

Ph.D. Thesis

**SPARSE SIGNAL PROCESSING FOR UNDERSEA
ACOUSTIC LINKS**

Submitted to

THE COCHIN UNIVERSITY OF SCIENCE AND TECHNOLOGY

in partial fulfilment of the requirement for the award of the degree of

Doctor of Philosophy

by

SABNA N.

Under the guidance of

Prof. (Dr.) P. R. S. Pillai

DEPARTMENT OF ELECTRONICS
COCHIN UNIVERSITY OF SCIENCE AND TECHNOLOGY
COCHIN – 682 022, INDIA

JANUARY 2017

SPARSE SIGNAL PROCESSING FOR UNDERSEA ACOUSTIC LINKS

Ph.D. Thesis in the area of Ocean Electronics

Author

Sabna N.
Research Scholar
Department of Electronics
Cochin University of Science and Technology
Cochin– 682 022, India
e-mail: sabnan@yahoo.com

Research Advisor

Dr. P. R. S. Pillai
Professor (Retd.)
Department of Electronics
Cochin University of Science and Technology
Cochin – 682 022, India
e-mail : prspillai@cusat.ac.in

JANUARY, 2017

Dedicated to.....

God Almighty



COCHIN UNIVERSITY OF SCIENCE AND TECHNOLOGY
DEPARTMENT OF ELECTRONICS
Cochin – 682 022

CERTIFICATE

This is to certify that this thesis entitled, *Sparse Signal Processing for Undersea Acoustic Links* is a bonafide record of the research work carried out by Ms. Sabna N. under my supervision in the Department of Electronics, Cochin University of Science and Technology. The result presented in this thesis or parts of it have not been presented for any other degree(s).

Cochin - 682022
JANUARY 2017

Prof. (Dr.) P.R.S. Pillai
Supervising Guide

DECLARATION

I hereby declare that the work presented in this thesis entitled *Sparse Signal Processing for Undersea Acoustic Links* is a bonafide record of the research work carried out by me under the supervision of Dr. P.R.S. Pillai, Professor, in the Department of Electronics, Cochin University of Science and Technology. The result presented in this thesis or parts of it have not been presented for other degree(s).

SABNA N.

Cochin – 22
JANUARY 2017



COCHIN UNIVERSITY OF SCIENCE AND TECHNOLOGY
DEPARTMENT OF ELECTRONICS
Thrakkara, Cochin – 682 022

CERTIFICATE

This is to certify that this thesis entitled, *Sparse Signal Processing for Undersea Acoustic Links* has been modified to effect all the relevant corrections suggested by the Doctoral Committee and the audience during Pre-synopsis Seminar.

Cochin - 682022
JANUARY 2017

Prof. (Dr.) P.R.S. Pillai
Supervising Guide

Acknowledgements

I would like to express my deepest sense of gratitude to my research guide, **Prof. (Dr.) P.R.S. Pillai**, Department of Electronics, Cochin University of Science and Technology for his excellent guidance and incessant encouragement. It has been a great pleasure and privilege to work under him and he was always there when I needed help.

I am much grateful to **Prof. (Dr.) Supriya M.H.**, Professor & Head, Department of Electronics, Cochin University of Science and Technology, for the whole hearted support and constant encouragement.

Sincere thanks are due to **Prof. (Dr.) K. Vasudevan, Prof. (Dr.) P.Mohanam, Dr. C. K. Aanandan, Dr. Tessamma Thomas** and **Dr. James Kurian** Department of Electronics, Cochin University of Science and Technology, for providing adequate help and fruitful suggestions.

I take this opportunity to express my sincere thanks to **Mr. Arun A. Balakrishnan, Dr. Bijoy A. Jose** and **Mr. Mithun Haridas**, Department of Electronics, for the constant encouragement rendered to me.

I would like to give a special word of thanks to the research fellows in the *Centre for Ocean Electronics (CUCENTOL)*, Dr. Binesh T., Dr. C. Prabha, Mr. Prasanth P.P., Mr. Sujith Kumar S.Pai, Mr. Suraj Kamal, Mr. Shameer, Mr. Satheesh Chandran, Mr. Mohan Kumar K., Mr. Prajas John, Ms. Revathy R., Mrs. Sreelakshmi K., Mrs. Sherin B.M. and Mrs. Rithu James.

I thankfully bear in mind the sincere co-operation and support I received from the **library and administrative staff** of the Department.

I also take this opportunity to thank all the **Research Scholars, M.Tech. and M.Sc. students**, Department of Electronics, Cochin University of Science and Technology who contributed and helped me in completing my thesis.

I would also acknowledge the **Kerala State Council for Science, Technology and Environment** for the financial assistances granted to me, without which I would not have completed my thesis work as a Full-Time Research Scholar.

It is beyond words to express my gratitude to my husband **Mr. Sajoon A. A.**, my kids **Hadi** and **Raaina**, my parents, **Mr. T. S. Naushad** and **Mrs. Sarina Naushad** as well as my **in-laws**, for their sacrifice in connection with preparation of my thesis. I am sure I could not have completed this great task without their support and cooperation.

SABNA N.
JANUARY 2017.

ABSTRACT

The oceans encompass almost two-thirds of the earth's surface and possess significant explored as well as unexplored marine living and non-living resources. This necessitates the need and requirements for the exploration and *in-situ* online almost real time, monitoring of the ocean in a general perspective. Undersea communication channel is one of the most difficult and challenging communication media in use today. As radio frequency waves are not suitable for undersea communication due to its high propagation loss in water, acoustic waves are used as the mode of communication in undersea wireless networks, though it suffers from innumerable limitations such as low bandwidth, high and variable latency, power constraints, high failure rate on account of biofouling and corrosion, unpredictable propagation characteristics, etc. This thesis entitled, *Sparse Signal Processing for Undersea Acoustic Links* envisages the implementation of a prototype system for undersea communication between static sensor nodes employing Orthogonal Frequency Division Multiplexing (OFDM) concepts and the estimation of underwater channel exploiting its sparse features. It also addresses the use of compressive sensing for effectively utilizing the available scarce bandwidth in undersea acoustic links.

Contents

	Page No
<i>Acknowledgements</i>	<i>xi</i>
ABSTRACT	<i>xiii</i>
<i>Contents</i>	<i>xv</i>
<i>List of Figures</i>	<i>xix</i>
<i>List of Tables</i>	<i>xxiii</i>
<i>Abbreviations</i>	<i>xxv</i>
CHAPTER 1	1
INTRODUCTION	1
1.1 Background	1
1.2 Undersea Acoustic Communication	2
1.3 Underwater Acoustic Sensor Networks	2
1.3.1 Static Topology	3
1.3.2 Hybrid Topology - Networks with mobile sensor nodes	5
1.4 Factors Affecting Propagation of Sound in Water	6
1.4.1 Spreading	7
1.4.2 Attenuation	8
1.4.3 Sound Speed Profile	8
1.4.4 Ambient Noise	10
1.4.5 Multipath	11
1.5 Compressive Sensing	13
1.6 Sound Propagation Models	14
1.6.1 Bellhop Model	14
1.6.2 Rayleigh Model	15
1.7 Scope of Work Done	16
1.8 Summary	20
CHAPTER 2	21
REVIEW OF PAST WORK	21
2.1 Background	21
2.2 Underwater Acoustic Communication	21
2.3 Compressive Sensing	27
2.4 Modulation and Coding Schemes	33

2.5	Synchronization Issues in OFDM	38
2.6	Channel Estimation.....	39
2.7	Multiple-Input Multiple-Output Systems	48
2.8	Summary.....	49
CHAPTER 3		51
METHODOLOGY		51
3.1	Background.....	52
3.2	Compressive Sensing Algorithms	54
3.3	Sparsification and Recovery	56
3.4	Propagation Theory	57
3.5	Modulation techniques for Undersea Acoustic Links	57
3.6	Orthogonal Frequency Division Multiplexing	58
3.6.1	Advantages of OFDM	59
3.6.2	Disadvantages of OFDM	60
3.7	Channel Estimation.....	60
3.7.1	Channel Estimation techniques in use	61
3.7.2	Dictionary based Sparse Channel Estimation Technique	62
3.8	Summary.....	63
CHAPTER 4		65
SYSTEM MODEL		65
4.1	Background.....	66
4.2	Sparse Signal Reconstruction.....	66
4.2.1	Matrix Padding	69
4.2.2	LMS Based Adaptation	71
4.3	Undersea Acoustic Channel Effects.....	74
4.3.1	Ambient Noise.....	74
4.3.2	Generation of Channel Impulse Response.....	77
4.3.3	CTD (conductivity, temperature and depth) Instrument	79
4.4	OFDM for Undersea Acoustic Links	79
4.5	Coded OFDM	81
4.6	BCH Coded OFDM.....	82
4.7	STBC MIMO	83
4.7.1	Normal STBC.....	83
4.7.2	Coded STBC.....	84
4.8	Channel Estimation and Synchronization	85
4.9	Summary.....	86
CHAPTER 5		89
MODULATION AND CODING.....		89
5.1	Background.....	89
5.2	Orthogonal Frequency Division Multiplexing	90
5.2.1	Use of Guard band	91

5.2.2	OFDM Variants	92
5.2.3	Modulation Techniques	93
5.2.4	Subcarrier Generation	95
5.2.5	Signal Estimation.....	96
5.2.6	Peak to Average Power Ratio (PAPR) Issue in OFDM.....	96
5.3	Forward Error Correction	98
5.3.1	Block codes	99
5.3.2	Convolutional codes	100
5.4	Puncturing	101
5.5	Interleaving.....	102
5.6	Diversity Techniques.....	103
5.6.1	Space-time coding	105
5.6.2	Alamouti STBC for 2x1 System.....	106
5.6.3	Alamouti STBC for 2x2 System.....	108
5.7	Spatial Multiplexing.....	110
5.8	Dictionary based Sparse Channel Estimation Technique	111
5.8.1	Algorithm for Sparse Channel Estimation.....	115
5.9	Synchronization Issues in Practical OFDM Scenario	115
5.9.1	STO Estimation	116
5.9.2	CFO Estimation	118
5.10	Summary.....	121
CHAPTER 6		123
RESULTS AND DISCUSSIONS.....		123
6.1	Background.....	124
6.2	Performance of Matrix Padding Technique	125
6.2.1	Performance Comparison under Noiseless Scenario	126
6.2.2	Performance Comparison under Gaussian Noise	128
6.3	BER Performance of OFDM for Undersea Acoustic Links	131
6.4	BER Performance of Coded OFDM for Undersea Acoustic Links .	136
6.4.1	Simulation Parameters	137
6.4.2	Simulation Results	138
6.4.3	Performance Comparison of BCH (15, 11) and (15, 7) Coded OFDM for Undersea Acoustic Links.....	141
6.5	Performance of Space-Time Block Coding for Undersea Acoustic Links.....	145
6.5.1	Simulation Steps	145
6.5.2	Simulation Results	145
6.6	Effect of channel on BER Performance	148
6.6.1	Synchronization	148
6.6.2	Channel Estimation.....	149
6.7	Data Rate Computation for OFDM in undersea acoustic links	156
6.7.1	Comparison of Data Rates for BPSK, QPSK and 16-PSK based OFDM schemes.....	157
6.7.2	Comparison of Data Rates for normal OFDM, Convolutional Coded OFDM and BCH Coded OFDM schemes.....	157
6.7.3	Comparison of Data Rates for normal OFDM with pilot based scheme for channel estimation	158

6.8	Summary.....	159
	CHAPTER 7.....	161
	CONCLUSIONS.....	161
7.1	Background.....	161
7.2	Highlights of the Thesis.....	162
7.2.1	Importance of Undersea Sensor Networks	162
7.2.2	Matrix Padding method for Sparse Signal Reconstruction.....	163
7.2.3	OFDM for Undersea Acoustic Links.....	163
7.2.4	Effect of Coding and Interleaving on BER performance of OFDM systems .	164
7.2.5	BER performance of BCH Coded OFDM systems	164
7.2.6	Normal STBC and Coded STBC for Undersea Acoustic Links	165
7.2.7	Synchronization and Channel Estimation for an Undersea Acoustic Link.....	165
7.3	Future Scope for Research	166
7.3.1	Trials in the Open Ocean	166
7.3.2	Use of other Modeling techniques/simulators for Undersea Acoustic Communication	166
7.3.3	Other coding schemes.....	166
7.3.4	Coded STBC-OFDM for Undersea Acoustic Links	167
7.3.5	Possibility of utilization of proposed technique for real-time data transmission in the SOFAR channel.....	167
7.4	Summary.....	167
	References.....	169
	Publications brought out in the field of research.....	187
	Other Publications.....	189
	Subject Index	191

List of Figures

	Page No
Fig. 1.1 A typical Underwater Acoustic Network {Courtesy: [1]}.....	3
Fig. 1.2 Two-dimensional underwater network {Courtesy: [2]}.....	4
Fig. 1.3 Three-dimensional underwater network {Courtesy: [2]}.....	5
Fig. 1.4 Hybrid Underwater Network {Courtesy: [3]}	6
Fig. 1.5 Geometry for (a) Spherical Spreading (b) Cylindrical Spreading {Courtesy: [4,5]}	7
Fig. 1.6 Sound speed profile using Munk equation {Courtesy: [6]}	9
Fig. 1.7 Layered structure of ocean {Courtesy: [4,5]}	11
Fig. 1.8 Shallow water multipath propagation: direct as well as reflected paths {Courtesy: [7]}.....	12
Fig. 1.9 Multipath Channel Model {Courtesy: [8]}.....	12
Fig. 1.10 Various sound propagation paths in deep sea {Courtesy: [5]}.....	13
Fig. 3.1 Concept of compressive sensing	53
Fig. 3.2 Block diagram representation of compressive sensing	54
Fig. 3.3 Block diagram of the proposed matrix padding technique	56
Fig. 3.4 Pilot arrangement (a) block type (b) comb type	61
Fig. 4.1 Block Diagram for Compressive Sensing and Recovery.....	68
Fig. 4.2 Tapped delay line structure of the LMS filter	73
Fig. 4.3 Variation of PSD of Overall Ambient Noise with respect to wind speed and shipping factor.....	75
Fig. 4.4 PSD of Overall Ambient Noise with respect to frequency and shipping factor	76
Fig. 4.5 PSD of Overall Ambient Noise with respect to frequency and wind speed....	77
Fig. 4.6 A typical Sound Speed Profile from real ocean	78
Fig. 4.7 Normalised Channel Impulse Response	79
Fig. 4.8 General block diagram of an OFDM System for Undersea Acoustic Links..	80
Fig. 4.9 System Model of Interleaved Coded OFDM.....	82
Fig. 4.10 General block schematic of a 2x2 STBC system	84
Fig. 4.11 General block schematic of a coded interleaved 2x2 STBC system.....	85
Fig. 4.12 Block Diagram of an OFDM Receiver with synchronization and channel estimations	86

Fig. 5.1 General structure of an OFDM symbol	92
Fig. 5.2 Constellation diagram for the transmitted 16-QAM symbols.....	94
Fig. 5.3 Constellation diagram for the transmitted 16-PSK symbols.....	95
Fig. 5.4 DFT Spreading	98
Fig. 5.5 Subcarrier mapping.....	99
Fig. 5.6 General block diagram of a convolutional encoder.....	102
Fig. 5.7 Structure of a block interleaver	103
Fig. 5.8 Time diversity	104
Fig. 5.9 Frequency Diversity	105
Fig. 5.10 Space-time diversity	105
Fig. 5.11 Space-frequency diversity	106
Fig. 5.12 Alamouti Space-time block coding	107
Fig. 5.13 2x1 System	107
Fig. 5.14 2x2 System	109
Fig. 5.15 MIMO System	111
Fig. 5.16 STO Estimation	117
Fig. 5.17 Illustration of ICI due to frequency offset	120
Fig. 6.1 Comparison of Signal-to-noise ratio Performance of the proposed matrix padding method with the other compressive sensing methods	126
Fig. 6.2 Comparison of the Correlation Performance of the proposed matrix padding method with the other compressive sensing methods	127
Fig. 6.3 Comparison of the Mean Squared Error Performance of the proposed matrix padding method with the other compressive sensing methods	128
Fig. 6.4 Comparison of Signal-to-noise ratio Performance of the proposed matrix padding method with the other compressive sensing methods	129
Fig. 6.5 Comparison of the Correlation Performance of the proposed matrix padding method with the other compressive sensing methods	130
Fig. 6.6 Comparison of the Mean Squared Error Performance the proposed matrix padding method with the other compressive sensing methods	131
Fig. 6.7 Comparison of bit-error-rate performances of the AWGN channel with an Underwater Acoustic channel.....	132
Fig. 6.8 Constellation Diagram of Received 16-QAM Symbols.....	132
Fig. 6.9 Constellation Diagram of Received 16-PSK Symbols	133

Fig. 6.10 Comparison of bit-error-rate performances of 16-QAM and 16-PSK based OFDMs for an Undersea Acoustic channel.....	134
Fig. 6.11 Original and recovered data stream for 16-QAM based OFDM through underwater channel	134
Fig. 6.12 Comparison of bit-error-rate performances of 4-QAM, 16-QAM and 256-QAM based OFDMs for an Undersea Acoustic channel	135
Fig. 6.13 Comparison of bit-error-rate performances for BPSK, DPSK, QPSK and 16-PSK based OFDMs for an Undersea Acoustic channel.....	136
Fig. 6.14 Comparison of bit-error-rate performances of normal OFDM as well as Convolutional Coded and BCH coded OFDMs, with and without interleaving for an undersea acoustic channel using BPSK modulation.....	138
Fig. 6.15 Comparison of bit-error-rate performances of normal OFDM as well as Convolutional Coded and BCH Coded OFDMs, with and without interleaving for an undersea acoustic channel using DPSK modulation.....	140
Fig. 6.16 Comparison of bit-error-rate performance of normal OFDM as well as...	142
Fig. 6.17 Comparison of bit-error-rate performances of normal OFDM as well as.	143
Fig. 6.18 Comparison of bit-error-rate performances of 16-QAM and 16-PSK for a 2x1 case, as well as 2x1 and 2x2 cases, for 16-QAM based system.....	146
Fig. 6.19 Comparison of bit-error-rate performances of a 2x2 STBC system for 16-QAM modulation with and without coding	147
Fig. 6.20 Effect of CFO on bit-error-rate under various SNR conditions for BPSK based OFDM in an undersea acoustic channel.....	149
Fig. 6.21 Comparison of CFO Estimation by using Cyclic Prefix and Pilot based approaches for an Undersea Acoustic channel.....	150
Fig. 6.22 Comparison of bit-error-rate performances of LS, MMSE and the dictionary based sparse channel estimation method using 16 pilots for an Undersea Acoustic channel	151
Fig. 6.23 Comparison of bit-error-rate performances using different number of pilots for a BPSK based OFDM for a range of 200m.....	152
Fig. 6.24 Comparison of bit-error-rate performances using different number of pilots for a BPSK based OFDM for a range of 500m.....	153
Fig. 6.25 Comparison of bit-error-rate performances using different number of pilots for a BPSK based OFDM for a range of 1km.....	153

**Fig. 6.26 Comparison of bit-error-rate performances using different number of pilots
for a BPSK based OFDM for a range of 10km..... 155**

Fig. 6.27 Bit-error-rate plotted against Pilot Overhead for an SNR of 25dB..... 156

List of Tables

	Page No
Table 3.1 Available Bandwidth for different ranges in Underwater Acoustic Channels	52
Table 5.1 Number of correctable errors using various BCH codes	101
Table 5.2 Encoding scheme with 2 transmitters	107
Table 6.1 Simulation Parameters for PSK based OFDM	136
Table 6.2 Simulation Parameters for Coded OFDM	137
Table 6.3 Bit-error-rates for various SNR for BPSK based OFDM system	139
Table 6.4 Bit-error-rates for various SNR for DPSK based OFDM system	141
Table 6.5 Simulation Parameters for BCH Coded OFDM	142
Table 6.6 BER values for normal OFDM as well as BCH (15, 11) and (15, 7) Coded OFDM systems, with and without interleaving, under various SNR conditions	144
Table 6.7 BER values 16-QAM and 16-PSK based STBC systems	147
Table 6.8 STO Estimation by correlation and difference methods	149
Table 6.9 Simulation Parameters for channel estimation	150
Table 6.10 BER values for various ranges for channel estimated using 16 pilots for channel estimation	154
Table 6.11 Minimum number of pilots needed for an L -sparse channel	155
Table 6.12 Data Rate Computation for PSK based OFDM schemes	157
Table 6.13 Data Rate Computation for BPSK based OFDM schemes with and without coding	158
Table 6.14 Data Rate Computation for BPSK based OFDM schemes with and without pilots	158

Abbreviations

AUV	- Autonomous Underwater Vehicles
AWGN	- Additive White Gaussian Noise
BCH	- Bose, Chaudhuri and Hocquenghem
BER	- Bit-error-rate
BPSK	- Binary Phase Shift Keying
CFO	- Carrier Frequency Offset
CIR	- Channel Impulse Responses
COFDM	- Coded Orthogonal Frequency Division Multiplexing
CoSaMP	- Compressive Sampling Matching Pursuit
CP	- Cyclic Prefix
CTD	- Conductivity, Temperature, Depth
DCT	- Discrete Cosine Transform
DPSSK	- Differential Phase Shift Keying
DSC	- Deep Sound Channel
FFT	- Fast Fourier Transform
ICI	- Inter Carrier Interference
ISI	- Inter symbol Interference
l_1	- l_1 -Regularized Least Squares
LP	- Linear Program
LMS	- Least-Mean-Square
LS	- Least Squares
MIMO	- Multiple-Input Multiple-Output
MMSE	- Minimum Mean Square Error
OFDM	- Orthogonal Frequency Division Multiplexing
OMP	- Orthogonal Matching Pursuit
PSD	- Power Spectral Density
PSK	- Phase Shift Keying
QAM	- Quadrature Amplitude Modulation
RAP	- Reliable Acoustic Path

RIP	- Restricted Isometry Property
ROV	- Remotely Operated Vehicles
SOFAR	- Sound Fixing And Ranging Channel
SM	- Spatial Multiplexing
SNR	- Signal-to-Noise Ratio
SSP	- Sound Speed Profile
STBC	- Space-Time Block Coding
STO	- Symbol Time Offset
UUV	- Unmanned Underwater Vehicles
UWA	- Underwater Acoustics
WOFDM	- Wideband OFDM
YALL1	- Your Algorithm for L1 Optimization
ZP	- Zero Padding

CHAPTER 1

INTRODUCTION

Underwater acoustic channels are generally recognized as one of the most difficult and challenging communication media in use today. This chapter addresses the various factors affecting the propagation of sound in water. Underwater acoustic communication is characterised by certain undesirable effects like multipath, ambient noise, attenuation, spreading, etc. Evaluation of new communication schemes and devices under realistic conditions being very expensive and time-consuming, simulators for modeling the acoustic underwater communication channel accurately like Bellhop and Rayleigh models have been studied.

1.1 *Background*

Undersea links are complex due to the effects of multipath, scattering, absorption, ambient noise, etc. Even though complex, a reliable communication is achievable using acoustic waves. During the last three decades, the realm of undersea communication scenario has witnessed remarkable progress and there was an exponential migration from systems with low bit rate to high bit rate and high power to low power consumption, which facilitated the development and deployment of undersea acoustic networks. Current research in this area focuses on judiciously formulating an integrated solution for meeting the emerging demands for applications of undersea networks in environmental data collection, pollution monitoring, offshore surveillance, coastal surveillance, etc.

1.2 Undersea Acoustic Communication

Acoustic signals are widely used in ocean exploration, oceanographic data collection, underwater communication, etc. Optical waves and electromagnetic waves do not propagate over long distances in underwater environment. The underwater channel is too complex due to various phenomena like multipath propagation, spreading, attenuation, etc. The available bandwidth of an underwater acoustic channel depends on the transmission loss, which increases with range and frequency. Moreover, the ambient noise also affects the performance of underwater acoustic communication systems. The sound speed is typically 1500m/s; but varies with depth, climatic conditions, etc. Sea trials being very expensive and time consuming, various toolboxes available for simulating the underwater acoustic communication have been used in this thesis, for investigating the behavior of the underwater channels.

1.3 Underwater Acoustic Sensor Networks

Underwater sensor network consists of a number of sensor nodes deployed to perform collaborative monitoring tasks over a given area for applications like oceanographic data collection, pollution monitoring, offshore exploration, mapping of the ocean floor for detection of objects, offshore oil/gas field monitoring, etc. A typical underwater acoustic sensor network is shown in Figure 1.1. Sensor nodes are mounted on the seabed by using anchors for observations of environmental conditions such as temperature, pollution data and other parameters of strategic and civilian applications.

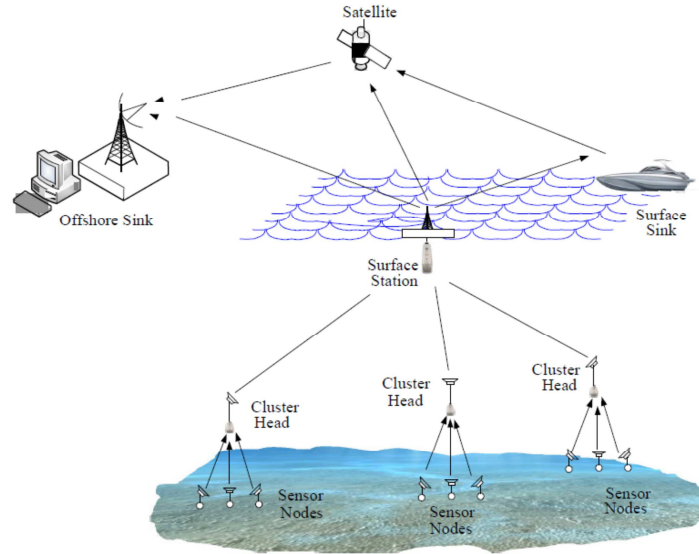


Fig. 1.1 A typical Underwater Acoustic Network {Courtesy: [1]}

1.3.1 Static Topology

1.3.1.1 Two dimensional

In two-dimensional underwater networks, a group of sensor nodes are anchored to the bottom of the ocean with deep ocean anchors for applications like environmental monitoring. The topology of a two-dimensional underwater network is shown in Figure 1.2. Underwater sensor nodes are interconnected to one or more cluster heads by means of wireless acoustic links. Cluster heads are network devices in charge of relaying data from the ocean bottom network to a surface station. To achieve this objective, cluster heads are equipped with two acoustic transceivers, namely a vertical and a horizontal transceiver. The horizontal transceiver is used by the cluster head to communicate with the sensor nodes in order to send commands and configuration data to the sensor nodes and collect monitored data. The vertical link is used by the cluster heads to relay data to a surface station. In deep water applications, vertical

transceivers must be long range transceivers as the ocean can be as deep as 10km. The surface station is equipped with an acoustic transceiver that is able to handle multiple parallel communications with the cluster heads. It is also endowed with a long range RF and/or satellite transmitter to communicate with the onshore sink and/or to a surface sink.

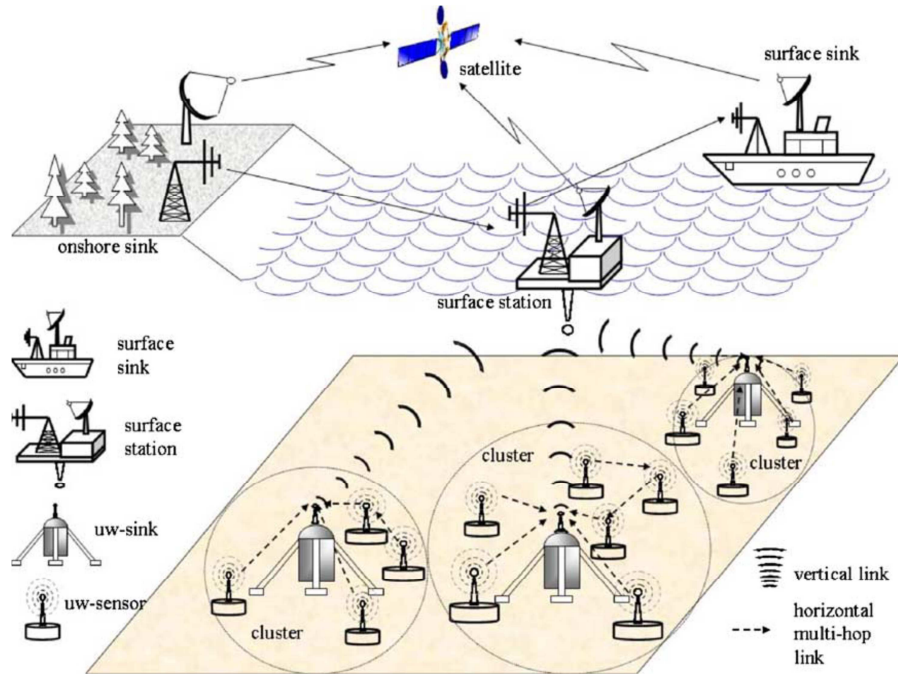


Fig. 1.2 Two-dimensional underwater network {Courtesy: [2]}

1.3.1.2 Three-dimensional

Three-dimensional underwater networks are used to detect and observe phenomena that cannot be adequately observed by means of ocean bottom sensor nodes, *i.e.*, to perform cooperative sampling of the 3D ocean environment. In three-dimensional underwater networks, sensor nodes are anchored to the bottom of the ocean and they float at different depths in order to observe a given phenomenon.

In three-dimensional topology, as depicted in Figure 1.3, each node is equipped with a floating buoy that can be inflated by a pump. The buoy pushes the node towards the ocean surface. The depth of the node can then be regulated by adjusting the length of the wire that connects the node to the anchor, by means of an electronically controlled engine that resides on the node. A challenge to be addressed in such a topology is the effect of ocean currents on the described mechanism to regulate the depth of the sensor nodes.

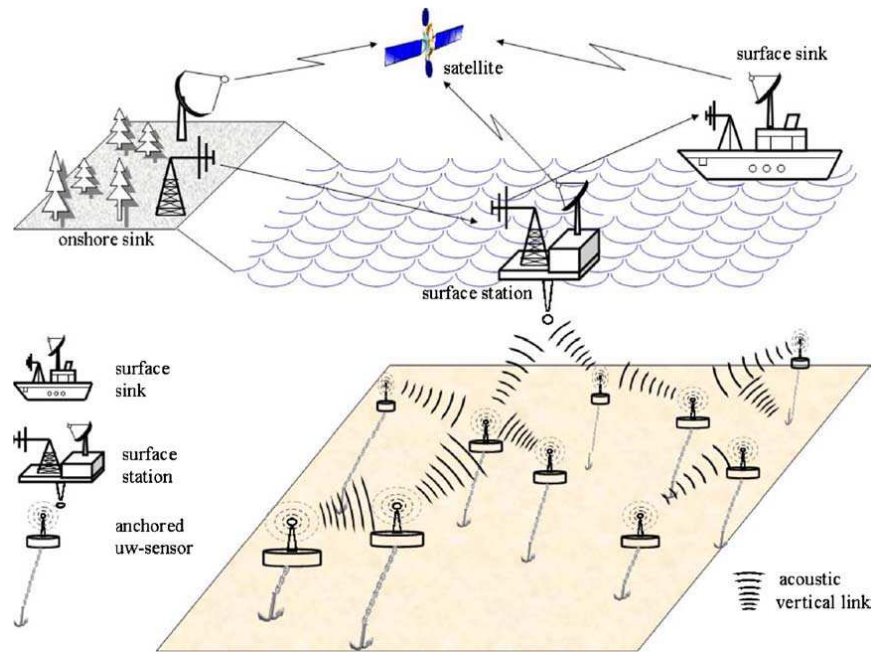


Fig. 1.3 Three-dimensional underwater network {Courtesy: [2]}

1.3.2 Hybrid Topology - Networks with mobile sensor nodes

Autonomous Underwater Vehicles (AUVs) can function without tethers, cables, or remote control, and therefore they have a multitude of applications in oceanography, environmental monitoring, and underwater resource study. Hence, they can be used to enhance the capabilities of underwater sensor networks in many ways. The integration and

enhancement of fixed sensor networks with AUVs, Remotely Operated Vehicles (ROVs) or any other sea gliders, is a promising area of research in undersea networks. This is called a Hybrid topology where an underwater acoustic sensor network consists of lots of static nodes together with a number of mobile nodes, as shown in Figure 1.4. In hybrid topology, mobile nodes play a key role for additional support in accomplishing the task, perhaps for data harvesting or enhancing the network capacity. Mobile nodes could be considered as super nodes which has more energy and can move independently, it could be a router between fixed nodes, a manager for network reconfiguration, or even a normal node for data sensing.

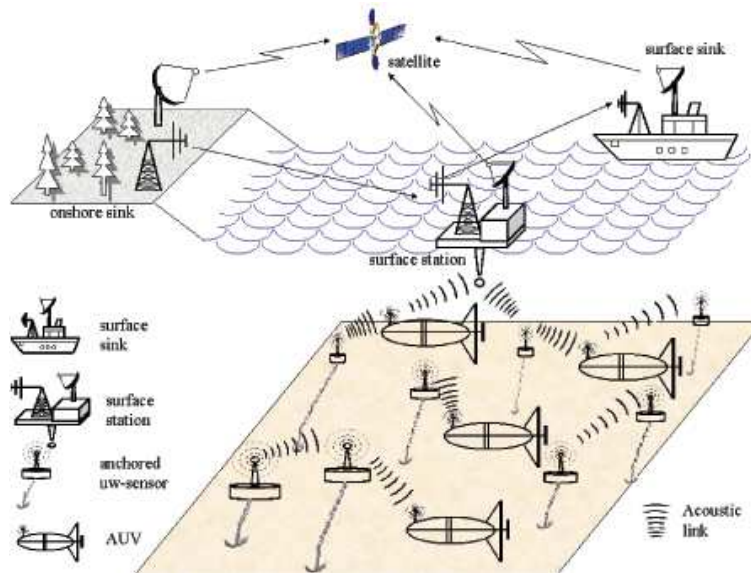


Fig. 1.4 Hybrid Underwater Network {Courtesy: [3]}

1.4 Factors Affecting Propagation of Sound in Water

Ocean forms a complex medium for the propagation of sound. Underwater acoustic communications include undesirable effects like ambient noise, attenuation, spreading, etc. Transmission loss (TL) can be

defined as ten times the log (base 10) of the ratio of the reference intensity (I_{ref}) measured at a point 1m from the source, to the intensity (I), measured at a distant point, and is expressed in units of decibels (dB):

$$TL = 10 \log \frac{I_{ref}}{I}. \quad (1.1)$$

Transmission loss may be considered to be the sum of loss due to spreading and attenuation. Spreading effect is the regular weakening of sound as it spreads outwards from the source. Attenuation loss includes the effects of absorption, scattering and leakage out of sound channels.

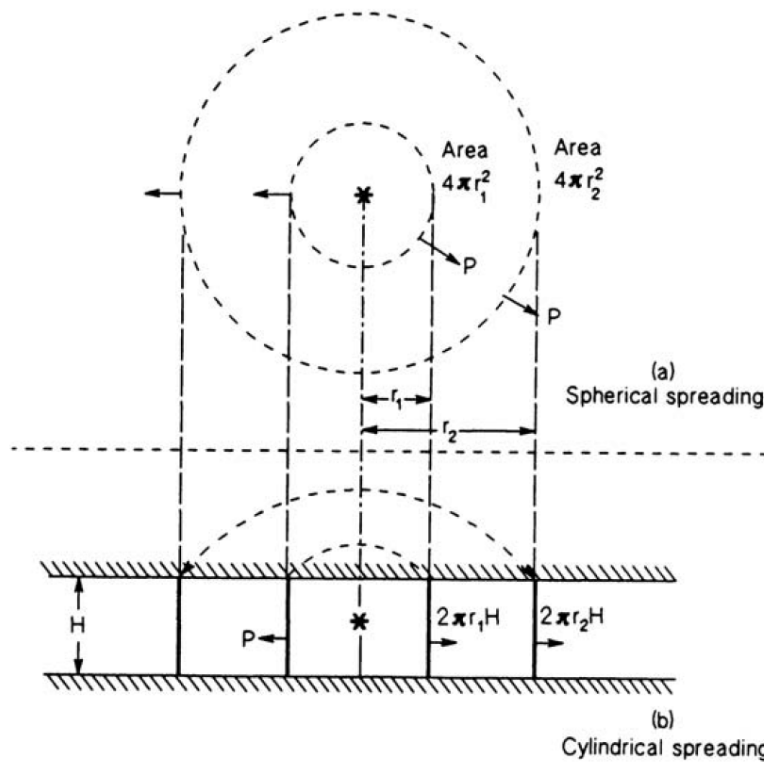


Fig. 1.5 Geometry for (a) Spherical Spreading (b) Cylindrical Spreading {Courtesy: [4,5]}

1.4.1 Spreading

Spreading can be cylindrical, in which, the intensity decreases proportional to the range or spherical, in which the intensity decreases as

the square of the range. Figure 1.5 shows the geometry for spherical spreading and cylindrical spreading. Cylindrical spreading occur when the medium has plane parallel upper and lower bounds and is given by

$$\text{Transmission Loss} = 10 \log r, \quad (1.2)$$

where r is the range from the transmitter. For spherical spreading, the transmission loss varies as,

$$\text{Transmission Loss} = 20 \log r. \quad (1.3)$$

1.4.2 Attenuation

Absorption involves conversion of acoustic energy into heat. The Thorpe attenuation model for absorption is given by

$$\alpha(f) = 0.1 \frac{f^2}{1+f^2} + 40 \frac{f^2}{4100+f^2} + 0.000275f^2, \quad (1.4)$$

where attenuation $\alpha(f)$ is in decibels per kiloyard and frequency f is in kHz. Thus, for every kiloyard travelled, the sound intensity gets diminished due to the absorption by an amount α dB. It is known that absorption of sound in sea water is high compared to that in distilled water due to the dissolved minerals in the sea.

1.4.3 Sound Speed Profile

The sound speed profile (SSP) represents a plot of the speed of sound with depth from the surface to bottom. The Sound Speed Profile may be constructed from any number of actual data points and then subjecting it to a fitting algorithm to produce a smoother graph. Given the Conductivity, Temperature, Depth (CTD) data, the Sound Speed Profile can be computed using the Leroy's formula given by

$$C = 1492.9 + 3(T - 10) - 6 \times 10^{-3}(T - 10)^2 - 4 \times 10^{-2}(T - 18)^2 + 1.2(S - 35) - 10^{-2}(T - 18)(S - 35) + \frac{z}{61}, \quad (1.5)$$

where C is the sound velocity in m/s, T is the temperature in degree centigrade, S is salinity in parts per thousand and z is the depth in meters.

The sound speed varies non-linearly with depth, due to the variation of temperature, salinity and pressure from surface to bottom. At lower depths, temperature determines the sound speed, but as the water depth increases, pressure becomes the main determining factor in the speed of sound propagation at larger depths.

When the measurements are not available, standard models like Munk profile, can be used for many ocean regions. Walter H. Munk introduced an equation for sound velocity as function of depth, with the exponential increase dominating in the upper waters and the linear term dominating in deep waters. Figure 1.6 shows a Munk profile and the Munk equation is given as

$$c(z) = 1492.0[1.0 + \varepsilon(e^{-\eta} + \eta - 1)], \quad (1.6)$$

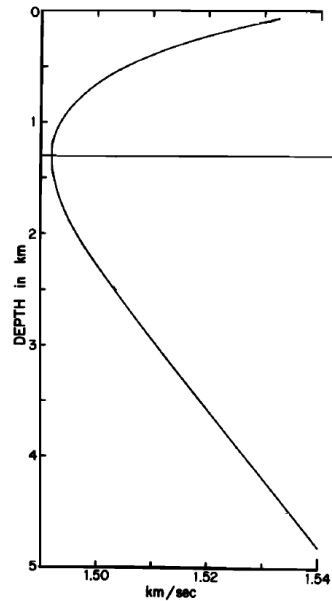


Fig. 1.6 Sound speed profile using Munk equation {Courtesy: [6]}

where

$$\eta = \frac{2(z-1300)}{1300}, \quad (1.7)$$

$\varepsilon = 7.4 \times 10^{-3}$ is the Perturbation coefficient, the fractional adiabatic velocity increase over a scale depth and z is the water depth.

A typical deep sea profile may be divided into several layers such as the *surface layer*, *seasonal thermocline*, *main thermocline* as well as the *deep isothermal layer* as shown in Figure 1.7. In the surface layer, the velocity of sound is susceptible to daily and local changes of heating, cooling and wind action. In the seasonal thermocline, temperature, and hence velocity decreases with depth. The main thermocline, which lies below the seasonal thermocline, is affected only slightly by seasonal changes. Close to the sea bottom, there is the deep isothermal layer with positive velocity gradient due to the effect of pressure on sound velocity. As a consequence of the characteristic velocity profile of the deep sea, a sound channel also called the *SOFAR (sound fixing and ranging) channel* or *deep sound channel (DSC)* occurs in the deep sea. This sound channel offers low transmission loss, and hence, very long ranges are achievable.

1.4.4 Ambient Noise

Noise in underwater communication scenario consists of *ambient noise* which is always present in the background of the sea, and *site-specific noise* which exists only in certain regions. The sources of ambient noise include tides, seismic disturbances, oceanic turbulences, thermal noise, biological sources, etc. At low frequencies (0.1 - 100Hz), earthquakes, underwater volcanic eruptions, turbulence in the ocean and atmosphere, etc. are the main noise sources. In the frequency band 50 - 300Hz, underwater noise is mainly due to remote shipping traffic, while in the frequency band

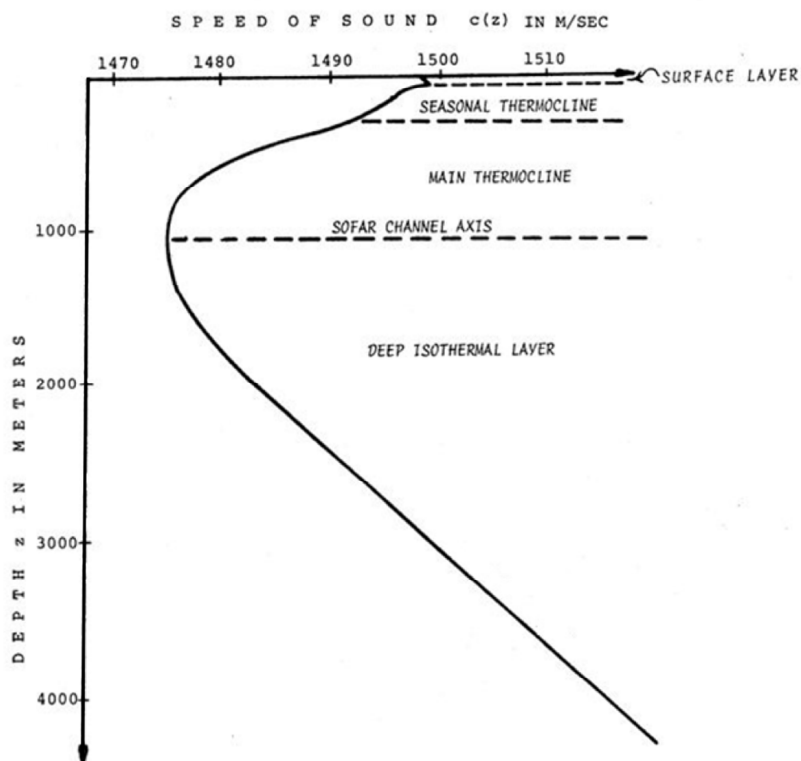


Fig. 1.7 Layered structure of ocean {Courtesy: [4,5]}

0.5 - 50kHz, underwater noise is directly associated with the state of the ocean surface and the winds in the area of interest. At frequencies greater than 100kHz, thermal noise is dominant. Biological noise produced by marine animals for communication with each other, locating the prey, frightening enemies and so on, is seasonal and spatial in nature.

1.4.5 Multipath

Multipath effects occur due to the reflection of sound by the sea surface and sea bottom as well as due to the refraction of sound in the water. As a result, the receiver gets a bewildering mix of signals from the transmitter in direct path as well as multipath as shown in Figure 1.8.

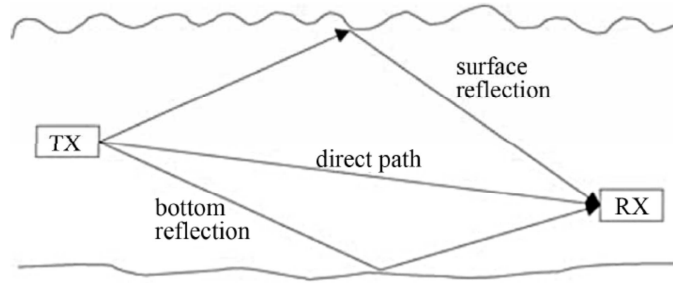


Fig. 1.8 Shallow water multipath propagation: direct as well as reflected paths {Courtesy: [7]}

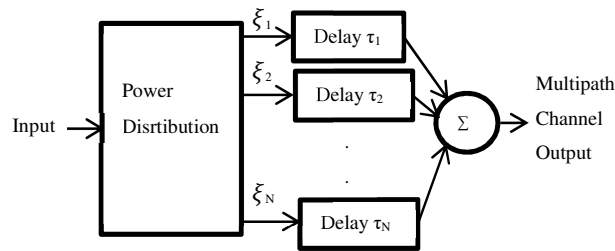


Fig. 1.9 Multipath Channel Model {Courtesy: [8]}

The channel impulse response of a multipath channel can be modeled as in Figure 1.9 and expressed as

$$h = \sum_{n=1}^N \xi_n \delta(\tau - \tau_n), \quad (1.8)$$

where N is the number of multipaths, τ_n is the n^{th} path delay and ξ_n is the amplitude associated with n^{th} path.

The different types of propagation paths that exist between a source and a receiver in the deep sea are as shown in Figure 1.10. Sound propagates in the sea by way of a variety of paths depending on the sound speed structure in the water column and the source–receiver geometry. These paths are direct path (A), surface duct (B), bottom bounce (C), convergence zone (D), deep sound channel (E) and reliable acoustic path (F), where x is the source and o is the receiver.

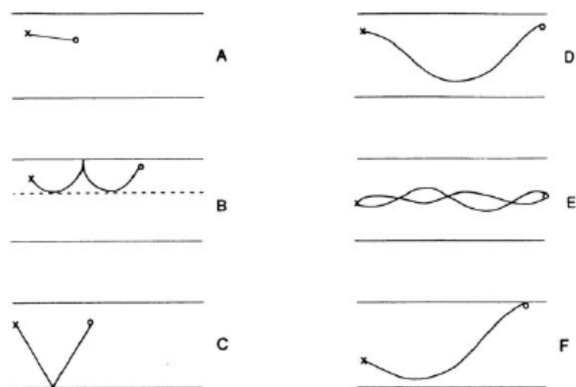


Fig. 1.10 Various sound propagation paths in deep sea {Courtesy: [5]}

1.5 *Compressive Sensing*

Nyquist sampling theorem forms the basis of nearly all the signal acquisition, transmission and reconstruction techniques widely used in almost all the systems. Sampling a signal at the Nyquist rate and transmitting it at the same rate in situations where the bandwidth is a scarce resource may adversely affect the system throughput and efficiency. This warrants the need and requirement for devising systems and techniques for transmitting a signal at a rate lower than the Nyquist rate. If the signal is transmitted at par with the Nyquist criteria, it might result in too many samples. This necessitates the need for compressing the signal before it is stored or transmitted. The signals so compressed can be reconstructed at a later stage following certain optimization techniques.

The available bandwidth of an underwater acoustic channel depends on the transmission loss, which increases with range and frequency. This implies that the transmission loss limits the available bandwidth for underwater acoustic communication. The bandwidth available for underwater acoustic communication is of the order of 1kHz, which is much lower than that available for RF communication links. If the information

could be stored or transmitted by fewer numbers of samples than the Nyquist rate, it would have been advantageous in underwater acoustic communication scenario.

A new method called compressive sensing is used to represent and reconstruct certain classes of signals at a rate below the Nyquist rate. Compressive Sensing is a new paradigm that gained the attention of researchers in signal processing, communication as well as mathematics. It helps in reconstructing the signal from far less samples than that required by the sampling theorem, which paves the way for saving memory and catering low data rate requirements in communication applications.

1.6 *Sound Propagation Models*

This section discusses the Bellhop and Rayleigh models, which are used widely for undersea acoustic modeling.

1.6.1 Bellhop Model

Bellhop is a highly efficient ray tracing toolbox for predicting the acoustic pressure fields in ocean environments. It was developed by Michael Porter from Heat, Light & Sound (HLS) Research, Inc. and is available as free software. Bellhop model can generate a variety of useful outputs including transmission loss, Eigen rays, Channel Impulse Response, etc. for the environment specified by the user.

To utilize the ray tracing capabilities of the Bellhop model, a precise description of the physical characteristics of the targeted environment is important, which include the depth of the ocean, sound speed profile in the location, information concerning the bottom contour and roughness, information about the surface, etc. The environmental data can be gathered from the real measurements or are available from known data sets for the particular ocean environments. In general perspective, the

real measurement data are preferred so that the model will generate more realistic results. The environmental file specified should include the frequency of operation, depth-speed pairs, number of sources as well as receivers and their depths. Bellhop model allows for range-dependence on the top and bottom boundaries (altimetry and bathymetry), as well as the sound speed profile. Additional input files allow the specifications of directional sources and geo-acoustic properties of the bounding media as well as the surface/ bottom reflection coefficients.

1.6.2 Rayleigh Model

The effects of multipath in underwater acoustic channel causes constructive and destructive interferences and phase shifting of the signal. The shallow water medium range channel, where the multipath fading is predominantly due to reflections from the sea bed and the sea surface, exhibits Rayleigh fading properties. Rayleigh fading, which is used for modeling the effect of propagation in a wireless environment, assumes that the magnitude of a signal that has passed through such a transmission medium will fade according to certain well known (Rayleigh) distribution.

The Rayleigh probability density function (pdf) is defined as,

$$f(x) = \left(\frac{x}{\sigma^2}\right) \exp\left(\frac{-x^2}{2\sigma^2}\right), \quad (1.9)$$

and the Cumulative Distribution Function (CDF) is expressed as,

$$F(x) = 1 - \exp\left(\frac{-x^2}{2\sigma^2}\right), \quad (1.10)$$

where σ is the scale parameter and x lies in the range $[0, \infty)$.

1.7 Scope of Work Done

This thesis addresses one of the emerging topics in Underwater Acoustics, *viz.* the various modulation and coding techniques for realising reliable OFDM for Undersea Acoustic Links. This thesis proposes a matrix padding method for sparse recovery, which is robust even in the presence of noise. Orthogonal Frequency Division Multiplexing and coded interleaved OFDM as well as coded interleaved STBC have been investigated. The synchronization and channel estimation issues in OFDM systems have also been investigated.

Chapter 2 is devoted to the review of the works reported in open literature in the areas of compressive sensing, propagation of sound in sea, channel modeling, various modulation schemes, various coding schemes, channel estimation techniques, synchronization issues in OFDM (Orthogonal Frequency Division Multiplexing), etc. Compressive sensing methods have been reported and various reconstruction methods have also been consolidated by various researchers. Many compressive sensing solvers do exist, which include ℓ_1 -magic, ℓ_1 -Regularized Least Squares (ℓ_1 ls), Convex Optimization (CVX), Your Algorithm for L1 Optimization (YALL1), Orthogonal Matching Pursuit (OMP), Compressive Sampling Matching Pursuit (CoSaMP), etc. Various research works relating to modeling of underwater channel using Bellhop and Rayleigh models as well as OFDM, diversity techniques and channel estimation techniques were also covered in the literature survey.

Compressive sensing has been evolved as a very useful technique for sparse reconstruction of signals that are sampled at sub-Nyquist rates. Compressive sensing helps to reconstruct the signals from few linear projections of the sparse signal. Chapter 3 presents the background of

compressive sensing and the various compressive sensing algorithms that are reported in open literature. A method for Sparsification and Recovery has also been proposed with a block diagram. Undersea acoustic links have numerous applications in pollution monitoring, environmental data collection, offshore and coastal surveillance, etc. Chapter 3 also provides a brief description of the various modulation techniques in use for undersea acoustic links. Orthogonal Frequency Division Multiplexing, which is a multicarrier modulation technique, is widely employed in undersea acoustic applications because of its numerous advantages. OFDM requires an estimate of the channel parameters at the receiver for undoing the channel effects. The sparsity of the channel impulse response of undersea links can be used for estimating the channel characteristics. A brief overview of the dictionary based sparse channel estimation is also included.

Compressive sensing recently gained immense attention due to the commendable advantages the technique offers in recovering certain target signals from a few random measurements. With the help of compressive sensing, the salient information in a signal can be preserved in a relatively small number of linear projections. A new technique which converts the signal into sparse domain by applying Discrete Cosine Transform (DCT) and then compressing it using a modified measurement matrix, followed by an LMS based adaptation, has been proposed in chapter 4. Making use of this proposed matrix padding technique, a computationally efficient sparse signal reconstruction has been achieved. Ambient noise is always present in the background of the undersea channel and the four basic sources that can model the ambient noise in the ocean are noise effects due to turbulence, shipping, wind and thermal processes. A study of variation of power spectral density (PSD) of the overall ambient noise has also been performed. Generation of channel impulse response using the Bellhop

model utilizing the environmental data like the sound speed profile of the water column, the number of transceivers and their depths has also been described. OFDM is a good choice in underwater communication, because of its numerous advantages. Chapter 4 also introduces the system models for normal OFDM as well as coded and interleaved OFDM, for undersea acoustic links. Space-time block coding (STBC) offers higher link reliability and this thesis combines STBC with coding and interleaving for improving the bit-error-rate performances. Synchronization and channel estimation are critical in practical OFDM communication scenario. A system model of an OFDM Receiver with Symbol Time Offset (STO) and Carrier Frequency Offset (CFO) estimation as well as channel parameter estimation has also been described.

Orthogonal Frequency Division Multiplexing is widely employed nowadays because of its advantages like resilience to intersymbol interference, higher spectral efficiency, simpler channel equalization, etc. Various modulation techniques like Quadrature Amplitude Modulation and Phase Shift Keying are used in conjunction with OFDM. Coding techniques like convolutional and BCH coding, as well as interleaving techniques can be used along with OFDM for improving the error correction capability of the receiver. Chapter 5 discusses OFDM as well as some of the modulation and coding techniques which can effectively improve underwater acoustic communication. Diversity techniques improve reliability of data transfer by transmitting the same data on two or more communication channels with different characteristics. The most commonly used space-time block coding (STBC) technique, the Alamouti STBC, has also been described. For undoing the channel effects and demodulating the signal with fairly acceptable accuracies, the channel parameters need to be estimated. Channel estimation is performed in

orthogonal frequency division multiplexing by inserting pilots into the subcarriers of an OFDM symbol. Underwater channels exhibit sparse channel impulse response which implies that very few of the channel taps have a nonzero value and the channel can be estimated using the compressive sensing techniques to achieve better performance. The dictionary based sparse channel estimation technique has also been analytically explained.

The performance of the matrix padding method is compared with other existing compressive sensing algorithms like l_1 -ls, l_1 -magic, YALL1, OMP, CoSaMP, etc. and the results of comparison in terms of signal-to-noise ratio, correlation and mean squared error, have been investigated in chapter 6. OFDM has been simulated using QAM (Quadrature Amplitude Modulation) and PSK (Phase Shift Keying) based modulation techniques for undersea acoustic links. The performances of various orders of QAM based OFDM systems for undersea acoustic communications have been studied and the bit-error-rates under various Signal to Noise Ratio conditions have also been compared for Additive White Gaussian Noise (AWGN) and Underwater Channels for 16-QAM based OFDM. The bit-error-rate performances of normal as well as coded OFDM with and without interleaving schemes have been simulated for various signal-to-noise ratio levels for both convolutional and Bose, Chaudhuri and Hocquenghem (BCH) codes. The performances of Alamouti STBC for a 2x1 and a 2x2 system were studied. It has been observed that the proposed STBC system with coding and interleaving offers better performance compared to the normal 2x1 and a 2x2 STBC systems. The performances of various STO as well as CFO estimation methods have been compared and it has been observed that STO estimation using difference method and CFO estimation using pilot based method guarantee acceptable performances. The undersea

channel has been estimated using dictionary based sparse channel estimation technique for various ranges and it has been found that by using a minimum number of pilots, acceptable bit-error-rate (BER) performance can be achieved. Chapter 7 brings out the salient highlights of the research work undertaken for realizing an underwater acoustic communication system and the general inferences gathered. This chapter also enlists the scope and direction for future research in this area.

1.8 Summary

The importance of underwater acoustic communication as well as various topologies for underwater acoustic sensor networks were covered. The factors affecting the propagation of sound in water as well as modeling of undersea channel using the Bellhop and Rayleigh models have also been discussed. This chapter also gives an introduction to Compressive Sensing, which helps in efficient use of the available scarce bandwidth of the undersea channel. Sparsity, an inherent characteristic of many natural signals, enables the signal to be stored in a fewer samples than that has been dictated by the Nyquist rate and subsequently be recovered, by means of compressive sensing. The scope of the work carried out in this thesis has also been briefly outlined.

CHAPTER 2

REVIEW OF PAST WORK

This chapter is devoted to the review of the research work reported in open literature in the areas of compressive sensing, propagation of sound in sea, channel modeling, various modulation schemes, various coding schemes, channel estimation techniques, synchronization issues in OFDM, etc. Compressive sensing methods have been reported and the various reconstruction methods have also been consolidated by various researchers. Many compressive sensing solvers exist, which include ℓ_1 -magic, l_1 _ls, SPARLS, YALL1, OMP, CoSaMP, etc. Various research works relating to modeling of underwater channel using Bellhop and Rayleigh models as well as OFDM, diversity techniques and channel estimation techniques were also covered in the literature survey.

2.1 Background

This chapter is devoted to the review of the research work reported in open literature in the fields of compressive sensing, modulation and coding schemes, communication in underwater environments, effects of underwater channel, underwater channel modeling, channel estimation, etc. as included in the following sections.

2.2 Underwater Acoustic Communication

Acoustic waves, which are used as the mode of communication in underwater wireless sensor networks, suffer from innumerable constraints such as low bandwidth, high latency, high failure rates, etc. The available bandwidth of an underwater acoustic channel depends on the transmission loss, which increases with range and frequency. This implies that the

transmission loss limits the available bandwidth for underwater acoustic communication. Studies on the underwater acoustic channel have been included in this section.

Tri Budi Santoso *et al.* [1] discussed the research and development of underwater acoustic communication systems. Acoustic propagation in the underwater channel influenced by three factors: signal attenuation, multipath propagation, and low speed of sound propagation. The experimental planning for underwater acoustic propagation characteristics has also been presented and the characterization results are used to evaluate the performance of communication system through simulation. Ian F. Akyildiz *et al.* [2] investigate several fundamental key aspects of underwater acoustic communications. Different topologies for two-dimensional and three-dimensional underwater sensor networks are discussed. The main challenges for the development of efficient networking solutions posed by the underwater environment has been analyzed and a cross-layer approach for the integration of all communication functionalities has been suggested.

The applications of two dimensional, three dimensional and hybrid underwater networks are discussed in [3]. Static two-dimensional networks can be used for applications like environmental monitoring or monitoring of underwater plates in tectonics. Static three-dimensional networks may be used for surveillance applications or monitoring of ocean phenomena (ocean bio-geo-chemical processes, water streams, pollution, etc.). Hybrid underwater networks can be used in both shallow as well as deep water and these networks can be used for distributed target classification and tracking.

Sonar, active and passive, the sonar equations and the factors that affect the propagation of sound in the sea are described by Robert J. Urick [4]. Sound propagation is affected by spreading, attenuation, multipath,

absorption, etc. Also velocity structure and thermocline of the sea, effects of sea surface and sea bottom on sound propagation, etc. are also described. Moreover, radiated noise and self-noise as well as the methods to reduce them are considered. Spreading loss, which is a geometrical effect representing the regular weakening of a sound signal as it spreads outward from the source, can be either cylindrical or spherical.

Paul C. Etter [5] provides an authoritative overview of currently available propagation, noise, reverberation and sonar-performance models. Sound propagates in the sea by way of a variety of paths. The particular paths traveled depend upon the sound speed structure in the water column and the source–receiver geometry. These paths include the direct path, surface duct, bottom bounce, convergence zone, deep sound channel and reliable acoustic path. Walter H. Munk [6] introduces an equation for computing sound velocity in ocean as function of depth. The exponential stratification model leads to an equation with the exponential increase dominating in the upper waters and the linear term dominating in deep waters. The Munk profile is an idealized sound speed profile; however, it allows us to illustrate many features that are typical of the deep-water sound speed profiles.

Milica Stojanovic *et al.* [7] discuss the acoustic propagation in underwater communication channels. There are three major factors in underwater acoustic communication: attenuation that increases with signal frequency, time-varying multipath propagation, and low speed of sound, approximately 1500m/s. Fangkun Jia [8] *et al.* studies time-variant characteristics of underwater acoustic channels. With the characteristics of high ambient noise level, very narrow bandwidth, low carrier frequency, enormous propagation latency and time-space-frequency variant multipath

effect, the stochastic ocean channel is very complex and difficult to achieve reliable underwater acoustic communications.

Gordon M. Wenz [9] discusses on the spectra and the sources of acoustic ambient noise in the ocean. The results of ambient noise investigations, after appropriate processing are compared on the basis of pressure spectra in the frequency band 1Hz to 20kHz. In the past, active and passive military sonar systems have dominated the activity in the field. With passive sonar systems, one listens to signals that are radiated by the various sources of acoustic energy in the ocean. A. B. Baggeroer [10] discusses active and passive sonar and their corresponding digital signal processing schemes.

William C. Knight *et al.* [11] describe the sonar digital signal processing functions along with the associated implementational considerations. The unwieldiness of the undersea propagation medium has been explained in detail. The theory of sound propagation in the ocean in its most fundamental form is systematically presented by L. M. Brekhovskikh *et al.* [12]. An important characteristic of the ocean is its underwater ambient noise and the various sources of ambient noise as well as their frequency ranges have also been touched upon.

Multipath transmission has the great beneficial effect in producing stronger sound fields than would exist in their absence as explained by R. J. Urick [13]. Yet these stronger signals are not always utilizable, in that they are smeared in time and frequency, and tend to become rapidly decorrelated with hydrophone separation in arrays. These effects are not predictable, because of the complexity of the existing multipath, and one has to devise elaborate processing techniques, such as replica correlation and matched filter approaches, which will not result in any signal enhancement. John G. Proakis [14] explains that in underwater,

electromagnetic waves do not propagate over long distances except at extremely low frequencies. In contrast, acoustic signals propagate over distances of tens and even hundreds of kilometers. An underwater acoustic channel is characterized as a multipath channel due to signal reflections from the surface and the bottom of the sea. In spite of this hostile environment, it is possible to design and implement efficient and highly reliable underwater acoustic communication systems for transmitting signals over large distances.

A. D. Waite [15] provides an understanding of the basic principles of sonar and investigates the sonar design and performance analysis. He describes the deep sound channel, reliable acoustic path, surface duct propagation as well as convergence zone propagation. Between the negative gradient of the main thermocline and the positive gradient of the deep layer there is a *sound speed minimum*, where sound tends to be focused by refraction. Seaweb networks interconnect fixed and mobile nodes distributed across a wide area in the undersea environment. Acoustic communications between neighboring DSP equipped tele-sonar modems is the basis for the physical layer. Node-to-node ranging is a byproduct of tele-sonar signaling, permitting localization of sensor nodes and navigation of mobile nodes such as submarines and autonomous vehicles. Joseph Rice [16] reviews the concept of operations for undersea networks with illustrative examples of actual Seaweb deployments.

It is well known that the frequency-dependency of the acoustic path loss imposes a bandwidth limitation on an underwater communication system, such that a greater bandwidth is available for a shorter transmission distance. Milica Stojanovic [17] offers an insight into the relationship between an acoustic link capacity and distance. Mandar Chitre, *et al.* [18] explain various challenges posed by the underwater channel. The

bandwidth available for communication is severely limited due to the strong absorption of high frequency sounds by the sea water. Extended multi-path and severe fading are also common in many underwater channels. A good understanding of the communications channel is important in the design and simulation of a communication system. Andrew C. Singer [19] *et al.* provide a brief overview of signal processing methods and advances in underwater acoustic communications, discussing both single-carrier and emerging multicarrier methods.

In underwater channel model, the attenuation, transmission distance, power consumption, Signal to Noise Ratio, Bit Error Ratio, inter symbol interference, error coding and alternative modulation strategies, etc. are of primary concern in the whole study and design of the transceiver structure. Nejah Nasri *et al.* [20] aim to survey the existing transceiver and its applicability to underwater communication based on the simulation parameters.

The depths of the oceans have a high potential for future industrial development and applications. However, communications must face harsh conditions that hinder the performance. Due to this, acoustic equipment is envisaged as the most appropriate technology, even though it suffers from several adverse effects such as strong attenuation at high (ultrasonic) frequencies, Doppler shifts and a time-varying multipath. The characteristics of the acoustic underwater channel and how it affects the mechanisms at the link and network layers have been described by J.Poncela *et al.* [22].

A new multipath channel model for shallow underwater acoustic communications has been proposed by F. De Rango *et al.* [23]. In particular, this model takes into account the effects due to spreading loss, scattering and reflections. José S. G. Panaro *et al.* [24] describe an

empirical model for the noise of the shallow underwater channel based on the analysis of the measured field data. A probability density function for the noise amplitude distribution has been proposed and the associated likelihood functions have been derived, based on which, an expression for the probability of error for binary signaling has been arrived at. The results of simulations carried out using the field noise data samples paved the way for establishing the noise effect on the performance of underwater acoustic communication systems.

Michael B. Porter *et al.* [25] discuss the application of four principal approaches: normal modes, ray/beam tracing, parabolic equations, and wavenumber integration to shallow waters with an eye on coastal security. As a particular application of interest, acoustic modems are considered which may be used to provide communications links with underwater vehicles. The basic physics, the modeling approaches, and the implications for modem performance have also been discussed.

Nan Jing *et al.* [26] describe a shallow water acoustic channel model based on the actual acoustic propagation characteristics with path attenuation, ambient noise, multiple paths, and Doppler effects. The channel model has been implemented in MATLAB and the simulation results show that the absorption coefficient and path losses are both dependent on the frequencies as well as propagation distances and the path gain is seen to have improved with Line of Sight (LOS)/ short range acoustic propagations.

2.3 Compressive Sensing

Compressive Sensing (CS) is a new signal acquisition technique that enables the reduction of the number of measurements required for the

recovery of sparse or compressible signals in an appropriate basis. Signal recovery is carried out by means of certain optimization techniques.

Emmanuel J. Candes [27] consolidates an emerging theory which goes by the name of compressive sensing or compressed sensing, making use of which, it is possible to reconstruct images or signals of scientific interest accurately and sometimes even exactly from a much less number of samples. This new sampling theory may come to underlie procedures for sampling and compressing data simultaneously. Justin Romberg [28] gives an introduction to compressive sensing and recovery via convex programming. A way to avoid the large digital data set to begin with and a way to build the data compression directly into the acquisition is what compressive sensing is all about. The mathematical theory draws from diverse fields including harmonic analysis, convex optimization, random matrix theory, statistics, approximation theory, and theoretical computer science.

Xiao Wang *et al.*, [29] describe current researches on the applications of compressive sensing in wireless communication networks, and then enumerate burning questions and the master keys of their corresponding solutions in these fields. The techniques of using compressive sensing in communication networks have been studied. Saad Qaisar *et al.* [30] give a brief background on the origins of this idea, reviews the basic mathematical foundation of the theory and then goes on to highlight different areas of its application with a major emphasis on communications and network domain. Finally, the survey concludes by identifying new areas of research where compressive sensing could be beneficial. Richard G. Baraniuk [31] explains that in many applications, including digital image and video cameras, the Nyquist rate is so high that too many samples result, making compression a necessity prior to storage

or transmission. In other applications, including imaging systems and high-speed analog-to-digital converters, increasing the sampling rate is very expensive. Compressive sensing employs non adaptive linear projections that preserve the structure of the signal and the signal is then reconstructed from these projections using an optimization process.

Compressive Sensing has attracted a lot of interests over the past few years as a revolutionary signal sampling paradigm. While the sampling process is simply a random linear projection, the reconstruction process to recover the original signal from the measurements is highly nonlinear. The measurement matrix should be incoherent with the basis matrix and the incoherence between the two matrices is mathematically quantified by the mutual coherence coefficient, the formula for which is given by Thong T. Do *et al.* [32]. Mark D. Plumbley, *et al.* [33] give an overview of a number of current and emerging applications of sparse representations in areas from audio coding, audio enhancement and music transcription to blind source separation solutions that can solve the cocktail party problem.

Supatana Auethavekiat [34] reviews the compressive sensing fundamentals and describes the implementation of compressive sensing reconstruction by basis pursuit (BP) and matching pursuit (MP) algorithms. Joel A. Tropp *et al.* [35, 36, 37] give an overview of the algorithms for sparse approximation, describing their computational requirements and the relationships between them. Pursuit method for sparse approximation includes orthogonal matching pursuit (OMP), compressive sampling matching pursuit (CoSaMP), etc.

Compressive sensing is a new type for signal reconstruction, which predicts that sparse signals and images can be reconstructed from what was previously believed to be incomplete information. The theory has many

potential applications in signal processing and imaging. In [38], Jagdeep Kaur *et al.* present the compressive sensing study carried out by many researchers. A theoretical framework of compressive sensing is presented by Shuai Yu *et al.* [39], for real audio signals, which are compressive and the performance of different reconstruction algorithms have been studied for original audio signals based on a number of measurements. It was concluded that OMP offered good reconstruction performance. Deanna Needell *et al.* [40] describe a recent algorithm, called CoSaMP that accomplishes the data recovery task. It was the first known method to offer near-optimal guarantees on resource usage, which is a greedy iterative method for reconstructing a signal from compressive samples.

Leveraging the concept of transform coding, compressive sensing has emerged as a new framework for signal acquisition and sensor design as explained by Richard Baraniuk *et al.* [41]. Compressive sensing enables a potentially large reduction in the sampling and computation costs for sensing signals that have a sparse or compressible representation. Emmanuel J. Candès *et al.* [42] give a detailed introduction to compressive sensing and survey the theory of compressive sampling or compressive sensing as a novel sensing/sampling paradigm that goes against the common wisdom in data acquisition. Compressive sensing relies on two principles: *sparsity* and *incoherence*.

Christian R. Berger, *et al.* [43] discuss an application of Compressive Sensing to Sparse Channel Estimation. There are large classes of matrices that obey the Restricted Isometry Property (RIP) with high probability. A simple technique for verifying the RIP for random matrices that underlies Compressive Sensing have been proposed by Richard Baraniuk *et al.* [44]. Emmanuel Candès *et al.* [45] formulated a condition for sparse signal reconstruction when the measurements are noisy

and the signal is not exactly sparse. The mathematical framework to recover the signal when the available information is not only severely incomplete, but also, the few available observations are inaccurate, has been given. The recovery procedure has been substantiated by using a 256 x 256 pixel boat image.

A unified view of the area of sparse signal processing has been presented by Farokh Marvasti *et al.* [46]. The key application domains of sparse signal processing have also been elaborated. Emmanuel J. Candes *et al.* [47] establish that it is possible to recover an input sparse vector by solving a simple convex optimization problem. The computational intractability of ℓ_0 -norm has recently led researchers to develop alternatives to ℓ_0 -norm, and a frequently discussed approach considers a similar program in the ℓ_1 -norm which goes by the name of basis pursuit. The ℓ_1 -norm is convex and it can be recast as a linear program (LP).

It is well known that compressive sensing problems reduce to solving large under-determined systems of equations. If we choose the compressed measurement matrix according to some appropriate distribution and the signal is sparse enough, the ℓ_1 optimization can exactly recover the ideally sparse signal with overwhelming probability. The case of approximately sparse signals has also been considered by Mihailo Stojnic *et al.* [48]. Vidya L. *et al.* [49] review some of the compressive sensing algorithms like basis pursuit, orthogonal matching pursuit, compressive sensing matching pursuit, etc. and try to find the best algorithm to make use of that in launch vehicle telemetry system. The recovery of the original signal from compressive sensing measurements becomes difficult when the compressive sensing data acquisition is noisy.

In [50], Vivekanand V. *et al.* review the robustness of some of the compressive sensing algorithms in recovering the original signal in presence of data acquisition noise. The results of the experimental evaluation using generic sparse data have been presented. In general, the relaxation based algorithms are found to have better recovery precision. A comparison of the performance of several algorithms for Compressive Sensing reconstruction has been carried out by Radomir Mihajlović *et al.* [51].

Moreno-Alvarado, *et al.* [52, 53], propose application of both DCT and the compressive sensing to the compression of audio signals. For the problem of making a sparse representation of an audio signal, DCT is used, which is one of the most widely used transform for image and video compression systems. Deanna Needell [54] analyzes a modified version of ℓ_1 -minimization problem, called the reweighted ℓ_1 -minimization method in the noisy case. The results of the experiments demonstrate large improvements in the error of the reweighted reconstruction compared to the reconstruction from the standard method.

Many ℓ_1 -minimization solvers exist. These include ℓ_1 -magic [55], `l1_ls` [56], SPARLS [57], YALL1 [58], etc. A sparse vector can be recovered from a small number of linear measurements by solving a convex program. Junfeng Yang *et al.* [59] propose the use of alternating direction algorithms for the basis pursuit and the basis pursuit de-noising problems in compressive sensing. Two classes of algorithms derived from either the primal or the dual form of ℓ_1 -problems have also been investigated.

Convex optimization problems arise frequently in many different fields. The convex optimization, a special class of mathematical optimization problems, includes least-squares and linear programming problems. Interior-point methods, developed in the 1980s to solve linear

programming requirement has been used to solve the convex optimization problems. The advantages in recognizing or formulating a problem as a convex optimization problem has been elaborated and various algorithms such as Newton's method, barrier method, primal-dual interior-point methods, etc. have been explained in detail by Stephen Boyd *et al.* [60]. Richard G. Baraniuk *et al.* [61] discuss some of the applications of compressive sensing. A number of low-dimensional signal models that support stable information-preserving dimensionality reduction are compared from a geometric perspective by Richard G. Baraniuk *et al.* [62]. There are large classes of diverse signal models that support stable dimensionality reduction and thus can be used to effect data acquisition, analysis, or processing more efficiently. Convex optimization (CVX) [63] is another effective software for finding solutions for complex convex optimization problems, including non-differentiable functions, such as ℓ_1 -norms.

2.4 Modulation and Coding Schemes

This section discusses some of the modulation schemes used in the area of underwater acoustic communication. In [64], Hamada Esmail *et al.* attempt to provide an overview of the key developments, both theoretical and applied, in topics relating to multicarrier communication for realising underwater acoustic links. This paper also includes acoustic propagation properties in seawater and underwater acoustic channel representation.

The application of OFDM for high speed data transmission in underwater scenario has been studied by Jeong-woo Han, *et al.*[66]. Underwater channel simulation modeling and experimentation has been performed and OFDM exhibits better performances than QPSK. Discrete

Cosine Transform based Orthogonal Frequency Division Multiplexing (DCT-OFDM) has been proposed for underwater acoustic communication by Prashant Kumar *et al.* [67]. This system provides higher peak to average power ratio (PAPR) reduction as well as achieve better noise immunity and hence better BER performance than standard OFDM has been achieved, while maintaining a low implementation cost.

M. C. Domingo [68] presents a detailed survey on ray-theory-based multipath Rayleigh underwater channel models for underwater wireless communication and outlines the research challenges for an efficient communication in this environment which are valid for shallow or deep waters, based on acoustic propagation physics which captures different propagation paths of sound in underwater and considers all the effects of shadow zones, multipath fading, operating frequency, depth and water temperature. Further simulations have been carried out to study the bit-error-rate effects and the maximum internode distances for different networks and depths, considering a 16-QAM modulation scheme with OFDM as the multicarrier transmission technique. Ghorpade *et al.* [71] introduce the design of OFDM transceiver system, simulated in MATLAB.

Bellhop beam tracing has been used to model two regions in the north of Arabian Sea by Rehan Khan *et al.* [72]. Multipath with delay channel model has been obtained using the Bellhop ray tracing algorithm with random Doppler shifts on each block and also in the complete OFDM packet. Simulation results yielded low BER even in high relative speed between transmitter and receiver. Neha Pathak [74] also discusses the design and implementation of an OFDM modem used in wireless communication.

Guoqing Zhou *et al.* [75] present an adaptive transmission technique to adapt the channel fluctuations based on a statistical channel

model. Simulation analysis shows that the data rate can be optimized allowing the transmit power to vary with SNR, subject to an average power constraint and also establishes that the data rate can be increased adaptively. Under the optimum data rate, the MATLAB Simulink of underwater acoustic channel QPSK communication system gives a benchmark for the experiments in the open ocean. The design aspects of adaptive modulation based on orthogonal frequency-division multiplexing (OFDM) for underwater acoustic communications are explored by Andreja Radosevic *et al.* [76] and its performance using real-time *in-situ* experiments have been studied.

Implementation and design of the real-time underwater speech communication system based on orthogonal frequency division multiplexing (OFDM) technology, was used to compress the speech coding by Lu Yin *et al.* [78]. The feasibility of underwater acoustic speech communication system based on OFDM technology has been experimentally proved. Baosheng Li *et al.* [80] propose an approach to mitigate the Doppler effect and focus on zero-padded orthogonal frequency-division multiplexing (OFDM) to minimize the transmission power. Null subcarriers have been used to facilitate Doppler compensation while the pilot subcarriers carry out the channel estimation. The data from two shallow-water experiments near Woods Hole, Massachusetts, has been used to demonstrate the receiver performance. Acceptable validation results have been obtained even when the transmitter and the receiver are moving.

Xuefei Ma *et al.* [81] present underwater acoustic communication using OFDM. An LMS adaptive equalizer has been used for equalization. Simulation and pool trial show that the method has rapid convergence and the system has good performance. This approach is very attractive for high

speed implementation of an underwater acoustic OFDM receiver. The effectiveness of different spread OFDM techniques with transmit diversity used for underwater acoustic communications has been compared by Prashant Kumar *et al.* [82]. Spreading by Walsh-Hadamard codes, discrete Fourier transform, discrete cosine transform, etc. have been combined with the application of space-time and space-frequency transmit diversity in OFDM for underwater acoustic communication.

The performance of differentially encoded quadrature phase shift keying (DQPSK) modulated orthogonal frequency division multiplexing (OFDM) for underwater acoustic communication has been evaluated by Prashant Kumar *et al.* [83]. The combination of OFDM and the non-coherent detection scheme maintains the receiver design simple, reliable and spectrally efficient. The performance of orthogonal frequency division multiplexing (OFDM) with $\pi/4$ -differential quadrature phase shift keying modulation over underwater acoustic (UWA) channels has also been studied by Prashant Kumar *et al.* [84]. This result in spectrally efficient, reliable and simple receiver design and it has been shown that with a pair of hydrophones for reception and maximum-ratio combining (MRC) technique, considerably low bit-error-rate (BER) at practical signal-to-noise ratio (SNR) value can be achieved.

Suzi Seroja Sarnin *et al.* [86] describe performance evaluation of phase shift keying modulation technique such as Binary Phase Shift Keying (BPSK) and QPSK using error correcting code. Three error correcting codes - Bose-Chaudhuri-Hocquenghem (BCH), Cyclic as well as Hamming codes were used to compute the bit-error-rate in an AWGN channel. It has been concluded that BCH codes demonstrate the best performance compared to Hamming and Cyclic codes for both BPSK and QPSK.

The gain of the BCH code has been investigated by applying it to BPSK modulation scheme in symmetric AWGN channel by Mahmoud A. Smadi [87]. The bit error probability of coded (63, 36) BCH system has been evaluated and compared with the performance of un-coded system. The price to be paid for this performance improvement is the higher transmission data rate and hence higher transmission bandwidth. Jitendra Prakash Shreemukh *et al.* [88] proposed some selection criteria for the puncturing vector to achieve excellent performance in terms of BER and offer useful guidelines for the design of puncturing vector based on simulation results. The performance of turbo codes for different puncturing location for two parity branches has also been studied.

Jyoti Kataria *et al.* [89] compare the Coded Orthogonal Frequency Division Multiplexing (COFDM) with OFDM and the study shows that COFDM outperforms the OFDM with respect to reliable transmission, BER performance and bandwidth efficiency. Ch Sekhararao K. *et al.* [90] present a novel combination of Coding techniques and OFDM to combat impulsive noise. The simulation results show that, in the presence of impulsive noise, convolutional coding improves the performance of OFDM based Power Line Communication systems significantly.

Fernando H. Gregorio [91] presents coding and interleaving techniques applied in WLAN systems. An overview of coding, decoding and puncturing of convolutional codes as well as time and frequency interleaving have been presented. The improvement in performance has been measured in terms of bit-error-rate and packet error rates. Mandar Chitre *et al.* [92] tested coded OFDM in a very shallow water channel in Singapore waters. The results show that it is a promising technique for use in very shallow, warm water channels.

2.5 Synchronization Issues in OFDM

Due to the unpredictable practical conditions, the receiver in OFDM may sample a new frame at the incorrect time instant, which is called Symbol Time Offset (STO). Also, in practical situations, frequency mismatch between local oscillators at the transmitter and receiver or Doppler frequency shift can occur, leading to Carrier Frequency Offset (CFO) problems in OFDM which destroys orthogonality among the subcarriers leading to inter carrier interference. Hence, estimation of STO and CFO are very important and critical in any practical scenario. The effects of STO are studied and correspondingly W.Aziz *et al.* [93] have proposed different precautionary schemes in the receiver.

Praween Kumar Nishad *et al.* [94] present a basic useful technique for CFO estimation in OFDM over frequency selective fading channel. The performances of cyclic prefix (CP) based estimation, training symbol based estimation and pilot based methods are compared. Abdul Gani Abshir *et al.* [95] have examined the effects of CFO on the OFDM signals. The deterioration in bit-error-rate as well as the loss in Signal to Noise Ratio due to the CFO for an OFDM system have been investigated. The paper also presents comparative analysis between CP based estimation technique, Symbol based estimation method and Pilot Tone based estimation schemes. CFO and its effects have been analysed in detail for OFDM symbols and the techniques to estimate CFO are also described in detail by W.Aziz *et al.* [96]. The estimation techniques cover the time and frequency domains for OFDM system.

Mahmood A.K. Abdulsattar *et al.* [97] describe real-time implementation of a timing and frequency synchronization for OFDM system using MATLAB software Simulink and a DSP processor. The

practical results and performance evaluation of the synchronization algorithms in OFDM system are presented and discussed. The results are plotted for different offsets of CFO and STO at different values of signal to noise ratio. Ferdinand Classen *et al.* [101] consider the problem of carrier synchronization of OFDM systems in the presence of a substantial frequency offset. The two-stage structure considered in this paper is able to cope with frequency offsets in the order of multiples of the spacing between subchannels. This ensures high-speed synchronization at a low implementation effort.

Seung Hee Han *et al.* [102] describes some of the important peak to average power ratio reduction techniques for multicarrier transmission including amplitude clipping and filtering, coding, partial transmit sequence, selected mapping, interleaving, tone reservation, tone injection, and active constellation extension. Single Carrier Frequency Division Multiple Access (SC-FDMA) is currently adopted as the Long Term Evolution standard for the uplink due to its high data rate and low PAPR. In SC-FDMA, two methods of choosing subcarriers for transmission are used-distributed using Interleaved (IFDMA) and localized (LFDMA). In [103], the PAPR for LFDMA and IFDMA techniques are simulated and compared by Mohammed Melood *et al.*

2.6 Channel Estimation

Evaluation of new communication schemes and devices under realistic conditions in the open ocean is very expensive and time-consuming, as it involves ship time, diver resources and other related components. Hence various channel modeling schemes are widely used before realizing an implementable system. Studies of the channel modeling efforts reported by various researchers are included in this section.

A survey of the characteristics of all existing seawaters has been made by C. C. Leroy [104], covering all the previous methods and formulated two equations for the speed of sound in the waters, one of which fits with Wilson's second equation for seawater to within 0.1m/sec in the domain described, and the other fits with the Wilson's corresponding data with a better accuracy than does Wilson's equation.

Michael B. Porter *et al.* [105] describes Gaussian beam tracing for computing ocean acoustic fields. The method of Gaussian beam tracing has recently received a great deal of attention in the seismological community. Compared to standard ray tracing, the method has the advantage of being free of certain ray-tracing artifacts such as perfect shadows and infinitely high energy at caustics. BELLHOP [106 – 107] is a beam tracing model for predicting acoustic pressure fields in ocean environments. The beam tracing structure leads to a particularly simple algorithm. BELLHOP can produce a variety of useful outputs including transmission loss, eigen rays, arrivals and the received time-series.

Peter King *et al.* [108], present the development of an improved channel model based on the BELLHOP beam tracing program. The BELLHOP program provides path computations that connect a given source-receiver pair which are dependent on a description of the environment provided by the user. This model is an efficient ray tracing tool for performing two-dimensional analysis of an ocean environment. The BELLHOP program was selected because of its efficacy and accuracy in generating acoustic data sets consisting of amplitude, phase, and delay for each path between a given transmitter-receiver pair. Lars Michael Wolff, *et al.* [109], use channel impulse responses (CIRs) generated by the BELLHOP ray tracing model to simulate multipath propagation. The CIRs for fixed nodes are post-processed to simulate mobile nodes.

Modeling and Simulation plays an important role in understanding the performance of underwater acoustic sensor networks before its implementation, as the design, development and testing of actual system turns out to be expensive and time consuming. The research community working in the underwater acoustic network area is faced with limited options as far as simulation tools are concerned. Sumi. A. Samad [112] *et al.* discuss some details of the underwater communication model generally used to accurately model the behavior of underwater communication channel.

Hou Pin Yoong *et al.* [113] carried out a study on modeling of underwater wireless communication with a detailed model on the channel characteristic, environmental noise, signal to noise ratio and the Doppler Effect. Simulation of a modified Rayleigh fading communication channel model has been presented by Mario A. Muñoz *et al.* [114], which takes into account the boundary reflections and Doppler shift effects. The statistical characteristics of underwater acoustic channels using experimental measurements have been analyzed by Jesse Cross [115]. CIRs are estimated in the time domain using a least squares method with sliding windows applied to the received data. The experimental results demonstrate that underwater channels often offer poorer communication quality than Rayleigh fading channels.

Xueyi Geng *et al.* [117], reviewed and discussed the properties of underwater acoustic channels. Based on some experimental results and analytical considerations, the limitations of the Rayleigh fading channel model commonly used to model underwater acoustic channels has been pointed out and a novel underwater acoustic communication channel model simulator has been proposed, based on the concept of eigen paths that

consist of one dominant component and several sub-eigen path components.

An Underwater Acoustic Signals Separation method based on prior information about the Channel Impulse Response (CIR) has been attempted by S. Bonnifay *et al.* [118]. Using a sound speed profile measured in real world environment, the channel impulse response of the ocean is estimated with normal mode theory and the ray tracing method. This preliminary work has shown that prior information on the transmission channel can lead to success in underwater signal separation in real world situations.

Milica Stojanovic [119] discusses the effects of attenuation, noise, multipath propagation and the Doppler effects in underwater acoustic communication scenario. Muhammad Ali Raza [120] models impulse response of a time-varying acoustic channel as a superposition of multiple propagation paths where each path is characterized by a frequency dependent path loss. Later, an estimation model based on adaptive filtering has been proposed, to model the impulse response of the underwater acoustic communication channel.

A statistical model was developed for underwater acoustic channels by Parastoo Qarabaqi *et al.* [122] that take into account physical aspects of acoustic propagation as well as the effects of inevitable random channel variations. John Heidemann *et al.* [123] examine the main approaches and challenges in the design and implementation of underwater wireless sensor networks. The key applications and the main phenomena related to acoustic propagation have also been summarized.

In [125], M. S. Chavan *et al.* proposed multipath fading channel simulation model for wireless communication. The model has been tested for sine wave and complex wave inputs. The effects of noise on fading and scattering property of the channel have been validated. The performance of

various channel models: Rayleigh model, AWGN channel model and Rician model have been evaluated, analyzed and compared. In [126], Joaquín Aparicio *et al.* presented an underwater acoustic channel model based on ray tracing. This model takes into account the common phenomena such as sound speed profiles and transmission loss. The model has also been used to simulate the sound propagation for a relative positioning system, which measures the surface current, yielding acceptable surface current estimates.

Adaptive filters have been used in many diverse applications in the past. An investigation of some of the adaptive filters and their possible applications are addressed here. Adaptive equalization removes the effect of the channel and allows subsequent demodulation of the signal. Bernard Widrow *et al.* [127] introduced the concept of adaptation as a property or characteristic of certain systems in engineering and adaptive linear combiner, which is the simplest and most widely used adaptive structure. Simon Haykin [128] examines the mathematical theory behind various linear adaptive filters. The adaptive filter is described as a device that is self-configuring one, which relies on a recursive algorithm for its operation that makes it possible for the filter to perform satisfactorily in an environment where complete knowledge of the relevant signal characteristics is not available. Yilun Chen *et al.* [129] propose a new approach to adaptive system identification when the system model is sparse. The approach applies ℓ_1 relaxation, common in compressive sensing, to improve the performance of LMS type adaptive methods. In order to improve the performance of LMS based system identification of sparse systems, a new adaptive algorithm has been proposed by Yuantao Gu *et al.* [130] which utilizes the sparsity property of such systems. A general approximation approach on ℓ_0 norm has been proposed and

integrated into the cost function of the LMS algorithm. The simulations demonstrate that the proposed algorithm can effectively improve the performance of LMS-based identification algorithms in sparse systems.

The function of channel estimation is to form an estimate of the amplitude and phase shift caused by the wireless channel. The estimated channel state information can be used in the receiver for undoing the channel effects. The following papers deals with estimation of channel which is critical in proper signal recovery.

Ons Benrhouma *et al.* [131] estimate the underwater acoustic channel and the method of channel estimation have been validated through experiments. A statistical study of the estimated underwater channel such as the number of paths, the attenuation of the principal path and the delay between the principal and the secondary paths have been demonstrated. Another method for estimating the underwater acoustic channel has been proposed by Oe-Hyung Lee *et al.* [132], which uses a probe signal. The underwater channel impulse responses are estimated and the received data signals are convolved with the time-reversed channel impulse responses.

The Channel Capacity of a point-to-point communication link in an underwater acoustic channel has been computed by B. Jagdishwar Rao *et al.* [133]. The approach takes into account the effects of various acoustic propagation models. A comparative assessment of the influence of various acoustic transmission loss models on the acoustic bandwidth and the capacity has been consolidated. Nina Wang *et al.* [134] propose a novel sparse channel estimation method with compressive sensing using CoSaMP algorithm for sparse multipath multicarrier underwater acoustic communication systems. Simulation results confirm that the proposed method offer high spectral efficiency, good performance guarantee and low computational complexity.

Channels with a sparse impulse response arise in a number of communication applications. Exploiting the sparsity of the channel, Shane F. Cotter *et al.* [135] show how an estimate of the channel may be obtained using a matching pursuit (MP) algorithm. This estimate has been compared with the least squares (LS) channel estimate. Among these sparse channel estimates, the MP estimate is computationally much simpler to implement and a shorter training sequence is required to form an accurate channel estimate leading to higher information throughput. C. Qi *et al.* [136] attempted underwater acoustic channel estimation based on sparse recovery. The underwater acoustic communication system under consideration employs orthogonal frequency division multiplexing (OFDM) and receiver preprocessing to compensate for the Doppler effect before channel estimation. The authors propose enhancements to the sparse recovery-based underwater acoustic channel estimator by exploiting the recursive least-squares algorithm for channel tracking. Moreover the authors propose a scheme to optimize the pilot placement over the OFDM subcarriers based on the discrete stochastic approximations.

It has been shown that sparse channel estimation, implemented with orthogonal matching pursuit (OMP) and basis pursuit (BP) algorithms, has impressive performance gains over alternatives that do not take advantage of the channel sparsity, for underwater acoustic communications. J.-Z. Huang *et al.* [138] compare the performance and complexity of three popular BP algorithms, namely *l1_ls*, *SpaRSA*, and *YALL1*, using both simulation and experimental data for underwater OFDM systems with both single and multiple transmitters. It was found that all BP solvers achieve similar block-error-rate performance, considerably outperforming OMP.

Sichuan Guo *et al.* [139] propose a new compressive sensing based channel estimation method with block-by-block channel tracking for

underwater acoustic communication. Compared with conventional channel estimation algorithms, the proposed method efficiently exploits the sparsity of the underwater acoustic channel and improves the channel tracking capability of underwater acoustic communication system. In [140], Guan Gui *et al.* introduce a novel channel estimation strategy using compressive sampling matching pursuit (CoSaMP) algorithm which combines the greedy algorithm with the convex program method. The effectiveness of the proposed algorithm has been confirmed through comparisons with the existing methods. It is seen that, when compared with the existing algorithms, this method is bandwidth efficient as well as computationally efficient.

Various efficient pilot based channel estimation schemes for OFDM systems have been investigated and compared by Srishtansh Pathak *et al.* [142]. Two major types of pilot arrangement such as block type and comb-type pilot have been focused employing LS (Least Squares) and MMSE (Minimum Mean Square Error) channel estimators. Block type pilot subcarriers are suitable especially for slow-fading radio channels whereas comb type pilots provide better resistance to fast fading channels. A full review of block-type and comb-type pilot based channel estimation has also been proposed by Sinem Coleri *et al.* [143]. The simulation results show that comb-type pilot based channel estimation with low-pass interpolation performs the best among all channel estimation algorithms. OFDM pilot-aided underwater acoustic channel estimation approaches, which involve in block-type pilot, comb-type pilot and grid-type pilots are investigated by Thomas Pedersen *et al.* [144]. Simulation revealed that based on different channel conditions, pilot types which give best performance has to be adopted.

Underwater acoustic channels have been regarded significantly different from wireless radio channels, due to their unique characteristics such as large temporal variations, abundance of transmission paths, etc. Shengli Zhou *et al.* [145] survey the challenges in underwater acoustic communications for orthogonal frequency division multiplexing and underwater acoustic channel estimation for OFDM in both time-invariant as well as time-varying environments has been performed. The underwater acoustic channel is well known to consist of sparsely distributed propagation paths and the channel sparsity can be exploited to reduce the number of unknown parameters to estimate.

The channel estimation in OFDM and its implementation in MATLAB using pilot based block type channel estimation techniques by LS and MMSE algorithms have been discussed by Sajjad Ahmed Ghauri *et al.* [146]. The paper starts with comparisons of OFDM using BPSK and QPSK on different channels, followed by modeling the LS and MMSE estimators. The results of different simulations have been compared and it has been established that the LS algorithm gives less complexity but the MMSE provides comparatively better results.

Various channel estimation techniques based on pilot arrangement with the communication system that uses QPSK and 16-QAM to transmit information using OFDM over multipath Rayleigh fading channel have been investigated and compared by Sanjay Kumar Khadagade *et al.* [147] for block type and comb type pilot arrangements and the bit-error-rate performance has been considered as the performance index in all the studies.

The channel estimation techniques for OFDM systems based on pilot arrangement are investigated by Sinem Coleri *et al.* [149]. The channel estimation based on comb type pilot arrangement has been studied

using different algorithms for estimating channel at pilot frequencies and interpolating the channel behavior. The estimation of channel at pilot frequencies is based on least squares and least mean squares approaches. The channel estimation based on block type pilot arrangement has also been performed. The performances of all the schemes have been compared by measuring the bit-error-rate with 16-QAM, QPSK, DQPSK and BPSK as the modulation schemes, and multi-path Rayleigh fading channels as channel model.

The computational complexity required in the channel estimation plays an important role in underwater acoustic communications (UAC) with orthogonal frequency duplex access (OFDM), especially when the channel is sparse. Chunguo Li *et al.* [150] develop an algorithm to carry out the orthogonal matching pursuit (OMP) for the sparse channel estimation based on the compressive sensing, where the goal is to obtain the minimum computational complexity. Numerical simulations are demonstrated that the proposed algorithm achieves the remarkable gain of the computational complexity compared to the existing algorithm.

2.7 Multiple-Input Multiple-Output Systems

Multiple Input Multiple Output (MIMO) transmission system is one of the recent and the most promising area of the smart antenna technology which uses multiple antennas in the transmitter and the receiver side and is currently followed for high-rate wireless communication. This section discusses some of the papers on Space-Time Block Coding (STBC), MIMO and their applications. A simple two-branch transmit diversity scheme has been presented by Siavash M. Alamouti [151]. Using two transmitter and one receiver antenna, the scheme provides the same diversity order as maximal-ratio receiver combining with one transmit antenna and two

receive antennas. It is also shown that the scheme may easily be generalized to two transmit antennas and M receive antennas.

The viability of using space-time processing methods to improve the robustness and/or capacity of underwater acoustic communication links has been tested experimentally by R.F.Ormondroyd *et al.* [152]. Alamouti space-time coding has also been investigated in conjunction with OFDM modulation for high-rate underwater acoustic communications over time varying channels by Baosheng Li *et al.* [153]. Performance has been demonstrated using experimental data transmitted in a 10kHz bandwidth over a 1km shallow water channel south of the Martha's Vineyard island in New England. The two-transmitter Alamouti scheme showed improved performance over the same-rate single-transmitter scheme.

The performance analysis of Alamouti STBC has been compared with SISO performance by Yamini Devlal *et al.* [155]. The paper includes study of SISO system, STBC, Alamouti STBC theory and its mathematical expressions. The results for each of the systems considered, SISO, 2x1 and 2x2 Alamouti STBC have also been plotted and 2x2 Alamouti STBC was found to have the smallest BER values. MIMO techniques for increasing the data rates in the area of underwater communications have been performed by Byung-Chul Gwun *et al.* [156]. The advantage of MIMO techniques is to increase the channel capacity without additional transmit power.

2.8 Summary

An attempt has been made in this chapter to present a state-of-the-art literature in the topic covered by the thesis, *the sparse signal processing* as well as *underwater acoustic communication*. Various compressive sensing reconstruction algorithms, problems in underwater acoustic

communication, modulation and coding schemes used for undersea links, underwater channel estimation, multicarrier modulation techniques, various synchronization issues, etc. have been included in the review of the papers reported in open literature.

CHAPTER 3

METHODOLOGY

Compressive sensing has been evolved as a very useful technique for sparse reconstruction of signals that are sampled at sub-Nyquist rates. Compressive sensing helps to reconstruct the signals from fewer linear projections of the sparse signal. This chapter presents a brief overview of the proposed method for sparsification and recovery. Undersea acoustic links have applications in pollution monitoring, environmental data collection, offshore and coastal surveillance, etc. Orthogonal Frequency Division Multiplexing (OFDM), which is a multicarrier modulation technique, is widely employed in undersea acoustic applications because of its numerous advantages. OFDM requires an estimate of the channel parameters at the receiver for undoing the channel effects. The sparsity of the channel impulse response for undersea links can be used for estimating the channel characteristics. A brief overview of the dictionary based sparse channel estimation is also included in this chapter.

The Nyquist sampling theorem specifies that in order to avoid information loss when capturing a signal, it must be sampled at least twice the maximum signal frequency. In many applications, the Nyquist rate is so high that too many samples result, making compression a necessity prior to storage or transmission. A new method called “Compressive Sensing” can be used to capture and represent compressible signals at a rate significantly below the Nyquist rate. Compressive sensing has applications in signal processing, in areas such as coding, signal level enhancement, source separation, etc. For example, a sparse representation has only a few

non-zero values, which necessitates encoding only these values for transmission and storage.

3.1 Background

Underwater channel is known to be bandwidth limited due to sound attenuation by sea water and interaction with ocean surface and bottom. Table 3.1 shows the available bandwidth for different ranges in underwater acoustic channels [2]. If the information could be stored or transmitted by fewer numbers of samples than the Nyquist rate, it would have been advantageous in underwater acoustic communication scenario. The method called compressive sensing can be used to represent and reconstruct certain classes of signals at a rate below the Nyquist rate.

Traditional methods make use of signal representations conforming to the sampling theorem that makes compression a necessity before storage or transmission in situations where the memory space and bandwidth are scarce resources. A signal with only a few non zero coefficients in any transform domain is called a sparse signal and a signal which can be approximated by a few non zero coefficients in any transform domain is called a compressible signal. For sparse or compressible signals, the compressive sensing technology is a paradigm shift.

Table 3.1 Available Bandwidth for different ranges in Underwater Acoustic Channels

	Range [km]	Bandwidth [kHz]
Very long	1000	<1
Long	10–100	2–5
Medium	1–10	≈10
Short	0.1–1	20–50
Very short	<0.1	>100

The recovery of the signal is carried out by using certain optimization techniques. The recovery becomes more difficult when the signal to be compressed is corrupted with noise. For resorting to compressive sensing, it is required that the compression and reconstruction techniques should be capable of transforming the data into a suitable representation domain. Many natural and manmade signals have underlying sparse representations in some basis functions. Basis functions like Discrete Fourier Transform, Discrete Cosine Transform, Wavelets, etc. can be used, depending on the information and type of the signal.

A discrete time signal $x(n)$ with N elements, can be viewed as an $N \times 1$ vector with $n=1, 2, \dots, N$. Consider a basis function ψ , which provides K sparse representations (*i.e.*, $\|\mathbf{x}\|_0 \leq K$) of $x(n)$, with $K < N$. $x(n)$ can be represented in the matrix form as $\mathbf{x} = \psi \mathbf{f}$, where ψ is the basis matrix of order $N \times N$ and \mathbf{f} is the weighting coefficient vector of order $N \times 1$. The vector $\mathbf{y} = \phi \mathbf{x}$, where ϕ is the measurement matrix of order $M \times N$ with $M < N$, is the linear projection of the signal $x(n)$. The matrix ϕ is often referred to as a dictionary [35]. The vector \mathbf{y} preserves the information content of the signal, while being much smaller than the signal, effectively constituting a compression. Figure 3.1 illustrates the concept of compressive sensing.

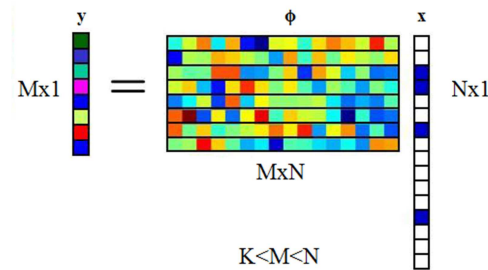


Fig. 3.1 Concept of compressive sensing

Recovering the original signal \mathbf{x} requires solving an underdetermined system of simultaneous linear equations. Given the knowledge that \mathbf{x} is sparse, the system regenerates the actual signal from the acquired small number of non-adaptive linear projections of the signal. Figure 3.2 shows a basic model of compressive sensing.

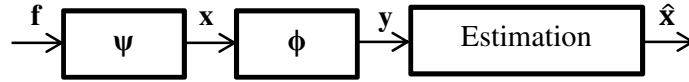


Fig. 3.2 Block diagram representation of compressive sensing

To recover the sparse signal, the condition that should be satisfied is

$$\text{minimize } \|\mathbf{x}\|_0 \text{ subject to } \mathbf{y} = \Phi \mathbf{x}, \quad (3.1)$$

where $\|\mathbf{x}\|_0$ is the number of non-zero elements of \mathbf{x} , which is also called ℓ_0 norm. Computing ℓ_0 norm is an NP-hard problem [33] which led to making use of the basis pursuit relaxation or convex optimization [47]. Such approaches have led to the establishment of an $\ell_1 - \ell_0$ equivalence [61] and hence, (3.1) can be represented as,

$$\text{minimize } \|\mathbf{x}\|_1 \text{ subject to } \mathbf{y} = \Phi \mathbf{x}, \quad (3.2)$$

where $\|\mathbf{x}\|_1$ is the sum of the absolute values of the elements in \mathbf{x} , which is also being referred to as the ℓ_1 -norm ($\|\mathbf{x}\|_1 = \sum_i |x_i|$). In the case of signals, which are contaminated with noise, the equality constraint has been relaxed to allow some error tolerance $\epsilon \geq 0$ [35], such that

$$\text{minimize } \|\mathbf{x}\|_1 \text{ subject to } \|\Phi \mathbf{x} - \mathbf{y}\|_2 \leq \epsilon, \quad (3.3)$$

will help to reconstruct \mathbf{x} with insignificant error [27],[45].

3.2 Compressive Sensing Algorithms

Solution to the sparse recovery problem can be achieved with *Relaxation Methods* or with *Greedy Algorithms*. Relaxation methods

replace the original sparse recovery problem with a convex optimization problem, whereas Greedy Algorithms focus on finding the non-zero values of \mathbf{x} at their respective locations, which are determined iteratively. ℓ_1 -norm based sparse recovery problems can be solved using a variety of existing solvers such as ℓ_1 -magic, YALL1, l1_ls, etc. ℓ_1 -magic involves recovery of a sparse vector \mathbf{x} from a small number of linear measurements $\mathbf{y}=\Phi\mathbf{x}$ or $\mathbf{y}=\Phi\mathbf{x}+\mathbf{e}$ using primal-dual method [55], where \mathbf{e} is the measurement noise. YALL1 is another solver that can be applied to ℓ_1 -optimization, which is a collection of fast ℓ_1 -minimization algorithms based on the dual alternating direction method [58-59]. It is a first order primal-dual algorithm, as it explicitly updates both primal and dual variables at every iteration. l1_ls is a specialized interior-point method [56] that uses the preconditioned conjugate gradients algorithm to compute the search direction. CVX [60, 63] is an effective software for finding solutions for complex convex optimization problems, including non-differentiable functions, such as ℓ_1 -norms.

Greedy Algorithms include Orthogonal Matching Pursuit (OMP), Compressive Sampling Matching Pursuit (CoSaMP), etc. Orthogonal Matching Pursuit, which is one of the earliest methods for sparse approximation, provides simple and fast implementation [37]. It is an iterative algorithm that selects at each step the dictionary element best correlated with the residual part of the signal [36]. New approximation is generated by projecting the signal on to the dictionary elements that have already been selected and solving a least squares problem. The residual is updated in every iteration. The number of iterations can be made equal to the sparsity of the signal or the stopping criteria can be based on the magnitude of the residual [35]. Compressive Sampling Matching Pursuit [40] which selects multiple columns per iteration [35], is an enhancement

to OMP. Each iteration of CoSaMP reduces the error in the current signal approximation.

3.3 Sparsification and Recovery

In view of the overwhelming limitations of the existing compressive sensing algorithms, in terms of computational complexities, response time, overall reconstruction capabilities, etc., there has been a constant search for high performance, more capable and reliable techniques for the sparsification and recovery of audio, speech and natural images. Hence, a new method has been proposed in this thesis which involves padding the matrix ϕ during compression phase for the purpose of solving the underdetermined system of simultaneous linear equations, followed by least mean square based adaptation during the reconstruction phase. The solution is obtained with the help of a Moore Penrose inverse matrix, which is then corrected using iterative least mean square based adaptation. Figure 3.3 shows the block diagram of the proposed technique.

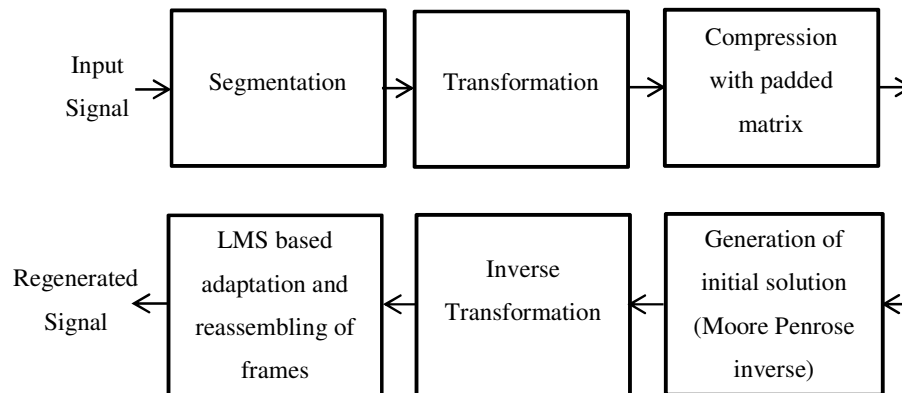


Fig. 3.3 Block diagram of the proposed matrix padding technique

3.4 Propagation Theory

The propagation of sound in a medium is described mathematically by solving the wave equation using the appropriate boundary and medium conditions for a particular condition. There are two approaches [15] for solving this equation, wave theory and ray theory. Ray theory (Ray acoustics) postulates wavefronts and the existence of rays, which indicate where the sound emanating from the source is being sent. It does not provide a good solution under conditions where the radius of curvature of the rays or the pressure amplitude changes significantly over the distance of a wavelength. Hence, ray theory is restricted to high frequencies or short wavelengths.

3.5 Modulation techniques for Undersea Acoustic Links

The modulation techniques widely used in underwater acoustic communication include frequency hopped FSK, direct sequence spread spectrum, single carrier transmission and multicarrier modulation.

In FSK modulation, information bits are used to select the carrier frequencies of the transmitted signal. This scheme does not require the estimation of the channel and is robust to channel variations. The guard bands help to avoid interference caused by frequency-spreading while the guard intervals help to avoid interference caused by time-spreading. However, the bandwidth efficiency is significantly low.

In Direct Sequence Spread Spectrum, a narrow band waveform is spread to a large bandwidth before transmission by multiplying each symbol with a spreading code. Multiple arrivals at the receiver can be handled with a de-spreading operation. This technique necessitates the need for channel estimation and tracking.

One major step towards high data rate communication is single carrier transmission of information symbols from constellations such as phase-shift-keying (PSK) and quadrature-amplitude-modulation (QAM). The channel introduces inter symbol interference (ISI) due to multipath. Channel equalization is also needed.

Multicarrier modulation is a technique for transmitting data by sending the data over multiple carriers. An advantage of multicarrier systems is that they are less susceptible to interference than a single carrier system as interference may only affect a small number of the carriers. Frequency-division multiplexing (FDM) and Orthogonal Frequency Division Multiplexing (OFDM) come under multicarrier modulation methods. FDM approach splits a large bandwidth into non-overlapping bands and guard bands are inserted between neighboring subbands. Band pass filtering can be used to separate the signal from different subbands. OFDM is also an FDM approach with overlapping subbands, leading to better spectral efficiency.

3.6 Orthogonal Frequency Division Multiplexing

Underwater channel is too complex compared to the terrestrial radio channels leading to the requirement of sophisticated equalization techniques at the receiver. Recently, Orthogonal Frequency Division Multiplexing (OFDM), which is used in several terrestrial radio communications standards, is also considered for underwater acoustic communications due to its high data transmission rate, efficient spectral utilization and ability to cope up with the multipath interference. OFDM has been applied in broadband wireless radio applications, including digital audio/video broadcasting, wireless local area networks and fourth generation cellular networks.

Coded OFDM is a form of OFDM where error correction mechanisms have been incorporated into the signal. This technique uses multiple orthogonal sub-carriers to carry the data along with the error correcting mechanisms, which adds extra bits at transmitters to recover many subcarriers affected by fading. Channel coding schemes include *block codes* in which, the input bit stream is segmented into blocks for adding redundant bits and *convolutional codes*, which encodes the bit stream continuously without any segmentation. Coding offers better security and interleaving reduces the effect of burst errors. Hence, OFDM combined with coding and interleaving, is a good choice for complex as well as bursty channels like the undersea acoustic links.

3.6.1 Advantages of OFDM

OFDM, which can be efficiently implemented using Fast Fourier Transform (FFT), has been used in many wired as well as wireless systems because of the following advantages:

- high spectral efficiency because of the use of overlapping subcarriers
- eliminates ISI with a guard band
- simpler channel equalization
- computationally efficient, as it uses FFT techniques to implement modulation and demodulation functions
- eliminates Inter Carrier Interference (ICI) by the use of orthogonal subcarriers

OFDM has gained a significant importance in the wireless market. The combination of high spectral efficiency and its resilience to interference due to multipath effects makes it a suitable candidate for undersea acoustic communication scenario.

3.6.2 Disadvantages of OFDM

The disadvantages of OFDM are

- Cyclic Prefix Overhead - A cyclic prefix at least as long as the channel response must be attached to each OFDM symbol to prevent the interference between symbols.
- Sensitivity to frequency synchronization problems - Frequency synchronization problems destroy the orthogonality between subcarriers, resulting in inter carrier interference and severe degradation in performance.
- High peak-to-average power - Peak to average power ratio (PAPR) in an OFDM system is usually high. Because of IFFT operation, data symbols across subcarriers add up to produce a high peak value OFDM symbol.

Due to the numerous advantages offered by OFDM, this thesis considers the application of coded OFDM with and without interleaving for an undersea acoustic link.

3.7 Channel Estimation

In OFDM, the transmitter modulates the message bits into symbols, assigns them to various sub carriers and sends them through the channel, which distorts the signal. For undoing the channel effects and demodulating the signal with reasonable accuracy, OFDM needs an estimate of the channel parameters. Channel estimation is performed by inserting pilots [149] into the subcarriers of an OFDM symbol. The transmitted signal can then be reconstructed by a single tap equalizer at the receiver using the estimated channel.

3.7.1 Channel Estimation techniques in use

The underwater channel causes spreading, attenuation, absorption, etc. of the transmitted signals and hence, the received OFDM signals will be distorted. For proper recovery of the transmitted data, the channel effect has to be estimated and compensated in the receiver. The channel characteristics can be estimated by sending symbols known to both the transmitter and receiver. Even though this approach provides acceptable performances, the transmission overhead is high, due to the requirement of pilot tones in addition to data symbols.

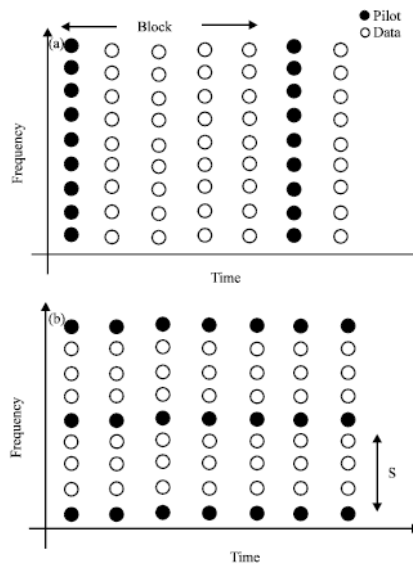


Fig. 3.4 Pilot arrangement (a) block type (b) comb type

Pilots can be inserted into all the subcarriers of an OFDM symbol periodically, leading to block type channel estimation. Block type pilots are suitable for a slow fading channel where the channel transfer function is fairly a constant over the period of transmission of a few OFDM symbols. Thus, the pilots are assigned to a particular OFDM block, which is sent periodically in time-domain. In Comb type channel estimation, pilots are

inserted into each OFDM symbol, at periodically located subcarriers and the comb type pilots are suitable for rapidly fading channels. Underwater channels are fast time-varying and as a result, comb type pilots are more appropriate for realising undersea acoustic links. Block type and comb type pilot arrangements are illustrated in Figure 3.4.

The traditional channel estimation methods [143] include Least Squares (LS) and minimum mean square error (MMSE) estimations. If S_p is the transmitted set of pilots and Y_p , the set of received pilots, the LS channel estimate is given as

$$\hat{H}_{LS} = \frac{Y_p}{S_p}. \quad (3.4)$$

The LS estimate of the channel is susceptible to noise and offers poor performance. The MMSE method gives a better estimate of the channel. But, the BER performance of both LS and MMSE are substantially lower, as these methods do not consider the sparsity of the channel. Since underwater channel is characterized by sparse multipath, a method based on compressive sensing can be used which will give excellent BER performance compared to the LS and MMSE based estimations.

3.7.2 Dictionary based Sparse Channel Estimation Technique

When a signal is sparse in a known transform domain, compressive sensing (CS) helps to reconstruct it with much fewer samples than that required by the dimensions of this domain. A channel impulse response with only a few significant coefficients is referred to as a sparse channel. Underwater channel exhibits sparse impulse response. Compressive sensing promises to estimate such channels with much less pilot overhead or at higher accuracy with a constant number of pilots. A dictionary based sparse channel estimation has been presented in the thesis and the results

have been compared for various environmental conditions as well as for various number of pilots. The number of pilots to be chosen is a trade-off between channel estimation accuracy and bandwidth efficiency. Also, the data rates for an OFDM system for different number of pilots have been computed and compared, in this thesis.

3.8 *Summary*

A brief overview of a method proposed for sparsification and recovery has been presented in this chapter. The advantages of OFDM as well as need for channel estimation have also been outlined briefly. A brief overview of the dictionary based sparse channel estimation has also included in this chapter.

CHAPTER 4

SYSTEM MODEL

Compressive sensing recently gained immense attention due to the commendable advantages the technique offers in recovering certain target signals from a few random measurements. A new matrix padding technique, which converts the signal into sparse domain by applying Discrete Cosine Transform (DCT) and then compressing it using a modified measurement matrix, followed by an LMS based adaptation, has been proposed. Making use of this matrix padding technique, a computationally efficient sparse signal reconstruction has been achieved. Ambient noise is always present in the background of the undersea channel and the four basic sources that can model the ambient noise in the ocean are the noise effects due to turbulence, shipping, wind and thermal processes. A study of the variation of power spectral density of the overall ambient noise has been performed. Generation of channel impulse response using the Bellhop model utilizing the environmental data like the sound speed profile of the water column, the number of transceivers and their depths has also been described. OFDM is a good choice in underwater communication and this chapter describes the system models for normal OFDM as well as coded and interleaved OFDM, for the undersea acoustic links. Space-time block coding offers higher link reliability and its combination with coding and interleaving has been proposed in this thesis, for improving BER performances. A system model of an OFDM Receiver with Symbol Time Offset (STO) and Carrier Frequency Offset (CFO) estimation as well as channel parameter estimation has also been described in this chapter.

4.1 Background

Modeling and simulation are very important in studying the performance of undersea acoustic links, as the design, development and testing of the actual system is very expensive as well as time consuming. One of the biggest advantages of OFDM is the ability to convert channels into parallel narrowband subchannels, thus significantly simplifying the equalization at the receiver end. Coding, is a method of adding redundancy to information so that it can be transmitted over a noisy channel and subsequently be checked and corrected for errors that occurred in transmission at the receiving end. This chapter discusses the system models used for simulating OFDM as well as coded interleaved OFDM for undersea acoustic links. The diversity techniques improve the reliability of communication by using two or more communication channels with different characteristics. This chapter also discusses the system models for normal and coded STBC systems for an undersea acoustic link.

4.2 Sparse Signal Reconstruction

The bandwidth constraint of an undersea acoustic link makes compressive sensing very useful for underwater acoustic communication. Compressive sensing, which has gained immense importance nowadays, bases its signal recovery capabilities on the *sparsity* and *incoherence* of the processes involved. *Incoherence* addresses the idea that the signals that are spread out in the domain in which they are acquired, may have a sparse representation in another domain. For effective reconstruction, it is mandatory that ϕ has to be incoherent with ψ . *Incoherence* implies that the mutual coherence or the maximum magnitude of entries of the product matrix $\phi\psi$ is relatively small. Coherence is measured according to

$$\mu(\Phi, \Psi) = \sqrt{N} \max |\langle \phi_k, \psi_j \rangle| \quad 1 \leq k, j \leq N, \quad (4.1)$$

where Ψ is the basis matrix of order $N \times N$ and Φ is the measurement matrix of order $M \times N$ with $M < N$.

If Φ and Ψ contain correlated elements, the coherence is large [42]. Coherence takes the values in the range $[1, \sqrt{N}]$. The random measurement matrices are largely incoherent with any fixed basis function Ψ . Hence the sparsity basis function need not even be known, when designing the measurement system.

The necessary and sufficient condition for the sparse signals to be uniquely determined is that the matrix $\mathbf{A} = \Phi\Psi$ should satisfy the Restricted Isometry Property of order K [35], such that

$$(1 - \delta_K)\|\mathbf{x}\|_2^2 \leq \|\mathbf{Ax}\|_2^2 \leq (1 + \delta_K)\|\mathbf{x}\|_2^2, \quad (4.2)$$

where δ_K is the isometry constant of the matrix \mathbf{A} and K is the sparsity of the signal. Evaluating Restricted Isometry Property (RIP) for a given matrix being computationally complex, this property is normally verified by computing the coherence of the matrix Φ . Certain random matrices such as Gaussian and Bernoulli matrices are known to obey RIP [44].

A signal \mathbf{x} is compressible if its sorted coefficient magnitudes α_n in the transform domain Ψ observe a power law decay [45], according to which,

$$|\alpha_n| \leq Rn^{-q}, n=1, 2, \dots, \quad (4.3)$$

where R and q are constants with $q \geq 1$.

The general block diagram for Compressive Sensing and recovery is shown in Figure 4.1. The data from the wave file is segmented into frames followed by a transformation of the signal into suitable domain for making it sparse. It is then compressed with the help of a measurement matrix. These values can either be stored or transmitted, depending on the

requirement. These signals are reconstructed with the help of a compressing sensing algorithm, followed by transforming it to the domain in which the data is acquired and the frames are reassembled to regenerate the signal.

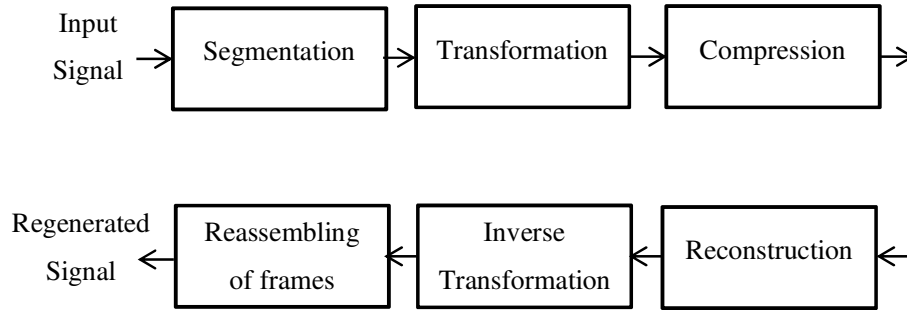


Fig. 4.1 Block Diagram for Compressive Sensing and Recovery

The signal has to be converted to the domain in which it is sparse, depending on the information and type of the signal. In the simulation studies, the domain chosen is Discrete Cosine Transform (DCT). Conversion of the audio signal to DCT results in a signal which is sparse with real valued coefficients, thus making the reconstruction easier [52]. The advantages of the Discrete Cosine Transform over Discrete Fourier Transform lies on the fact that it is real-valued, has better energy compaction and as such a sizeable fraction of the signal energy can be represented by a few initial coefficients. The DCT of a 1-D sequence $f(x)$ of length N is

$$c(u) = \alpha(u) \sum_{x=0}^{N-1} f(x) \cos \left[\frac{\pi(2x+1)u}{2N} \right], \quad (4.4)$$

for $u = 0, 1, 2, \dots, (N - 1)$.

where

$$\alpha(u) = \begin{cases} \sqrt{\frac{1}{N}}, & \text{for } u = 0 \\ \sqrt{\frac{2}{N}}, & \text{otherwise.} \end{cases} \quad (4.5)$$

The first coefficient, being the average value of the sample sequence, is referred to as the *dc coefficient*, while all other transform coefficients are called the *ac coefficients*. Similarly, the inverse DCT is defined as

$$f(x) = \sum_{u=0}^{N-1} \alpha(u) c(u) \cos \left[\frac{\pi(2x+1)u}{2N} \right], \quad (4.6)$$

for $x = 0, 1, 2, \dots (N-1)$.

Sections 3.1 and 3.2 presented a background on compressive sensing. A block diagram showing the proposed matrix padding technique has been briefly illustrated in Section 3.3. This section details the proposed matrix padding method. The proposed technique converts the signal into sparse domain by applying DCT, followed by compressing it using a modified measurement matrix. This modification of the measurement matrix has been effected by padding it with a suitable sub matrix for resolving the singularity problems, while solving the underdetermined system of simultaneous linear equations. Making use of this technique, a computationally efficient sparse signal reconstruction can be achieved.

4.2.1 Matrix Padding

The data from the wave file is divided into N' frames of N samples and these frames are then converted to the frequency domain by using DCT which resulted in a sparse data representation. The compression matrix used is a random Gaussian measurement matrix ϕ of size $M \times N$ with $M < N$. In order to make the computation of the matrix inverse feasible during the reconstruction phase at the receiver, it is padded with $(N-M) \times N$ ones

which makes the matrix size to $N \times N$. Operation of this modified matrix ϕ' upon the framed sparse data results in a signal matrix \mathbf{y} that has two sub matrices of which the first sub matrix \mathbf{y}_c gives the data pertaining to the matrix operation $\mathbf{y}=\phi\mathbf{x}$, while the other sub matrix \mathbf{y}_{am} provides certain redundant data consequent to the process of matrix padding. Removing the redundant data from \mathbf{y}_{am} results in a vector \mathbf{y}_{av} of size $l \times N'$. The matrix \mathbf{y}_c of order $M \times N'$ and the vector \mathbf{y}_{av} of order $l \times N'$ are to be transmitted or stored separately. The algorithmic procedure for the compression is given in ALGORITHM 4.1.

ALGORITHM 4.1: Compression Procedure

Begin
 Read the wave file
 Convert it into N' frames of N samples
 Create a matrix $\mathbf{x}(N,N')$ with the N' frames of samples
 Generation of modified Measurement matrix
 Generate Gaussian random measurement matrix ϕ
 Generate modified Measurement matrix ϕ'
 Compression Phase
 Multiply \mathbf{x} with DCT matrix ψ
 Compress the signal using ϕ'
 Generate \mathbf{y}_c (compressed data) and \mathbf{y}_{am} (auxiliary matrix)
 Store / transmit \mathbf{y}_c and \mathbf{y}_{av} (auxiliary vector) separately
 End

The signal is reconstructed at the receiver by generating the signal matrix \mathbf{y}' by appending the received \mathbf{y}_c' with \mathbf{y}_{am}' , which is generated from the received \mathbf{y}_{av}' by performing the reverse of the operations carried out at the transmitter. The Moore Penrose inverse [158] of ϕ' is taken and multiplied with \mathbf{y}' and the data so obtained is converted back to the time domain by the Inverse DCT operation to generate the initial solution, which

is refined further by iterative LMS adaptation. The procedure for the recovery of the signal at a later stage is furnished in ALGORITHM 4.2.

ALGORITHM 4.2: Recovery Procedure

```

Begin
  Generate the initial solution
    Retrieve / receive the signals  $\mathbf{y}_c'$  and  $\mathbf{y}_{av}'$ 
    Generate  $\mathbf{y}_{am}'$  from  $\mathbf{y}_{av}'$ 
    Append  $\mathbf{y}_{am}'$  to  $\mathbf{y}_c'$  and generate  $\mathbf{y}'$ 
    Generate Moore Penrose inverse of  $\Phi'$  and multiply it with  $\mathbf{y}'$ 
    Perform Inverse DCT operation and reassembling of frames
  Perform LMS based adaptation for signal refinement
  For  $n=1, \dots, \text{Length of } \mathbf{x}(n)$ 
    Compute the output  $\mathbf{y}(n)$ 
    Compute the error signal  $\mathbf{e}(n)$ 
    Update the filter coefficients  $\mathbf{w}(n+1)$ 
  End
  Reassembling of frames
End

```

4.2.2 LMS Based Adaptation

An adaptive filter is a self-designing one, which relies on a recursive algorithm for its operation that makes it possible for the filter to perform satisfactorily in an environment where complete knowledge of the relevant signal characteristics is not available [128]. For descending towards the minimum on the mean-square-error performance surface of the adaptive filter, least-mean-square or LMS algorithm can be used, which is simple and has less computational complexity. LMS filter is used in a large number of applications like echo cancellation, channel equalization, signal prediction, to name a few.

If $\mathbf{y}(n)$ is the n^{th} sample of the observed output signal [129], then

$$\mathbf{y}(n) = \mathbf{x}^T(n) \mathbf{w}(n), \quad (4.7)$$

where $\mathbf{w}(n) = [w_0(n) w_1(n) \dots w_{L-1}(n)]^T$ and $\mathbf{x}(n) = [x(n) x(n-1) \dots x(n-L+1)]^T$ denote the filter coefficient vector and input vector respectively and L is the filter length. The error of the adaptive filter output with respect to the desired response signal $\mathbf{d}(n)$ is

$$\mathbf{e}(n) = \mathbf{d}(n) - \mathbf{x}^T(n) \mathbf{w}(n). \quad (4.8)$$

By minimizing the cost function which is the mean squared error [130], the filter coefficients are updated iteratively, so that

$$\mathbf{w}(n+1) = \mathbf{w}(n) + \mu \mathbf{e}(n) \mathbf{x}(n), \quad (4.9)$$

where μ is the adaptation step size. If \mathbf{R} is the autocorrelation matrix of the input vector $\mathbf{x}(n)$ and λ_{max} , its maximum eigen value, the condition for convergence for the LMS is [129]

$$0 < \mu < \frac{1}{\lambda_{max}}. \quad (4.10)$$

The structure of adaptive LMS FIR filter is shown in Figure 4.2. It is known that the *optimum weight vector*, which is the point at the bottom of the performance surface, is

$$\mathbf{W}^* = \mathbf{R}^{-1} \mathbf{P}, \quad (4.11)$$

where \mathbf{R} is the input correlation matrix given by

$$\mathbf{R} = E[\mathbf{x}(n)\mathbf{x}(n)^T] \quad (4.12)$$

and

$$\mathbf{P} = E[\mathbf{d}(n)\mathbf{x}(n)]. \quad (4.13)$$

Taking expectation on both sides of (4.9),
 $E[\mathbf{w}(n+1)] = E[\mathbf{w}(n)] + \mu E[\mathbf{e}(n)\mathbf{x}(n)]$

$$\begin{aligned}
 &= E[\mathbf{w}(n)] + \mu E[\mathbf{d}(n)\mathbf{x}(n) - \mathbf{x}(n) \mathbf{x}^T(n) \mathbf{w}(n)] \\
 &= E[\mathbf{w}(n)] + \mu(\mathbf{P} - E[\mathbf{x}(n) \mathbf{x}^T(n) \mathbf{w}(n)]) \\
 &= E[\mathbf{w}(n)] + \mu(\mathbf{P} - E[\mathbf{x}(n) \mathbf{x}^T(n)] E[\mathbf{w}(n)]) \\
 &(\because \text{Coefficient vector } \mathbf{w}(n) \text{ is independent of input vector } \mathbf{x}(n)) \\
 E[\mathbf{w}(n + 1)] &= E[\mathbf{w}(n)] + \mu(\mathbf{P} - \mathbf{R} E[\mathbf{w}(n)]). \quad (4.14)
 \end{aligned}$$

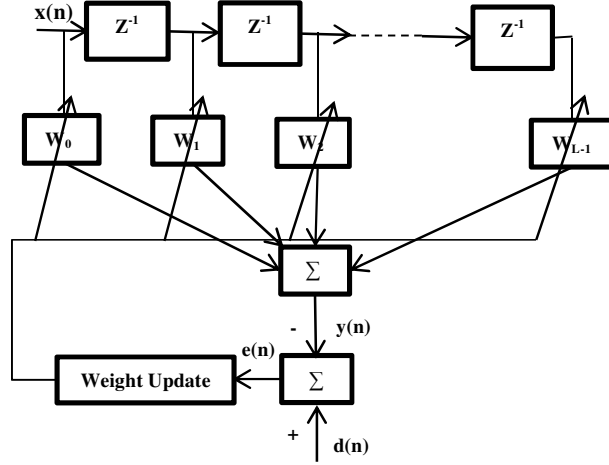


Fig. 4.2 Tapped delay line structure of the LMS filter

Let the error in coefficient vector $\mathbf{s}(n)$ be,

$$\mathbf{s}(n) = \mathbf{w}(n) - \mathbf{W}^*. \quad (4.15)$$

Substituting (4.14) in (4.15),

$$\begin{aligned}
 E[\mathbf{s}(n + 1)] &= E[\mathbf{s}(n)] + \mu(\mathbf{P} - \mathbf{R} (E[\mathbf{s}(n)] + \mathbf{W}^*)) \\
 &= E[\mathbf{s}(n)] + \mu(\mathbf{P} - \mathbf{R} E[\mathbf{s}(n)] - \mathbf{R}\mathbf{W}^*) \\
 &= E[\mathbf{s}(n)] - \mu \mathbf{R} E[\mathbf{s}(n)] \quad (\because \mathbf{P} = \mathbf{R}\mathbf{W}^*) \\
 &= (\mathbf{I} - \mu \mathbf{R}) E[\mathbf{s}(n)]. \quad (4.16)
 \end{aligned}$$

This implies that the mean error in filter coefficients at instant $n+1$ depend on the step size, autocorrelation of the input vector and the mean error in the filter coefficients at the instant n .

4.3 Undersea Acoustic Channel Effects

4.3.1 Ambient Noise

Ambient noise is always present in the background of the sea. The four basic sources that can contribute to the ambient noise in the ocean are the noise due to turbulence N_t , noise due to shipping N_s , noise due to wind N_w and thermal noise N_{th} .

The overall power spectral density $N(f)$ of the ambient noise is given by

$$N(f) = N_t(f) + N_s(f) + N_w(f) + N_{th}(f), \quad (4.17)$$

where the ambient noise due to turbulence, shipping, wind and thermal noise are described by the following equations:

$$N_t(f) = 17 - 30 \log(f), \quad (4.18)$$

$$N_s(f) = 40 + 20(s - 0.5) + 26 \log(f) - 60 \log(f + 0.03), \quad (4.19)$$

s being the shipping activity factor whose value ranges between 0 and 1 for low to high shipping activities and f is the frequency (in kHz).

$$N_w(f) = 50 + 7.5v_w^{1/2} + 20 \log(f) - 40 \log(f + 0.4), \quad (4.20)$$

v_w being the wind speed in m/s and

$$N_{th}(f) = -15 + 20 \log(f). \quad (4.21)$$

Figure 4.3 shows the variation of power spectral density of the overall Ambient Noise with respect to shipping traffic and wind speed. The black ones are for lower wind speed and the red ones are for higher wind

speeds. As seen from the plot, the curve in the region 500Hz to 100kHz shifts up as the wind speed increases.

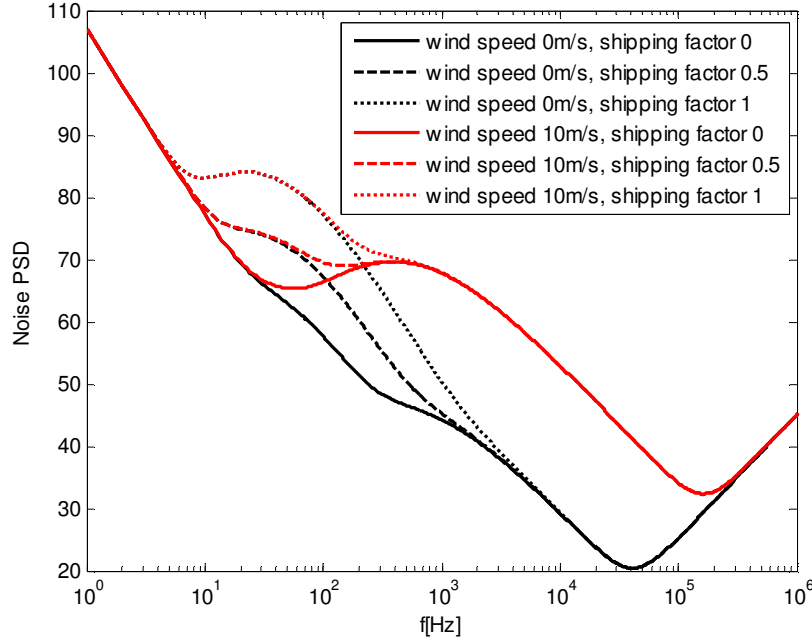


Fig. 4.3 Variation of PSD of Overall Ambient Noise with respect to wind speed and shipping factor

For computing the maxima or minima of the noise equations, the general practice is to equate the first derivative to 0 and compute the second derivative. Differentiating equations (4.18), (4.19), (4.20) and (4.21) with respect to f ,

$$\frac{\partial N_t}{\partial f} = \frac{-30}{f \ln 10}, \quad (4.22)$$

$$\frac{\partial N_s}{\partial f} = \frac{0.78 - 34f}{f(f + 0.03) \ln 10}, \quad (4.23)$$

$$\frac{\partial N_w}{\partial f} = \frac{8 - 20f}{f(f + 0.4) \ln 10}, \quad (4.24)$$

$$\frac{\partial N_{th}}{\partial f} = \frac{20}{f \ln 10}. \quad (4.25)$$

For shipping noise, equating (4.23) to 0, we get $f = 0.02294\text{kHz}$. Since, $\frac{\partial^2 N_s}{\partial f^2} < 0$, at $f = 22.94\text{Hz}$, there is a maxima at $f = 22.94\text{Hz}$. For wind noise, equating (4.24) to 0, we get $f = 0.4\text{kHz}$. Since, $\frac{\partial^2 N_w}{\partial f^2} < 0$, at $f = 400\text{Hz}$, there is a maxima at $f = 400\text{Hz}$. Similarly for turbulence noise, there is a minima at $f = \infty$ and for thermal noise, there is a maxima at $f = \infty$.

Figure 4.4 shows the variation of power spectral density of the overall Ambient Noise with respect to frequency and shipping traffic. As seen from the plot, the curve in the region 10Hz to 300Hz shifts up as the shipping traffic increases. Figure 4.5 shows the variation of power spectral density of the overall Ambient Noise with respect to frequency and wind speed. As seen from the plot, the curve in the region 500Hz to 100kHz shifts up as the wind speed increases.

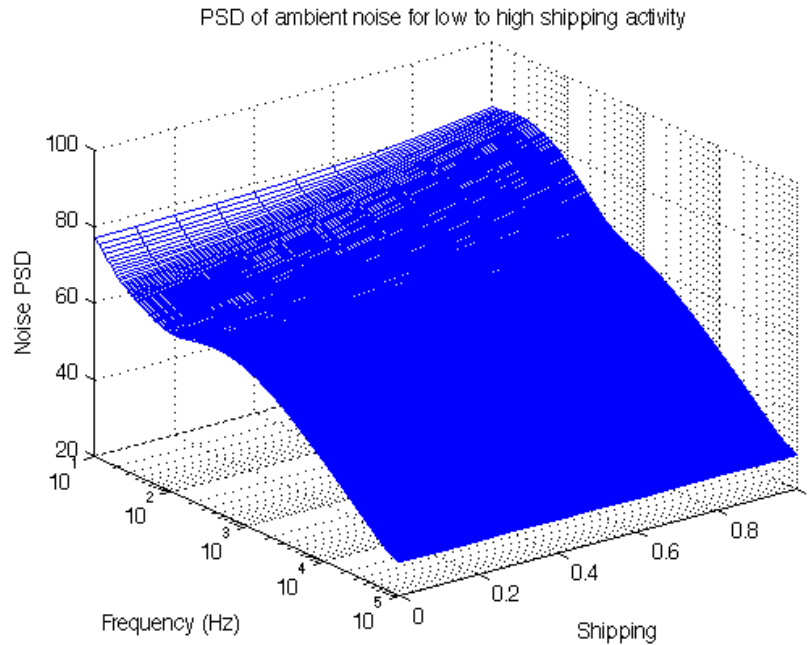


Fig. 4.4 PSD of Overall Ambient Noise with respect to frequency and shipping factor

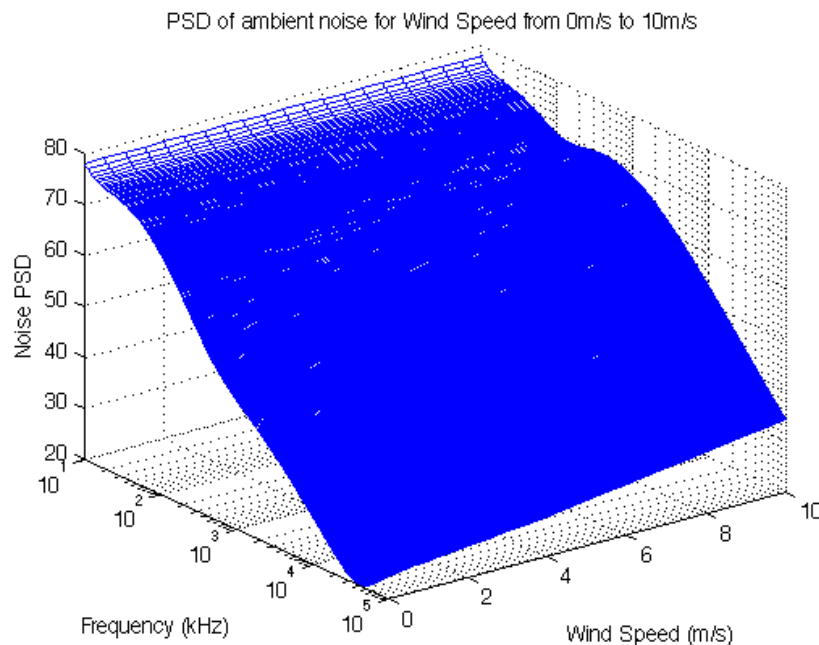


Fig. 4.5 PSD of Overall Ambient Noise with respect to frequency and wind speed

4.3.2 Generation of Channel Impulse Response

For simulation, Bellhop is used in order to obtain the channel impulse response based on a modeled underwater scenario. Therefore, environmental data like the sound speed profile of the water column, obtained from conductivity, temperature, depth (CTD) data sets, the number of transceivers and their depths, etc. are given as input to the Bellhop. The sound speed profile varies greatly with location and time of year. The channel impulse response represents multiple paths from any active transmitter to any receiver. By tracing a large number of rays through the inhomogeneous acoustic underwater channel that is characterized by the sound speed profile (SSP), the multipath sound propagation can be modeled. The rays are traced by numerically solving the differential ray equations given in [105]. The resulting rays travel on

bend curves rather than on straight lines due to the variation of sound speed with depth. Furthermore, rays are reflected at the surface and bottom, whereby absorption losses and phase shifts take place.

Sound Speed Profile from a real ocean region with the data collected using CTD and computed using Leroy's equation is shown in Figure 4.6. It can be seen that the sound speed varies non-linearly with the depth and the nonlinearity can be attributed as due to the variation of temperature, salinity and pressure from the surface to bottom. At lower depths, temperature determines the sound speed, but as the water depth increases, pressure becomes more and more prominent in influencing the speed of sound propagation. The corresponding normalized channel impulse response plot for source depth of 50m, receiver depth of 100m, receiver range of 1km and ocean depth of 1km, plotted using Bellhop is shown in Figure 4.7. The number of non-zero channel taps in channel

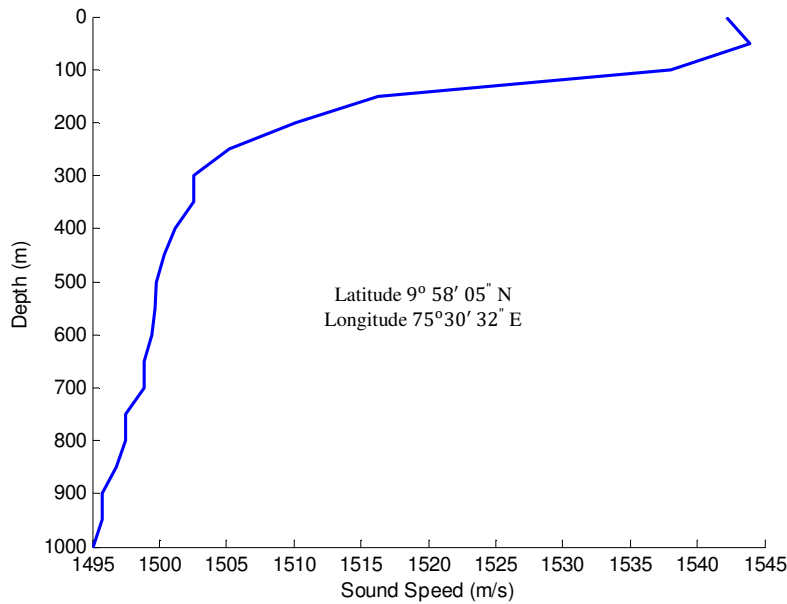


Fig. 4.6 A typical Sound Speed Profile from real ocean

impulse response varies, depending on the distance between the transmitter and the receiver as well as other environmental conditions.

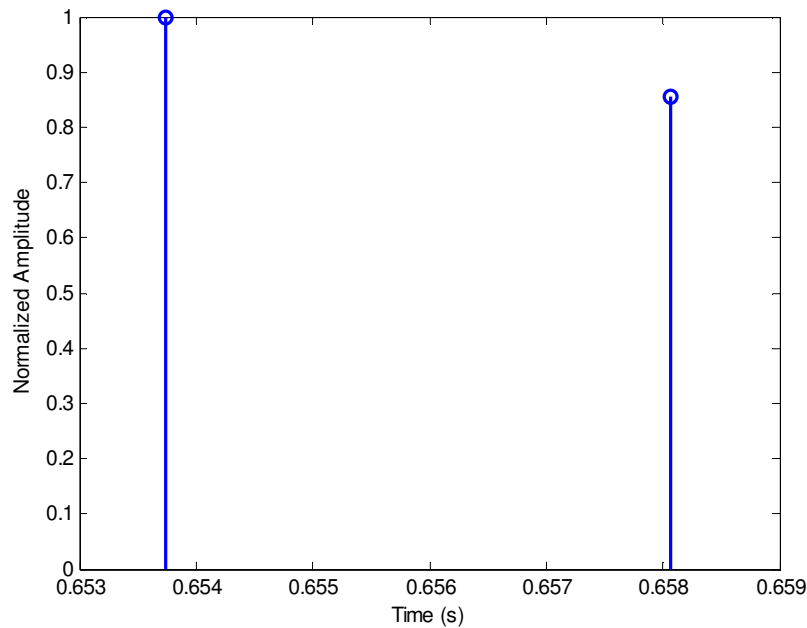


Fig. 4.7 Normalised Channel Impulse Response

4.3.3 CTD (conductivity, temperature and depth) Instrument

The CTD instrument refers to a package of electronic instruments that measures the conductivity, temperature and depth parameters. A CTD instrument's primary function is to detect how the conductivity and temperature of the water column changes relative to depth. Oceanographers usually measure underwater pressure in decibars (dbar) because an increase in pressure of 1dbar is approximately equal to an increase in depth of 1m.

4.4 OFDM for Undersea Acoustic Links

The orthogonal frequency division multiplexing has become a key technology for wireless communication systems because of its high spectral

efficiency, robustness against multipath fading, and reliable high speed transmission over complex channel conditions.

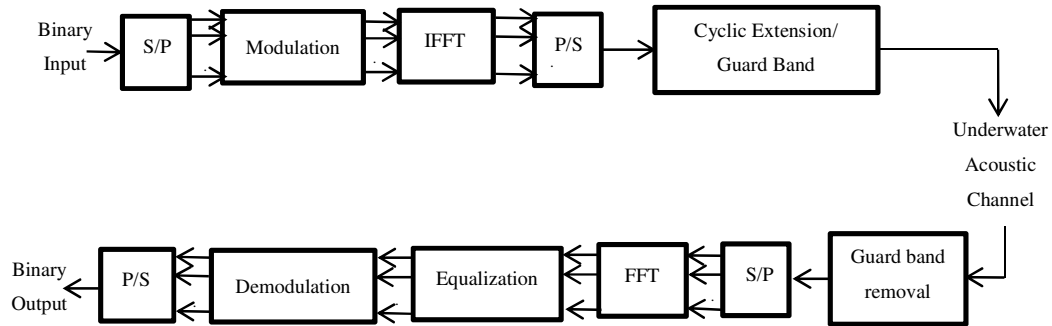


Fig. 4.8 General block diagram of an OFDM System for Undersea Acoustic Links

The block diagram of a general OFDM system is shown in Figure 4.8 and the OFDM for undersea acoustic link has been simulated using a data stream, which has been divided into parallel bit streams, followed by modulation and computation of its IFFT as well as insertion of the guard band for minimizing the inter symbol interference. The signal corrupted by the ambient noise is then convolved using the channel impulse response generated with the Bellhop model as

$$y(n) = [x(n) + a(n)] \otimes h(n), \quad (4.26)$$

where $x(n)$ is the transmitted signal, $a(n)$ is the ambient noise, $h(n)$ is the channel impulse response and $y(n)$ is the received signal. At the receiver, the guard band is removed, followed by the computation of FFT and equalization. The resultant signal is demodulated to reconstruct the binary data and the bit-error-rate has been computed. The bit-error-rates under various Signal to Noise Ratio conditions have been simulated and compared for various orders of QAM and PSK based OFDM schemes for undersea acoustic links. The bit-error-rate of underwater channel has also been compared with that of an AWGN channel, which assumes that noise is

the only source of disturbance in the channel and adds white Gaussian noise to the signal that passes through it.

4.5 Coded OFDM

Coded OFDM is a form of OFDM where error correction coding is incorporated into the signal. Coding offers better security and interleaving reduces the effect of burst errors. Hence, OFDM, combined with coding and interleaving, is a good choice for complex channels like undersea acoustic links. The thesis throws light on the application of interleaved coded OFDM (convolutional and BCH) for undersea acoustic links.

The system model for interleaved coded OFDM is similar to the one for the normal OFDM, except the encoding and interleaving at the transmitter side as well as deinterleaving and decoding at the receiver side. The Block Diagram of the Interleaved Coded OFDM is as shown in Figure 4.9. The data stream comprising of 64 bits per OFDM symbol has been encoded using convolutional and BCH coding for validating their performances. Convolutional coding has been performed by an encoder with a constraint length 7 and code rate $1/2$, where as a BCH (7,4) coding has been performed on 64 bits resulting in 112 bits. Thus, 128 and 112 sub carriers per OFDM symbol are required for convolutional coded and BCH coded OFDMs respectively. This data has further been subjected to interleaving, followed by the BPSK and Differential Phase Shift Keying (DPSK) based OFDM modulations.

If the channel is one which produces burst errors, an effective technique to reduce these errors is to shuffle the coded data through the method of interleaving in such a way that the error bursts get fairly and uniformly distributed in time. By doing so, the bursty channel effect is being manipulated into a channel characterized by statistically independent

errors. The data is written row-by-row into a 16×8 matrix for convolutional coded OFDM and 14×8 matrix for BCH coded OFDM respectively and read out column-by-column by the interleaver. The deinterleaver at the receiver performs the reverse process. The transmitted signal contaminated with the background noise is then convolved using the channel impulse response generated by the Bellhop model.

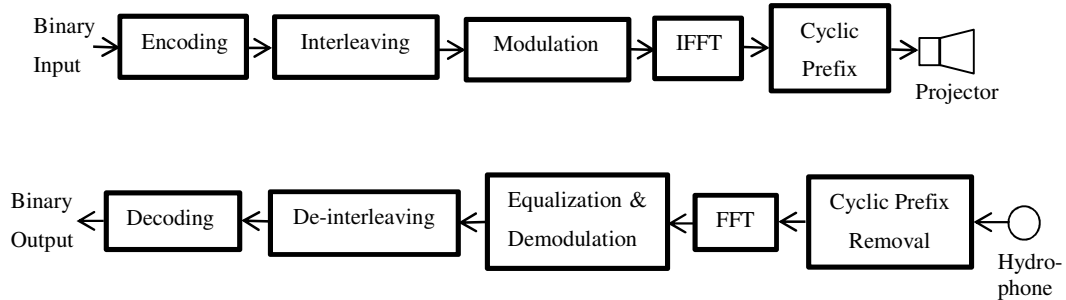


Fig. 4.9 System Model of Interleaved Coded OFDM

At the receiver, the OFDM demodulated signal is subjected to deinterleaving followed by decoding for regenerating the original data stream. The bit-error-rate performances, under various Signal to Noise Ratio conditions, have been simulated for BPSK and DPSK based convolutional coded OFDM with and without interleaving as well as BCH coded OFDM with and without interleaving. Also, the effect of interleaving has been investigated by quantitatively comparing the performances of both the coded OFDM schemes, with and without interleaving.

4.6 BCH Coded OFDM

Encoding introduces redundancy into a stream of data to correct errors and extract the original data. Using BCH codes, the number of errors that can be corrected, can be customized depending on the requirements. They can also be decoded easily via syndrome decoding. The

performances of BCH (15, 11) and (15, 7) coded interleaved OFDMs are also compared in the thesis.

The binary input undergoes BCH encoding followed by interleaving, which helps to reduce the effects of burst errors in the channel, followed by BPSK based OFDM modulation. The transmitted signal is convolved using the channel impulse response generated with the Bellhop model. At the receiver, the BPSK based OFDM demodulation is performed, followed by de-interleaving and BCH decoding to regenerate the original data stream.

4.7 STBC MIMO

Space-time block coding improves reliability and robustness of communication system by exploiting space and time diversity. The idea behind using a transmit diversity scheme is that some of the redundant signals transmitted may arrive in a better state at the receiver and by combining all the received versions, more accurate results can be obtained. The key feature of the Alamouti code is the orthogonality between the signals transmitted over the two transmitters. Using Alamouti STBC diversity scheme, the data rate is maintained the same, while improving the BER performance.

4.7.1 Normal STBC

The input bits undergo modulation, which can be 16-QAM or 16-PSK, followed by the Alamouti STBC encoding and the encoded symbols are transmitted by the respective transmitter. At the receiver, the channel impulse responses are estimated and STBC decoding is carried out, followed by demodulation to reconstruct the transmitted data. The performances of 16-QAM and 16-PSK systems have been simulated for the 2x1 case. It was found that 16-QAM based STBC system performed better

than 16-PSK based STBC system. As a result, 2x1 and 2x2 STBC systems were compared for 16-QAM based system. Figure 4.10 shows the general block schematic of a 2x2 STBC system.

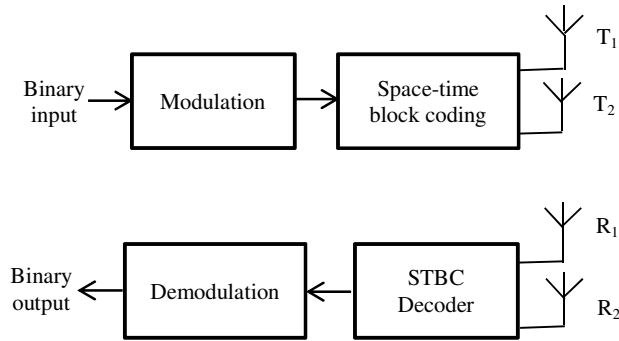


Fig. 4.10 General block schematic of a 2x2 STBC system

4.7.2 Coded STBC

A modification to the existing STBC is proposed in the thesis by incorporating coding and interleaving at the transmitter end followed by deinterleaving and decoding at the receiving end, as follows. In coded STBC, the input bits undergo channel coding, followed by interleaving. BCH (7, 4) encoder followed by 16-QAM modulation and Alamouti STBC encoding system has been simulated. The encoded symbols are transmitted by the respective transmitters. At the receiver, the channel impulse responses are estimated and STBC decoding is carried out, followed by demodulation, deinterleaving and decoding, to regenerate the transmitted data stream. Figure 4.11 shows the general block schematic of a coded interleaved 2x2 STBC system.

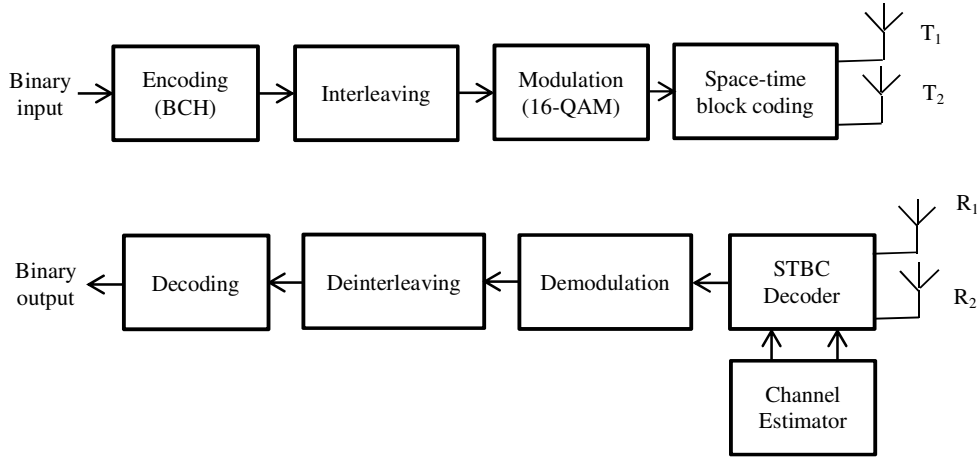


Fig. 4.11 General block schematic of a coded interleaved 2x2 STBC system

4.8 Channel Estimation and Synchronization

Synchronization is important in OFDM due to its great sensitivity towards timing and frequency offset errors. The performance of OFDM systems is particularly dependent on the synchronization error which occurs due to the Carrier Frequency Offset (CFO) and the Symbol Timing Offset (STO). The frequency mismatch between transmitter and receiver causes loss of orthogonality among the subcarriers giving rise to ICI. Incorrect symbol timing brings signals from adjacent frames into the target frame resulting in severe inter symbol interference too.

A dynamic estimation of the channel is necessary before the demodulation of OFDM signals since the channel is time-varying. Compressive sensing has been used in communications domain for sparse channel estimation. A sparse channel is the one whose impulse response consists of only a few significant values at certain time delays while the rest of the values are zero or negligible. The sparse channel estimation method offers lower reconstruction errors at the receiver, exploiting the sparsity of the channel impulse response. The thesis throws light on the effect of

varying the number of pilots for estimating the undersea channel for various ranges.

The system model of a generic OFDM receiver is shown in Figure 4.12. The synchronization errors, STO and CFO are estimated and compensated at the receiving front end. After guard band removal and computation of FFT, the received pilots have been extracted and the channel impulse response has been computed using the dictionary based sparse channel estimation method, followed by equalization procedure to undo the channel effects. The resultant signal has been demodulated to reconstruct the binary data and the bit-error-rates under various Signal to Noise Ratio conditions have been simulated and compared for BPSK based OFDM schemes.

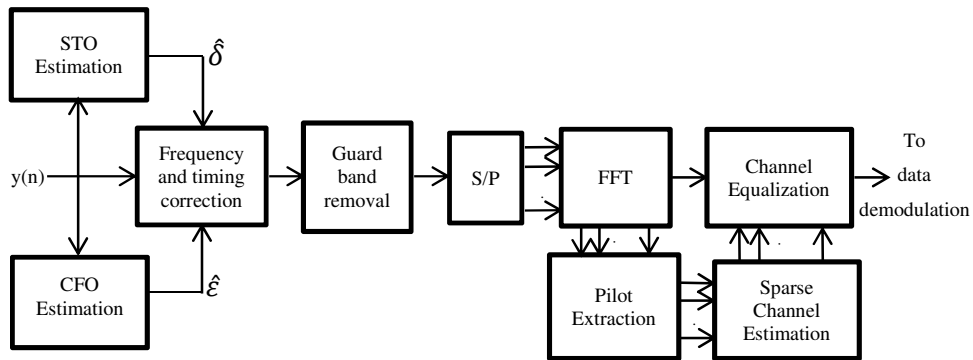


Fig. 4.12 Block Diagram of an OFDM Receiver with synchronization and channel estimations

4.9 Summary

A method for sparse signal reconstruction based on matrix padding and LMS based adaptation has been proposed. Ambient noise is always present in the background of sea and the effect four basic sources that contribute to the ambient noise in the ocean have been examined. Moreover, the maxima and minima values of the noise power spectral density equations have been computed and the variations of power spectral

density of the overall ambient noise with respect to frequency and shipping traffic as well as wind speed have been studied. The system models for normal OFDM, coded OFDM as well as normal and the proposed coded STBC have been described. Also, a system model of an OFDM Receiver with STO and CFO estimation as well as channel parameter estimation has also been described.

CHAPTER 5

MODULATION AND CODING

In the past few years, there has been a tremendous increase in research and development of underwater acoustic communication system. In underwater acoustic communication, the energy received is combination of energies contributed by different rays traversing through different paths due to multiple reflections of the waves at the boundaries, which results in inter symbol interference. Orthogonal Frequency Division Multiplexing is widely employed nowadays because of its advantages like resilience to inter symbol interference, immunity to selective fading, simpler channel equalization, etc. Various modulation techniques like Quadrature Amplitude Modulation and Phase Shift Keying are used in conjunction with OFDM. Coding techniques like convolutional and BCH coding, as well as interleaving techniques can be used along with OFDM for improving the error correction capability of the receiver. Diversity techniques improve reliability of data transfer by transmitting the same data on two or more communication channels with different characteristics. For undoing the channel effects and demodulating the signal with fairly acceptable accuracies, the channel parameters need to be estimated. Channel estimation is performed by inserting pilots into the subcarriers of an OFDM symbol. Underwater channels exhibit sparse channel impulse response and the channel can be estimated using the compressive sensing techniques to achieve good performance.

5.1 *Background*

Though various transmission schemes such as frequency division multiplexing, time division multiplexing, code division multiplexing and

the hybrid forms are in use for realizing undersea acoustic links, orthogonal frequency division multiplexing has been found to be an ideal choice for such links due to its numerous advantages. Multipath propagation is responsible for severe degradation of the acoustic communication signal in undersea scenario, since it generates Inter Symbol Interference (ISI). Maximum spectral efficiency is required to exploit the limited bandwidth available in the underwater acoustic channel. OFDM is a favorable communication scheme in underwater acoustic communications thanks to its resilience against multipath effects as well as high spectral efficiency.

Channel coding allows error detection and correction at the receiving end by introducing redundancy into transmitted data. Channel coding along with interleaving can be used to improve the performance of normal OFDM. Because of all the limitations of the underwater channel, the selection of the type of modulation and error correction techniques is of extreme importance.

5.2 Orthogonal Frequency Division Multiplexing

Multicarrier modulation, an approach to the design of a bandwidth-efficient communication system in the presence of channel distortion divides the available channel bandwidth into a number of subchannels, such that each subchannel is nearly ideal. Multicarrier modulation techniques attract a lot of attention in wireless communication because of its ability to efficiently combat multipath and fading effects in complex channels. Orthogonal Frequency Division Multiplexing is a multicarrier modulation technique which makes efficient use of the available bandwidth.

OFDM has evolved from Frequency-Division Multiplexing (FDM), which is a technique by which the total bandwidth available in a communication medium is divided into a series of non-overlapping

frequency sub-bands, each of which is used to carry a separate signal. If the FDM system had been able to use a set of subcarriers that were orthogonal to each other, a higher level of spectral efficiency could have been achieved. The guard bands that were necessary to allow individual demodulation of subcarriers in an FDM system would no longer be necessary. The use of orthogonal subcarriers would allow the spectra of subcarriers to overlap, thus increasing the spectral efficiency. As long as the orthogonality is maintained, it is possible to recover the data carried by individual subcarriers despite their overlapping spectrums.

In OFDM, the entire frequency band is divided into a number of sub bands. The data stream is also divided into several parallel data streams of lower rate and the individual subcarriers are modulated by individual low rate data streams and the resultant signals are added up and transmitted. Even though these sub carriers are overlapping, they are orthogonal and hence, there is no Inter Carrier Interference (ICI).

5.2.1 Use of Guard band

A guard band, which is zero padding or cyclic prefix, is used to ensure that the Inter Symbol Interference (ISI) is eliminated. In Cyclic prefixing, the tail end of each OFDM symbol is copied to its beginning. Even though the cyclic prefix has high power requirements compared to zero padding, it converts linear convolution to circular convolution problem, which helps in simplifying the equalization procedure at the receiver. Equalization is the removal of distortion/effects caused by the wireless channel to recover the transmitted symbols as accurately as possible. The length of the cyclic prefix is chosen to be greater than the expected multipath spread. The benefit gained in terms of simplified equalization is a sufficient justification to accept the reduced data rate. The general structure of an OFDM symbol is shown in Figure 5.1.

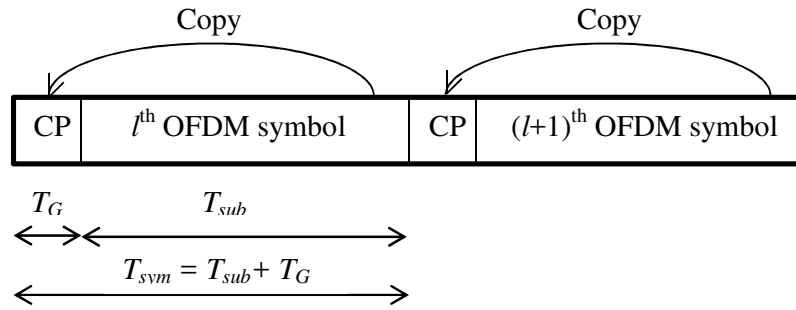


Fig. 5.1 General structure of an OFDM symbol

5.2.2 OFDM Variants

Since OFDM offers a lot of advantages, it can be used to offer better performance in a complex and challenging medium like the ocean. There are other variants of OFDM like COFDM (Coded Orthogonal Frequency Division Multiplexing), WOFDM (Wideband OFDM), Orthogonal Frequency Division Multiple Access (OFDMA) etc. which follow the basic format for OFDM, but have additional attributes.

- **COFDM (Coded Orthogonal frequency division multiplexing):** A form of OFDM where error correction coding is incorporated into the signal.
- **WOFDM (Wideband OFDM):** The concept of this form of OFDM is that it uses a degree of spacing between the channels that is large enough that any frequency errors between the transmitter and receiver do not affect the performance. It is particularly applicable to Wi-Fi systems.
- **OFDMA (Orthogonal frequency division multiple access):** A scheme used to provide a multiple access capability for applications such as cellular telecommunications when using OFDM technologies.

5.2.3 Modulation Techniques

With the fast developments in modern communication techniques, the demand for reliable high data rate transmission increased significantly, which diverted much interest in modulation techniques. Different modulation techniques aim to send different bits per symbol and thus achieve different throughputs or efficiencies. In the simulation studies, the modulation techniques used are Quadrature amplitude modulation (QAM) and Phase-shift keying (PSK).

5.2.3.1 Quadrature Amplitude Modulation

Quadrature amplitude modulation (QAM) is performed by changing the amplitude and phase of a carrier in accordance with the input data. In view of the fact that the signal undergoes both amplitude and phase variations, it may be considered to be a composite signal with amplitude and phase modulations. Normally the lowest order QAM encountered is 16-QAM because 2-QAM is similar to binary phase-shift keying (BPSK) and 4-QAM is similar to quadrature phase-shift keying (QPSK). Using higher order QAM, it is possible to transmit more bits per symbol. But, the points on the constellation move closer and the transmission becomes susceptible to noise, resulting in a higher bit-error-rate for higher order QAM than that for the lower order QAM variants. Hence, there exist a tradeoff between the data rates and bit-error-rates for a given system. 64-QAM and 256-QAM are often used in digital cable television and cable modem applications.

A graphical representation of the complex envelope of each possible symbol state is called a constellation diagram. The x-axis of a constellation diagram represents the in-phase component of the complex envelope, and y-axis represents the quadrature component of the complex envelope. The

distance between signals on a constellation diagram relates to how different the modulation waveform are, and how well a receiver can differentiate between all possible symbols when random noise is present. Figure 5.2 shows the constellation diagram for the transmitted 16-QAM symbols.

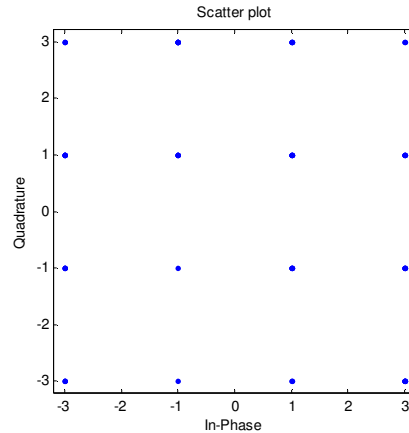


Fig. 5.2 Constellation diagram for the transmitted 16-QAM symbols

5.2.3.2 Phase-shift keying

Phase-shift keying (PSK) is a digital modulation scheme that conveys data by modulating the phase of a carrier wave according to the input. The demodulator, which is designed specifically for the symbol set used by the modulator, determines the phase of the received signal and maps it back to the symbol it represents, thus recovering the original data.

In binary phase-shift keying (BPSK), the phase of a constant amplitude carrier signal is switched between two values which are normally separated by 180° , corresponding to binary 1 and 0 respectively. Differential phase-shift keying (DPSK) is a non-coherent form of phase shift keying which avoids the need for a coherent reference signal at the receiver. Quadrature phase shift keying (QPSK) has twice the bandwidth efficiency of BPSK, since two bits are transmitted in a single modulation

symbol. In M-ary PSK (MPSK), the data can be transmitted at a faster rate compared to the simplest binary phase shift keying. Figure 5.3 shows the constellation diagram for the transmitted 16-PSK symbols.

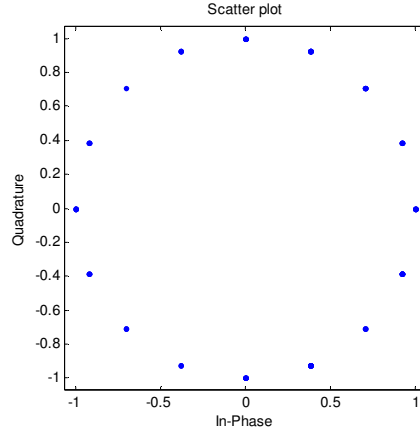


Fig. 5.3 Constellation diagram for the transmitted 16-PSK symbols

5.2.4 Subcarrier Generation

The modulation of the binary input is carried out by any of the schemes like QAM, FSK, PSK or their variants. The subcarriers of OFDM are modulated by the symbols generated from binary input and these subcarriers are made orthogonal so that the inter carrier interference (ICI) effect is minimized. If X_0, X_1, \dots, X_{M-1} are the M symbols and $\phi_0[n], \phi_1[n], \dots, \phi_{M-1}[n]$ are the M subcarriers, then the resulting signal is

$$x[n] = X_0\phi_0[n] + X_1\phi_1[n] + \dots + X_{M-1}\phi_{M-1}[n]. \quad (5.1)$$

The most popular set of orthogonal subcarriers can be generated by computing the IDFT. Thus,

$$x[n] = \frac{1}{\sqrt{M}} \sum_{i=0}^{M-1} X_i e^{j\frac{2\pi in}{M}} = IDFT\{X\}, \quad (5.2)$$

and can be easily implemented using IFFT efficiently. These orthogonal subcarriers being overlapping, helps OFDM to achieve higher spectral efficiency.

5.2.5 Signal Estimation

The use of zero padding or cyclic prefix guard band eliminates the inter symbol interference, if the length of guard band is greater than the length of channel impulse response. The cyclic prefix converts the channel effect into circular convolution, which corresponds to multiplication in the frequency domain. Equalizers, which are widely used in practical communication systems, help to undo the channel effects like the multipath, inter symbol interference, etc. OFDM enables simpler equalization at the receiver, which can be accomplished by a simple single tap frequency domain equalizer. This is equivalent to assuming that any fading is flat across the bandwidth of each subcarrier and the estimated signal at the receiver is given by

$$\hat{X}(f) = \frac{Y(f)}{H(f)}, \quad (5.3)$$

where $Y(f)$ and $H(f)$ are the frequency domain counterparts of the received signal $y(n)$ and the channel impulse response $h(n)$ respectively.

5.2.6 Peak to Average Power Ratio (PAPR) Issue in OFDM

The transmitted signals in an OFDM system can have high peak values in time domain because of IFFT operation. Data symbols across subcarriers add up to produce a high peak value OFDM symbol resulting in high peak-to-average power ratio (PAPR). PAPR of a signal x is the ratio of the maximum power to the average power of the signal and can be defined as

$$PAPR = \frac{\max|x(t)|^2}{E[|x(t)|^2]}. \quad (5.4)$$

The maximum possible value of PAPR is N , the number of subcarriers, which occurs when all the subcarriers add up constructively at

a single point. The largest PAPR rarely occurs and hence it is a common practice to find the probability that the PAPR of a symbol exceeds a given threshold $PAPR_0$. Hence, for representing PAPR, complementary cumulative distribution function (CCDF) is used, which can be defined as

$$CCDF = P(PAPR > PAPR_0). \quad (5.5)$$

Large PAPR means that the OFDM signal has a large variation between the average signal power and the maximum signal power.

5.2.6.1 PAPR Reduction Techniques

One simplest approach of reducing the PAPR is to clip the amplitude of the signal to a fixed level. The clipping technique employs clipping or nonlinear saturation around the peaks to reduce the PAPR. It is simple to implement, but it may cause in-band and out-of-band interferences while destroying the orthogonality among the subcarriers. Hence, clipping is followed by filtering.

Another approach commonly used for PAPR reduction is the DFT-spreading technique, which is used to spread the input signal with DFT and can be subsequently taken into IFFT. An M -point FFT block is inserted at the transmitter before the N -point IFFT in the block as in Figure 5.4 and the output of M -point FFT is assigned to the subcarriers of N -point IFFT. The effect of PAPR reduction depends on the way of assigning the subcarriers to each terminal. As depicted in Figure 5.5, there are two different approaches of assigning subcarriers among the users, *viz.*, DFDMA (Distributed FDMA) and LFDMA (Localized FDMA). DFDMA distributes M -point FFT outputs over the entire band (of total N subcarriers) with zeros filled in $(N-M)$ unused subcarriers, whereas LFDMA allocates FFT outputs to M consecutive subcarriers in N subcarriers. When DFDMA

distributes FFT outputs with equi-distance $N/M = S$, it is referred to as IFDMA (Interleaved FDMA) where S is called the bandwidth spreading factor.

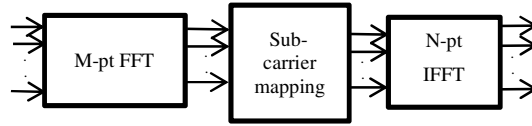


Fig. 5.4 DFT Spreading

5.3 Forward Error Correction

Forward error correction (FEC) or channel coding [14] addresses the process of mapping message vectors into code vectors using certain well-defined mapping procedures in such a way that the errors in the overall system can be corrected at the receiving end, leading to improved error rate performance. Coding helps to improve the transmission efficiency, security, quality and reliability. The American mathematician Richard Hamming invented the first error-correcting code in 1950: the Hamming (7,4) code.

FEC gives the receiver the ability to correct errors without needing a reverse channel to request retransmission of data, but at the cost of a fixed, higher forward channel bandwidth. FEC is therefore applied in situations where retransmissions are costly or impossible, such as one-way communication links and when transmitting to multiple receivers in multicast. The two main categories of FEC codes are *block codes* and *convolutional codes*.

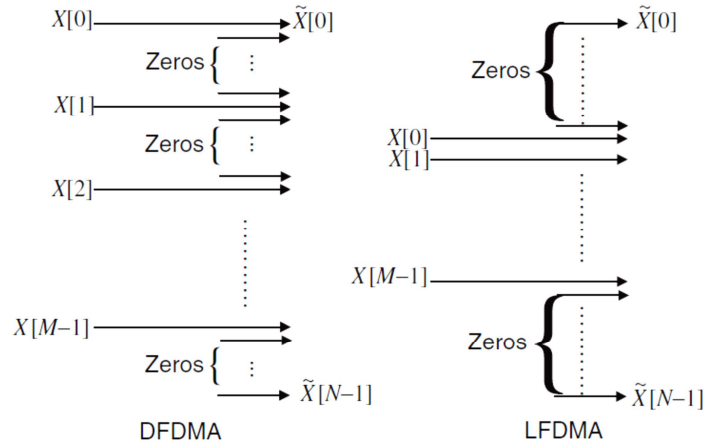


Fig. 5.5 Subcarrier mapping

5.3.1 Block codes

In block codes, the input bit stream is segmented into a block of k information bits and each block is appended with a group of r check bits or redundant bits that are derived from the respective block. At the receiver, these check bits are used for error detection and correction of the information bits in that block. The block code is referred to as an (n, k) code and the rate of the code is $R_b = k/n$.

5.3.1.1 BCH Coding

BCH code, which is a variant of the block code as well as a subclass of cyclic codes, has powerful built in properties for multiple error corrections and are supplemented with computationally efficient codec algorithms. Decoding of BCH codes involves computing the syndrome from the received code words, finding the error locations from the syndrome and finally correcting the errors. BCH codes are used in applications such as satellite communications, compact disc players, DVDs, disk drives, solid-state drives and two-dimensional bar codes.

For every block of k bits, r redundant bits are added and the number of bits in the code word is

$$n = k + r, \quad (5.6)$$

which can correct up to t errors, where

$$t = r/m. \quad (5.7)$$

The value of m is computed from

$$n = 2^m - 1, \quad (5.8)$$

where $m \geq 3$. The minimum distance between the code words for correcting t errors is found to be

$$d = 2t + 1. \quad (5.9)$$

One of the key features of BCH codes is that during code design, there is a precise control over the number of symbol errors correctable by the code. The communication system designer is provided with a large selection of block lengths and code rates. Table 5.1 lists the number of correctable bit errors for a block of k bits using BCH (7, 4), BCH (15, 11), BCH (15, 7) and BCH (15, 5) codes.

5.3.2 Convolutional codes

Convolutional coder encodes the bit streams continuously using a sequential logic in accordance with the coupled memory of the coder. For the purpose of generating the coded symbols, the input stream is fed into a shift register and the shift register contents are combined modulo-2 in such a way that the coder generates the resultant code vector in accordance with certain generator polynomial criteria. In view of the advantages offered by the nonsystematic convolutional codes, it has been used for error correction using the probabilistic Viterbi decoding algorithm. The Viterbi maximum

likelihood algorithm is found to be a very effective decoding procedure for codes with small constraint lengths. Both *hard* and *soft* decision decoding can be implemented for convolutional codes and usually soft decision decoding is superior by about 2-3dB.

Table 5.1 Number of correctable errors using various BCH codes

n	k	t
7	4	1
15	11	1
	7	2
	5	3

The general block schematic of a convolutional coder is shown in Figure 5.6. In general, the shift register contains N k -bit stages. The input data is shifted into and along the shift register, k bits at a time. The number of output bits for each k bit user input data sequence is n bits. The code rate is $R_c = k/n$. The parameter N is called the *constraint length* and indicates the number of input data bits that the current output is dependent upon. A *trellis diagram* gives a compact representation of the structure of the encoder.

5.4 Puncturing

Puncturing can be employed to increase the code rate at the expense of bit-error-rate performance. Puncturing involves eliminating certain redundant bits in the code word. It can be accomplished by using an encoder followed by a bit selector which deletes some of the parity bits according to the given puncturing rule. Puncturing is usually done to the parity bits since removing systematic bits will degrade the performance of the coder severely. At the receiver, before decoding, zeros are inserted at the punctured bit locations. Thus, the technique called puncturing helps in

improving the code rate of the system at the expense of bit-error-rate performance.

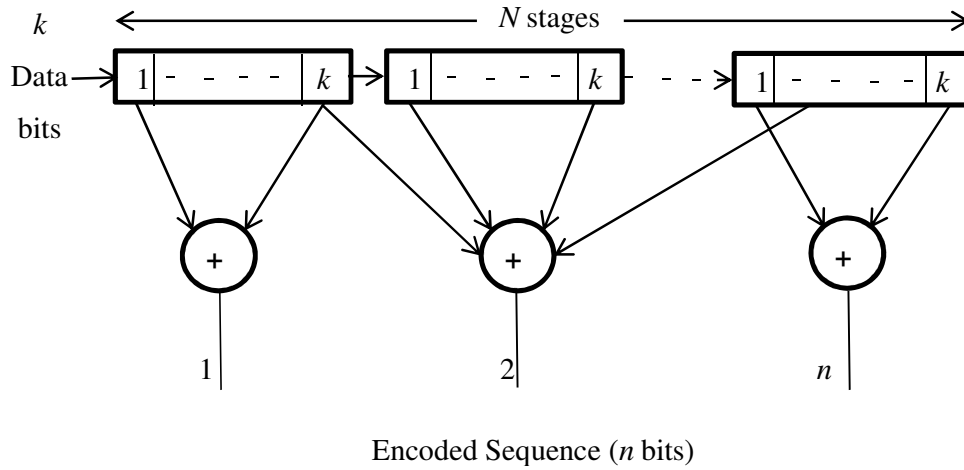


Fig. 5.6 General block diagram of a convolutional encoder

5.5 Interleaving

The errors occurring in a real communication scenario are often burst errors, which starts and ends with an error, the bits in between may or may not be erroneous. This results in unacceptable error rate performances in certain observation intervals. This problem can be resolved to some extent by changing the order of the sequence of transmitted symbols by the process of interleaving [14] and recovering the original order of sequence of the symbols at the receiver by a deinterleaver.

Figure 5.7 shows a block interleaver in which the data is written row-by-row into a rectangular array of m rows and n columns, and read out column-by-column by the interleaver before sending it over the channel. The reverse process is performed at the deinterleaver. The error bursts thus occurring due to channel effects get fairly distributed over time, resulting in an acceptable error rate performance. But, the use of interleaving results in

extra delay because deinterleaving can be started only after all the interleaved data (mn bits) is received.

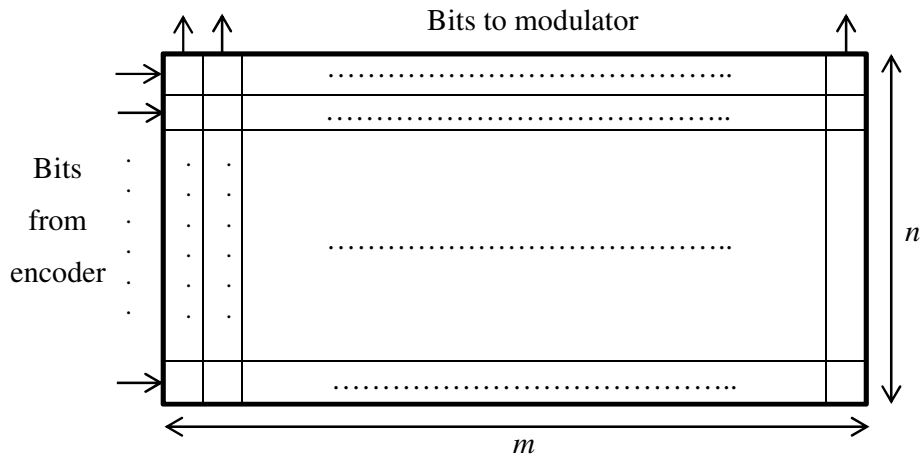


Fig. 5.7 Structure of a block interleaver

5.6 Diversity Techniques

Conventional point-to-point communication has a single transmitter communicating over the channel to a single receiver. Underwater acoustic communication environment is bandlimited by multipath due to reflections and scattering. To improve the error rate performance of underwater channel, diversity techniques can be employed. In telecommunications, a diversity scheme refers to a method for improving the reliability of a message signal by using two or more communication channels with different characteristics. Diversity is mainly used in radio communication and is a common technique for combatting fading, co-channel interference and avoiding error bursts. It is based on the fact that individual channels experience different levels of fading and interference. Multiple versions of the same signal may be transmitted and/or received and are combined in the receiver. Thus, diversity techniques may exploit the multipath propagation, resulting in better bit-error-rate performances.

The following classes of diversity schemes are possible:

- **Time diversity**, in which multiple versions of the same signal are transmitted at different time instants, as illustrated in Figure 5.8.
- **Frequency diversity**, in which, the signal is transmitted using multiple spectral bands, as illustrated in Figure 5.9.

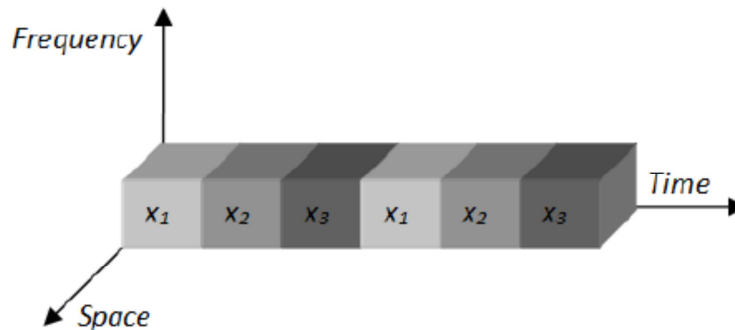


Fig. 5.8 Time diversity

- **Space diversity**, in which, the signal is transmitted over several different propagation paths. In the case of wired transmission, this can be achieved by transmitting via multiple wires. In the case of wireless transmission, it can be achieved by antenna diversity using multiple transmitters (transmit diversity) and/or multiple receivers (reception diversity). In the latter case, a diversity combining technique is applied before further signal processing takes place. Space-time diversity and space-frequency diversity are illustrated in Figures 5.10 and 5.11.

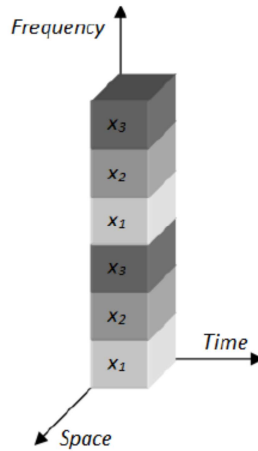


Fig. 5.9 Frequency Diversity

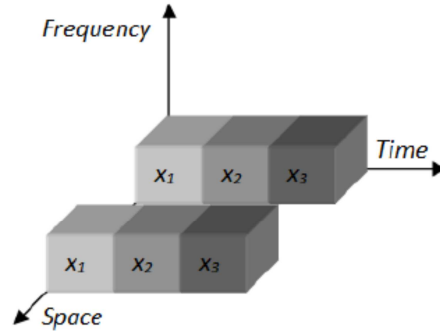


Fig. 5.10 Space-time diversity

5.6.1 Space-time coding

Space-time coding [155] is a method used in wireless communication to improve the reliability of the data transfer. Multiple copies of the symbols are transmitted from more than one transmitter in different time slots and the receiver uses the received versions in an optimal manner to reconstruct the signal. The space time coder encodes a single stream by sending each symbol at different time slots.

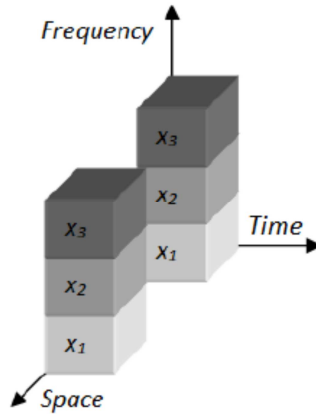


Fig. 5.11 Space-frequency diversity

One of the most commonly used space-time code is the Alamouti code. It is a complex orthogonal space-time code specialized for the case of two transmitters. The Alamouti Space-time block code [151] (STBC) for 2×1 and the 2×2 systems take two time-slots to transmit two symbols, thus maintaining the data rates fairly stable. The encoding scheme of Alamouti Space-time block code is as shown in Figure 5.12.

5.6.2 Alamouti STBC for 2×1 System

Figure 5.13 represents two transmitters and a single receiver system. In Alamouti STBC coding, two consecutive symbols x_1 and x_2 are encoded according to Table 5.2.

The Alamouti encoded signal is transmitted from two transmitters over two symbol periods. During the first symbol period, symbol x_1 is transmitted from the first transmitter and x_2 from the second transmitter simultaneously. During second symbol period, these symbols are

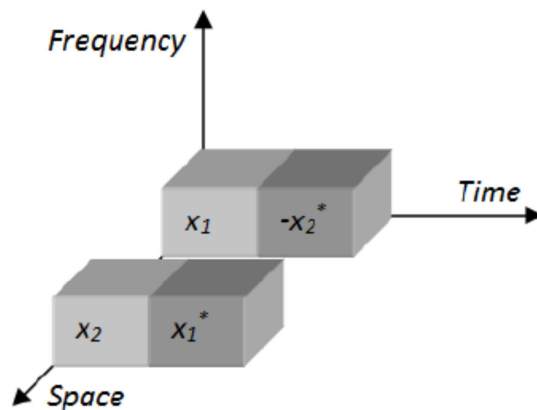


Fig. 5.12 Alamouti Space-time block coding

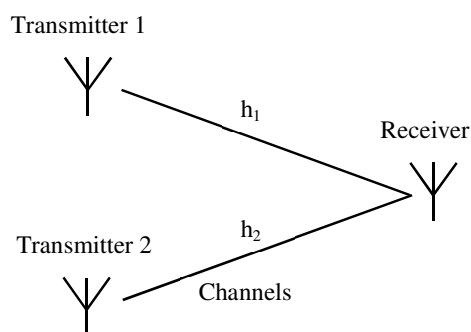


Fig. 5.13 2x1 System

Table 5.2 Encoding scheme with 2 transmitters

	Transmitter 1	Transmitter 2
Time Slot 1	x_1	x_2
Time Slot 2	$-x_2^*$	x_1^*

transmitted again, where $(-)x_2^*$ is transmitted from the first transmitter and x_1^* from the second transmitter simultaneously. It is assumed that the two channel impulse responses, $h_1(t)$ and $h_2(t)$ are time-invariant over 2 consecutive symbol periods, i.e. $h_1(t)=h_1$ and $h_2(t)=h_2$. Let y_1 and y_2 denote

the received signals during the first and second time slots respectively, so that

$$y_1 = h_1x_1 + h_2x_2 + z_1, \quad (5.10)$$

$$y_2 = h_1(-x_2^*) + h_2x_1^* + z_2, \quad (5.11)$$

where z_1 and z_2 denote the noise during the first and second time slots respectively. In matrix notation,

$$\begin{bmatrix} y_1 \\ y_2^* \end{bmatrix} = \begin{bmatrix} h_1 & h_2 \\ h_2^* & -h_1^* \end{bmatrix} \begin{bmatrix} x_1 \\ x_2 \end{bmatrix} + \begin{bmatrix} z_1 \\ z_2^* \end{bmatrix}, \quad (5.12)$$

where $H = \begin{bmatrix} h_1 & h_2 \\ h_2^* & -h_1^* \end{bmatrix}$ is a 2x2 channel matrix.

Multiplying both sides of equation (5.12) by the conjugate transpose of the channel matrix H yields the result:

$$\begin{aligned} \begin{bmatrix} h_1^* & h_2 \\ h_2^* & -h_1^* \end{bmatrix} \begin{bmatrix} y_1 \\ y_2^* \end{bmatrix} &= \begin{bmatrix} h_1^* & h_2 \\ h_2^* & -h_1^* \end{bmatrix} \begin{bmatrix} h_1 & h_2 \\ h_2^* & -h_1^* \end{bmatrix} \begin{bmatrix} x_1 \\ x_2 \end{bmatrix} + \begin{bmatrix} h_1^* & h_2 \\ h_2^* & -h_1^* \end{bmatrix} \begin{bmatrix} z_1 \\ z_2^* \end{bmatrix} \\ &= (|h_1|^2 + |h_2|^2) \begin{bmatrix} x_1 \\ x_2 \end{bmatrix} + \begin{bmatrix} h_1^*z_1 + h_2z_2^* \\ h_2^*z_1 - h_1z_2^* \end{bmatrix}. \end{aligned} \quad (5.13)$$

Equation (5.13) can be represented as,

$$\begin{bmatrix} \widetilde{y}_1 \\ \widetilde{y}_2 \end{bmatrix} = (|h_1|^2 + |h_2|^2) \begin{bmatrix} x_1 \\ x_2 \end{bmatrix} + \begin{bmatrix} \widetilde{z}_1 \\ \widetilde{z}_2 \end{bmatrix}, \quad (5.14)$$

where \widetilde{y}_1 and \widetilde{y}_2 represent the modified receiver versions of the transmitted symbols. Hence, from equation (5.14), the k^{th} symbol can be decoded as,

$$\widehat{x}_k = \frac{\widetilde{y}_k}{|h_1|^2 + |h_2|^2} \text{ for } k = 1, 2. \quad (5.15)$$

5.6.3 Alamouti STBC for 2x2 System

Figure 5.14 represent two transmitters and two receivers (2x2) system. Let h_{ij} denotes the channel impulse response from j^{th} transmitter to i^{th} receiver. Here also, the data is encoded as in Table 5.2 and the

channel parameters are assumed to remain constant during the two time slots, similar to the case of a 2x1 system.

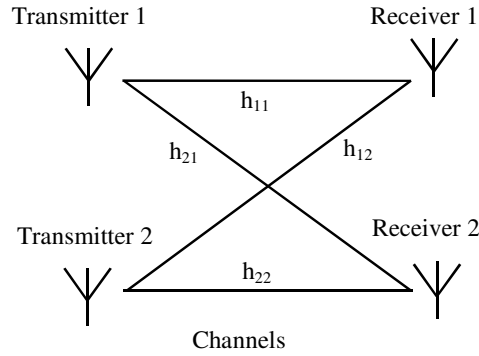


Fig. 5.14 2x2 System

The symbols received during first time slot by the two receivers, y_{11} and y_{12} , can be represented in the matrix form as

$$\begin{bmatrix} y_{11} \\ y_{12} \end{bmatrix} = \begin{bmatrix} h_{11} & h_{12} \\ h_{21} & h_{22} \end{bmatrix} \begin{bmatrix} x_1 \\ x_2 \end{bmatrix} + \begin{bmatrix} n_{11} \\ n_{12} \end{bmatrix}. \quad (5.16)$$

The symbols received during the second time slot by the two receivers, y_{21} and y_{22} , takes the matrix form,

$$\begin{bmatrix} y_{21} \\ y_{22} \end{bmatrix} = \begin{bmatrix} h_{11} & h_{12} \\ h_{21} & h_{22} \end{bmatrix} \begin{bmatrix} -x_2^* \\ x_1^* \end{bmatrix} + \begin{bmatrix} n_{21} \\ n_{22} \end{bmatrix}. \quad (5.17)$$

Combining (5.16) and (5.17),

$$\begin{bmatrix} y_{11} \\ y_{12} \\ y_{21}^* \\ y_{22}^* \end{bmatrix} = \begin{bmatrix} h_{11} & h_{12} \\ h_{21} & h_{22} \\ h_{12}^* & -h_{11}^* \\ h_{22}^* & -h_{21}^* \end{bmatrix} \begin{bmatrix} x_1 \\ x_2 \end{bmatrix} + \begin{bmatrix} n_{11} \\ n_{12} \\ n_{21}^* \\ n_{22}^* \end{bmatrix}, \quad (5.18)$$

where the channel matrix, $H = \begin{bmatrix} h_{11} & h_{12} \\ h_{21} & h_{22} \\ h_{12}^* & -h_{11}^* \\ h_{22}^* & -h_{21}^* \end{bmatrix}$.

Multiplying both the sides of equation (5.18) by the conjugate transpose of the channel matrix yields the result:

$$\begin{aligned}
& \begin{bmatrix} h_{11}^* & h_{21}^* & h_{12} & h_{22} \\ h_{12}^* & h_{22}^* & -h_{11} & -h_{21} \end{bmatrix} \begin{bmatrix} y_{11} \\ y_{12} \\ y_{21}^* \\ y_{22}^* \end{bmatrix} \\
&= \begin{bmatrix} h_{11}^* & h_{21}^* & h_{12} & h_{22} \\ h_{12}^* & h_{22}^* & -h_{11} & -h_{21} \end{bmatrix} \begin{bmatrix} h_{11} & h_{12} \\ h_{21} & h_{22} \\ h_{12}^* & -h_{11}^* \\ h_{22}^* & -h_{21}^* \end{bmatrix} \begin{bmatrix} x_1 \\ x_2 \end{bmatrix} \\
&\quad + \begin{bmatrix} h_{11}^* & h_{21}^* & h_{12} & h_{22} \\ h_{12}^* & h_{22}^* & -h_{11} & -h_{21} \end{bmatrix} \begin{bmatrix} n_{11} \\ n_{12} \\ n_{21}^* \\ n_{22}^* \end{bmatrix} \\
&= (|h_{11}|^2 + |h_{12}|^2 + |h_{21}|^2 + |h_{22}|^2) \begin{bmatrix} x_1 \\ x_2 \end{bmatrix} \\
&\quad + \begin{bmatrix} h_{11}^* n_{11} + h_{21}^* n_{12} + h_{12} n_{21}^* + h_{22} n_{22}^* \\ h_{12}^* n_{11} + h_{22}^* n_{12} - h_{11} n_{21}^* - h_{21} n_{22}^* \end{bmatrix}. \quad (5.19)
\end{aligned}$$

In line with the 2x1 STBC system, equation (5.19) can be represented as:

$$\begin{bmatrix} \widetilde{y}_1 \\ \widetilde{y}_2 \end{bmatrix} = (|h_{11}|^2 + |h_{12}|^2 + |h_{21}|^2 + |h_{22}|^2) \begin{bmatrix} x_1 \\ x_2 \end{bmatrix} + \begin{bmatrix} \widetilde{z}_1 \\ \widetilde{z}_2 \end{bmatrix}, \quad (5.20)$$

where \widetilde{y}_1 and \widetilde{y}_2 represent the modified receiver versions of the transmitted symbols. Similar to the 2x1 system, the k^{th} symbol can be decoded from equation (5.20) as:

$$\widehat{x}_k = \frac{\widetilde{y}_k}{|h_{11}|^2 + |h_{12}|^2 + |h_{21}|^2 + |h_{22}|^2} \text{ for } k = 1, 2. \quad (5.21)$$

It can be seen from equations (5.15) and (5.21) that Alamouti STBC offers a simple linear decoding mechanism, thus making the receiver structure less complex.

5.7 Spatial Multiplexing

Spatial Multiplexing is a method of MIMO in which original data stream is divided into independent data streams and are transmitted using

multiple radiators. The transmitted signals get mixed up in the channel and have to be detected in the receiver. Spatial Multiplexing uses multiple transmitters as well as receivers.

Given fixed bandwidth and transmission power, there is a trade-off between the data rate and error rate. Spatial Multiplexing is a way by which data rate can be improved. This technique uses multiple radiators at the transmitter and receiver to offer higher channel capacity. A high rate bit stream is divided into independent bit streams which are transmitted using multiple radiators. These signals get mixed in the channel as they use same frequency spectrum. At the receiver individual bit streams are separated, estimated and merged together to yield the original signal. The number of receive elements must be equal to or greater than the number of transmit elements, ie. $N \geq M$ required, where N is the number of receive elements and M is the number of transmit elements. The receiver must have proper channel knowledge so as to apply equalization techniques, to reconstruct the data. Figure 5.15 shows a general MIMO system.



Fig. 5.15 MIMO System

5.8 Dictionary based Sparse Channel Estimation Technique

When a signal is sparse in a known transform domain, compressive sensing (CS) helps to reconstruct it with much fewer samples than that required by the dimensions of the domain. Compressive sensing [31] has numerous applications like coding, image compression, source separation,

etc., of which sparse channel estimation in the field of communications is of significant importance.

A signal $x(n)$ of dimension $N \times 1$ can be compressed to \mathbf{y} of dimension $M \times 1$ as seen in section 3.1. The signal \mathbf{x} can be reconstructed from \mathbf{y} , which appears to be an incomplete set of observations by taking

$$M \geq L \log(N/L), \quad (5.22)$$

measurements [31].

Channel Estimation involves transmitting known signals (pilots) through an unknown channel H , and utilizing the received pilots to estimate the unknown channel with sufficient accuracy. Then, the estimated channel \hat{H} is used to decode the received signals that are unknown to the receiver. Compressive sensing based channel estimation is used to estimate channels whose impulse responses are sparse or at least approximately sparse.

Let T denote the OFDM symbol duration then, the subcarrier spacing is $\frac{1}{T}$ and the k^{th} subcarrier is at frequency $f_k = f_c + \frac{k}{T}$, $k = -\frac{K}{2}, \dots, \frac{K}{2} - 1$, where f_c is the carrier frequency and K is the number of subcarriers used. The multipath channel can be modeled as,

$$h = \sum_{n=1}^N \xi_n \delta(\tau - \tau_n), \quad (5.23)$$

where N is the number of multipaths, τ_n is the n^{th} path delay and ξ_n is the amplitude associated with n^{th} path. Let the transmitted set of pilots be represented as

$$S_P = \{p_1, p_2, \dots, p_P\}, \quad (5.24)$$

where P is the number of pilots used for channel estimation.

The signals gets distorted by the channel and added upon by the noise, which can be represented as

$$y(n) = s(n) \otimes h(n) + a(n), \quad (5.25)$$

where $s(n)$ is the transmitted signal, $a(n)$ is the noise, $h(n)$ is the channel impulse response and $y(n)$ is the received signal. Equation (5.25) can be represented in frequency domain as

$$Y = SH + Z, \quad (5.26)$$

where Y , S , H and Z are frequency domain counterparts of $y(n)$, $s(n)$, $h(n)$ and $a(n)$ respectively, which can also be written as

$$Y = \text{diag}(S)F\xi + Z, \quad (5.27)$$

where F is the DFT transformation matrix and ξ of size $N \times 1$ is the channel parameter to be estimated.

The input-output relation can be expressed from equation (5.27) as,

$$\begin{bmatrix} y_1 \\ \vdots \\ y_N \end{bmatrix} = \begin{bmatrix} s_1 & 0 & 0 & 0 \\ 0 & s_2 & 0 & 0 \\ 0 & 0 & \ddots & 0 \\ 0 & 0 & 0 & s_N \end{bmatrix} \begin{bmatrix} e^{-j2\pi\frac{k_1\tau_1}{T}} & e^{-j2\pi\frac{k_1\tau_2}{T}} & \dots & e^{-j2\pi\frac{k_1\tau_{max}}{T}} \\ e^{-j2\pi\frac{k_2\tau_1}{T}} & e^{-j2\pi\frac{k_2\tau_2}{T}} & \dots & e^{-j2\pi\frac{k_2\tau_{max}}{T}} \\ \vdots & \vdots & \dots & \vdots \\ e^{-j2\pi\frac{k_K\tau_1}{T}} & e^{-j2\pi\frac{k_K\tau_2}{T}} & \dots & e^{-j2\pi\frac{k_K\tau_{max}}{T}} \end{bmatrix} \begin{bmatrix} \xi_1 \\ \vdots \\ \xi_N \end{bmatrix} + \begin{bmatrix} \eta_1 \\ \vdots \\ \eta_N \end{bmatrix}, \quad (5.28)$$

where the set of subcarriers are $\{k_1, k_2, \dots, k_K\}$. The delays are

$$\tau \in \{\tau_1, \tau_2, \tau_3, \dots, \tau_{max}\}, \quad (5.29)$$

with $\tau_1 = 0$ and $\tau_{max} = T_g$, where τ_{max} is the maximum channel delay spread and T_g is the guard interval.

Equation (5.28) can be written using equation (5.29) as

$$Y = \text{diag}(S)\gamma\xi + Z, \quad (5.30)$$

where γ is the dictionary matrix [145].

Since underwater channels are usually sparse, the impulse responses can be estimated by using a limited number of pilots via CS-based algorithms. For P pilots, equation (5.30) can be written as

$$\begin{bmatrix} y_1 \\ \vdots \\ y_P \end{bmatrix} = \begin{bmatrix} s_{p_1} & 0 & 0 & 0 \\ 0 & s_{p_2} & 0 & 0 \\ 0 & 0 & \ddots & 0 \\ 0 & 0 & 0 & s_{p_P} \end{bmatrix} \begin{bmatrix} 1 & e^{-j2\pi\frac{p_1\bar{\tau}_2}{T}} & \dots & e^{-j2\pi\frac{p_1\bar{\tau}_P}{T}} \\ 1 & e^{-j2\pi\frac{p_2\bar{\tau}_2}{T}} & \dots & e^{-j2\pi\frac{p_2\bar{\tau}_P}{T}} \\ \vdots & \vdots & \dots & \vdots \\ 1 & e^{-j2\pi\frac{p_P\bar{\tau}_2}{T}} & \dots & e^{-j2\pi\frac{p_P\bar{\tau}_P}{T}} \end{bmatrix} \begin{bmatrix} \xi_1 \\ \vdots \\ \xi_N \end{bmatrix} + \begin{bmatrix} \eta_1 \\ \vdots \\ \eta_P \end{bmatrix}, \quad (5.31)$$

where $0, \bar{\tau}_2, \bar{\tau}_3, \dots, \bar{\tau}_P$ are the path delays.

Equation (5.31) can be represented as

$$Y_P = A\xi + Z, \quad (5.32)$$

where $A = \text{diag}(S_{pilots})\gamma_{pilots}$ is of size $P \times N$.

ℓ_1 minimization for estimation of $\hat{\xi}$ can be written as,

$$\text{minimize } \|A\xi - Y_P\|^2 + \lambda\|\xi\|_1, \quad (5.33)$$

where $\lambda > 0$ is the regularization or tuning parameter which controls the solution sparsity.

Convex optimization using CVX has been utilized for estimating the channel coefficients. CVX is a MATLAB based modeling system for handling complex convex optimization problems. It turns MATLAB into a modeling language, allowing constraints and objectives to be specified using standard expression syntax. Upon estimating the channel coefficients $\hat{\xi}$ using equation (5.33), the channel coefficients at all subcarriers are reconstructed from the dictionary as

$$\hat{H} = \gamma\hat{\xi}. \quad (5.34)$$

The equalization is performed to estimate the signal at the receiver as

$$\hat{X}(f) = \frac{Y(f)}{\hat{H}(f)}, \quad (5.35)$$

where $Y(f)$ is the received signal in the frequency domain.

5.8.1 Algorithm for Sparse Channel Estimation

During transmission, the data stream is divided into parallel bit streams, followed by modulation. Pilots are inserted at regular intervals and the IFFT of the modulated signal is computed followed by guard band insertion for eliminating ISI. The signal gets corrupted by the ambient noise as well as the channel. At the receiver, the guard band is removed and the modulated signal is extracted followed by dictionary generation from the received pilots. Depending on the received pilots Y_p , $\hat{\xi}$ and hence \hat{H} , are estimated by the dictionary based sparse channel estimation. Equalization is performed using the computed channel impulse response and the resultant signal is demodulated to reconstruct the binary data followed by bit-error-rate computation. The algorithmic procedure for the dictionary based sparse channel estimation at the receiver is given in ALGORITHM 5.1.

5.9 Synchronization Issues in Practical OFDM Scenario

OFDM carries data on orthogonal sub carriers and the orthogonality of the sub carriers has to be maintained in order to get all the advantages of OFDM. If the orthogonality is not properly maintained, the performance of OFDM will be degraded due to the phenomena of inter symbol interference (ISI) and inter carrier interference (ICI). Due to the unpredictable channel effects, the receiver in OFDM may sample a new frame at the incorrect time instant, which leads to Symbol Time Offset (STO). In practical situations, a frequency mismatch between local oscillators at the transmitter and receiver or Doppler frequency shifts may lead to Carrier Frequency Offset (CFO) problem in OFDM, as well. In underwater, Doppler shift is considerably a larger fraction of signal frequency than for radar due to higher ratio of vehicle speed to wave propagation speed [11]. Frequency

offset destroys orthogonality among the subcarriers leading to inter carrier interference (ICI). Hence, estimation of STO and CFO are very critical in practical scenarios [93, 96, 97].

ALGORITHM 5.1: Dictionary Based Sparse Channel

Estimation Procedure

Begin

Cyclic Prefix Removal

Computation of FFT of received signals ($Y(f)$)

Pilot extraction (Y_p)

Dictionary building (γ)

Convex optimization using CVX and $\hat{\xi}$ estimation

$\min \|A\xi - Y_p\|^2 + \lambda\|\xi\|_1$

Channel Construction from Dictionary $\hat{H} = \gamma\hat{\xi}$

Equalization $\left(\frac{Y(f)}{\hat{H}(f)}\right)$

Demodulation and BER computation

End

For taking the N-point FFT at the receiver the exact samples of the transmitted signal for OFDM symbol duration is an essential requirement. Thus, timing synchronization must be performed at the receiver to detect the beginning of the each OFDM symbol. The local oscillators at the transmitter and receiver perform up/down conversion of the baseband signal. Any Doppler frequency shift or a mismatch of frequency between the transmitter and receiver local oscillators will lead to ICI. Thus, frequency synchronization must also be performed at the receiver for minimizing the effects of ICI.

5.9.1 STO Estimation

Symbol Time Offset (STO) is the difference between the actual symbol start position and the expected symbol start position at the OFDM receiver. Let us consider an OFDM symbol with a cyclic prefix of N_G

samples over T_G duration and an effective data of N_{sub} samples over T_{sub} duration. The cyclic prefix and the corresponding data part share similarities since cyclic prefix is a replica of the last part of the data in a symbol and this similarity can be used for STO estimation. Two sliding windows, W_1 and W_2 are used to find the similarities between the samples in these windows [93], as shown in Figure 5.16. The point of maximum similarity between the values in the two windows can be found by correlation method or difference method. Thus, the beginning of the symbol can be identified perfectly without any additional transmission overhead with the help of STO estimation by correlation method or STO estimation by difference method.

Let y_l be the l^{th} symbol received and N , the distance between corresponding samples in cyclic prefix and the data part. The STO $\hat{\delta}$ can be estimated by finding the point of maximum correlation between the two blocks in windows, W_1 and W_2 as

$$\hat{\delta} = \max\{\sum_i |y_l[n+i]y_l^*[n+N+i]|\}. \quad (5.36)$$

STO can also be estimated by finding the point where the squared difference between the two blocks in windows, W_1 and W_2 , is minimum.

$$\hat{\delta} = \min\{\sum_i (|y_l[n+i]| - |y_l^*[n+N+i]|)^2\}. \quad (5.37)$$

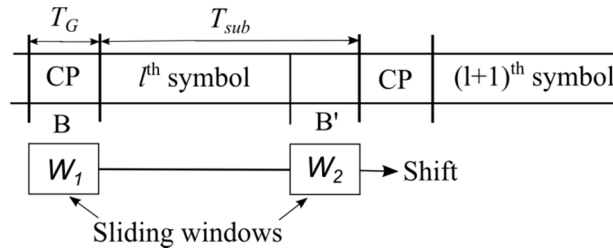


Fig. 5.16 STO Estimation

5.9.2 CFO Estimation

The Carrier Frequency Offset (CFO) is caused by the frequency mismatch between local oscillators at the transmitter and receiver or by the Doppler frequency shift, which is due to the relative motion between the transmitter and the receiver in mobile environments. The normalized CFO, ε is defined as a ratio of the frequency offset, f_o to the subcarrier spacing Δf .

$$i.e., \varepsilon = \frac{f_o}{\Delta f}. \quad (5.38)$$

The received signal in an OFDM receiver is,

$$Y(k) = H(k)X(k) + Z(k), \quad (5.39)$$

where $Y(k)$, $X(k)$, $H(k)$ and $Z(k)$ are frequency domain counterparts of the received signal, the transmitted signal, the channel impulse response and the noise, respectively. The received base band signal,

$$\begin{aligned} y(n) &= IDFT \{Y(k)\} = IDFT \{H(k)X(k) + Z(k)\} \\ &= \frac{1}{N} \sum_{k=0}^{N-1} H(k)X(k)e^{j2\pi kn/N} + z(n). \end{aligned} \quad (5.40)$$

When the effect of ε is incorporated, the base band signal becomes,

$$y(n) = \frac{1}{N} \sum_{k=0}^{N-1} H(k)X(k)e^{j2\pi(k+\varepsilon)n/N} + z(n). \quad (5.41)$$

Taking FFT of the received samples, the received symbol across the l^{th} subcarrier is,

$$\begin{aligned} Y(l) &= \sum_n y(n)e^{-j2\pi nl/N} \\ &= \frac{1}{N} \sum_n \sum_{k=0}^{N-1} H(k)X(k)e^{j2\pi(k+\varepsilon-l)n/N} + \sum_n z(n)e^{-j2\pi ln/N}. \end{aligned} \quad (5.42)$$

Splitting the R.H.S. of equation (5.42) for $k = l$ (Desired part) and $k \neq l$ (Interference part)

$$Y(l) = \frac{1}{N} H(l)X(l) \sum_n e^{j2\pi n\epsilon/N} + \frac{1}{N} \sum_n \sum_{\substack{k=0 \\ k \neq l}}^{N-1} H(k)X(k) e^{j2\pi(k+\epsilon-l)n/N} + Z(l). \quad (5.43)$$

Equation (5.43) consists of three parts, the first part is the desired signal, the second part is the ICI due to the presence of ϵ and the third part is the noise. Solving the summation as a sum of Geometric Progression, equation (5.43) can be written as,

$$Y(l) = \frac{1}{N} H(l)X(l) \frac{\sin(\pi\epsilon)}{\sin(\pi\epsilon/N)} e^{j\pi\epsilon(N-1)/N} + \frac{1}{N} \sum_{\substack{k=0 \\ k \neq l}}^{N-1} H(k)X(k) \frac{\sin(\pi(k+\epsilon-l))}{\sin(\frac{\pi(k+\epsilon-l)}{N})} e^{j\pi(k+\epsilon-l)(N-1)/N} + Z(l). \quad (5.44)$$

Hence,

$$Y(l) = \frac{1}{N} H(l)X(l) \frac{\sin(\pi\epsilon)}{\sin(\pi\epsilon/N)} e^{j\pi\epsilon(N-1)/N} + ICI + Noise. \quad (5.45)$$

Thus, any frequency offset destroys the orthogonality of the OFDM subcarriers and results in ICI as shown in Figure 5.17, which necessitates the estimation of CFO.

A CFO of ϵ results in a phase shift of $2\pi n\epsilon/N$. Let the l^{th} symbol be $x_l(n)$ and assuming that it gets affected by a CFO of ϵ yields $y_l(n)$ as,

$$y_l(n) = x_l(n) e^{j2\pi n\epsilon/N}. \quad (5.46)$$

Replacing n by $n+N$,

$$y_l(n+N) = x_l(n+N) e^{j2\pi(n+N)\epsilon/N}. \quad (5.47)$$

The cyclic prefix and the tail end of the data part, which are spaced N samples apart, are same, *i.e.*, $x_l(n+N) = x_l(n)$.

$$\text{Hence, } y_l(n+N) = x_l(n) e^{j2\pi n\epsilon/N} e^{j2\pi\epsilon}. \quad (5.48)$$

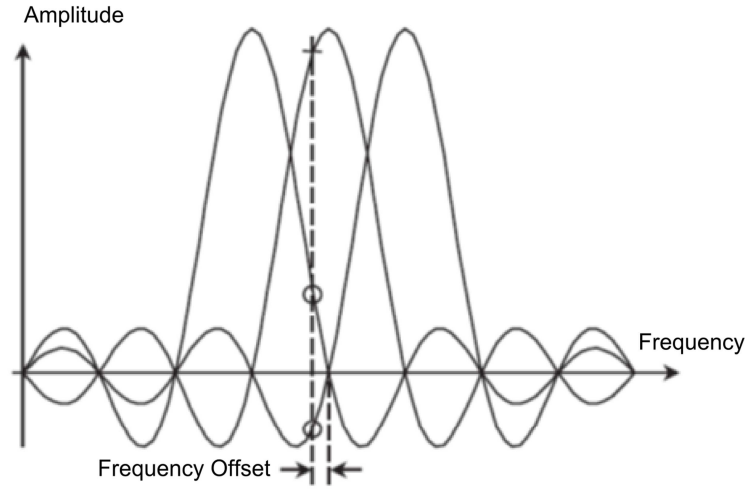


Fig. 5.17 Illustration of ICI due to frequency offset

Thus, the phase difference between cyclic prefix and the corresponding tail end of an OFDM symbol (spaced N samples apart) caused by CFO ε is, $\frac{2\pi N\varepsilon}{N} = 2\pi\varepsilon$. Thus, the CFO can be found from the phase angle of the product of cyclic prefix and the corresponding tail end of an OFDM symbol [94-95]. The estimated CFO, $\hat{\varepsilon}$ is given by,

$$\hat{\varepsilon} = \frac{1}{2\pi} \text{arg}\{\sum_{n=1}^{N_G} y_l^*[n]y_l[n+N]\}. \quad (5.49)$$

Pilots, which are inserted into an OFDM symbol can be used for tracking the carrier frequency. To facilitate this, the receiver transforms the symbols, $y_l[n]$ and $y_{l+D}[n]$, into frequency domain $Y_l[k]$ and $Y_{l+D}[k]$ via FFT, from which pilot tones and CFO are estimated, using [101]

$$\hat{\varepsilon} = \frac{1}{2\pi T_{sub}} \max\{|\sum_{j=0}^{L-1} Y_{l+D}(p(j))Y_l^*(p(j))X_{l+D}(p(j))X_l(p(j))|\}. \quad (5.50)$$

where T_{sub} denotes the valid symbol duration, L the number of pilot tones, $p(j)$, the location of the j^{th} pilot tone, $X_l(p(j))$ shows the pilot tone located

at $p(j)$ at the l^{th} symbol period, Y_{l+D} and Y_l are the received symbols and X_{l+D} and X_l are the respective transmitted symbols.

5.10 Summary

The characteristic property of the OFDM is orthogonality among the subcarriers, which are obtained by splitting the band into closely spaced orthogonal subcarriers. This property ensures the reduction in Inter Carrier Interference (ICI). Channel coding schemes like block codes and convolutional codes were briefly studied. The technique of interleaving and its advantages were also discussed. Different diversity techniques as well as the most commonly used Alamouti space-time diversity technique were also investigated. Estimation of channel by utilizing the sparsity of the channel has also been outlined. This chapter also presented the methodology of various STO and CFO estimation techniques.

CHAPTER 6

RESULTS AND DISCUSSIONS

The performance of the proposed matrix padding method is compared with l_1 -ls, l_1 -magic, YALL1, OMP, CoSaMP, etc. and the results of comparison in terms of signal-to-noise ratio, correlation and mean squared error, have been investigated. OFDM has been simulated using QAM and PSK based modulation techniques for undersea acoustic links. The performances of various orders of QAM based OFDM systems for undersea acoustic communications have been studied and the bit-error-rates under various Signal to Noise Ratio conditions have also been compared for AWGN and Underwater Channels for 16-QAM based OFDM. The bit-error-rate performances of normal as well as coded OFDM with and without interleaving schemes have been simulated for various signal-to-noise ratio levels for both convolutional and BCH codes. The performance of the proposed coded STBC system has been compared with 2x1 and 2x2 STBC systems. The performances of various STO as well as CFO estimation methods have been compared and it has been observed that STO estimation using difference method and CFO estimation using pilot based method guarantee acceptable performances. The undersea channel has been estimated using dictionary based sparse channel estimation technique for various ranges using different number of pilots and it has been found that by using a minimum number of pilots, acceptable BER performance can be achieved.

6.1 Background

A method for sparse signal reconstruction using matrix padding and LMS based adaptation had been presented in section 4.2. The sounds generated by 3-blade engine, music, speech, etc. (available in the databank of research lab) have been used to validate and compare the performance of the proposed technique with the other existing compressive sensing algorithms in ideal and noisy environments. The results of this method have been compared with some of the convex optimization methods as well as greedy methods, under section 6.2.

Ocean is a dynamic and complex environment, which demands advanced signal processing for optimum undersea acoustic communication. Multicarrier modulation in the form of OFDM facilitates high-rate transmission over complex channels. The results of comparison of performances of an acoustic channel with an AWGN channel for 16-QAM based OFDM are included in this chapter. These results motivated the investigation of performances of coded and interleaved versions of OFDM over underwater acoustic channels. The comparison of performances of convolutional coded and BCH (7,4) coded OFDM systems with and without interleaving for BPSK and DPSK based OFDM systems is also included in this chapter. The performances of BCH (15, 11) and BCH (15, 7) coded OFDM with and without interleaving have also been compared.

The higher reliability offered by STBC diversity technique created a curiosity for studying its performance for undersea acoustic links. The simulation results of normal STBC and the proposed coded STBC system for an undersea acoustic link are also studied. The importance of synchronization in OFDM motivated the investigation of various timing and frequency synchronization techniques. The results of STO and CFO

estimation techniques as well as dictionary based sparse channel estimation for undersea acoustic links have also been presented.

6.2 Performance of Matrix Padding Technique

The algorithms for compression (Algorithm 4.1) and reconstruction (Algorithm 4.2) using the matrix padding method has been given in Section 4.2.1. The proposed matrix padding method for compressive sensing has been simulated under noiseless and noisy environments and the performance of this approach has been *vis-a-vis* compared with a few of the widely used compressive sensing recovery methods like ℓ_1 -magic, ℓ_1 _ls, YALL1, OMP and CoSaMP discussed in section 3.2. Comparison of the performances of the various algorithms has been performed in terms of signal-to-noise ratio (SNR), correlation and mean squared error (MSE).

In the simulation studies, the number of samples per frame is chosen to be 2048, which resulted in 22 frames for the test signal and the tapped delay line structure has been used for the LMS adaptation with 32 weights, obtained on the basis of the well-established trial and error method.

Let x be the original signal and x' , the recovered signal. The signal-to-noise ratio is computed using

$$\text{SNR} = 10 \log \frac{\sum x^2}{\sum (x-x')^2}. \quad (6.1)$$

The correlation is computed as

$$R_{xx'} = \frac{\sum x x'}{\sqrt{\sum x^2 \sum x'^2}}. \quad (6.2)$$

The mean squared error is computed using

$$\text{MSE} = \frac{1}{n} \sum (x - x')^2. \quad (6.3)$$

6.2.1 Performance Comparison under Noiseless Scenario

Figures 6.1, 6.2 and 6.3 show the results of comparison of the performances of the proposed matrix padding method with the widely used compressive sensing recovery algorithms at 50% compression. The plots show the values of signal-to-noise ratio, correlation and mean squared error for the sparse recovery algorithms under consideration.

From figure 6.1, it can be seen that in the noiseless case, the proposed matrix padding method offers an SNR value of around 30dB and other convex optimization techniques offer an SNR above 29dB, whereas the greedy methods offer an SNR of nearly 27dB.

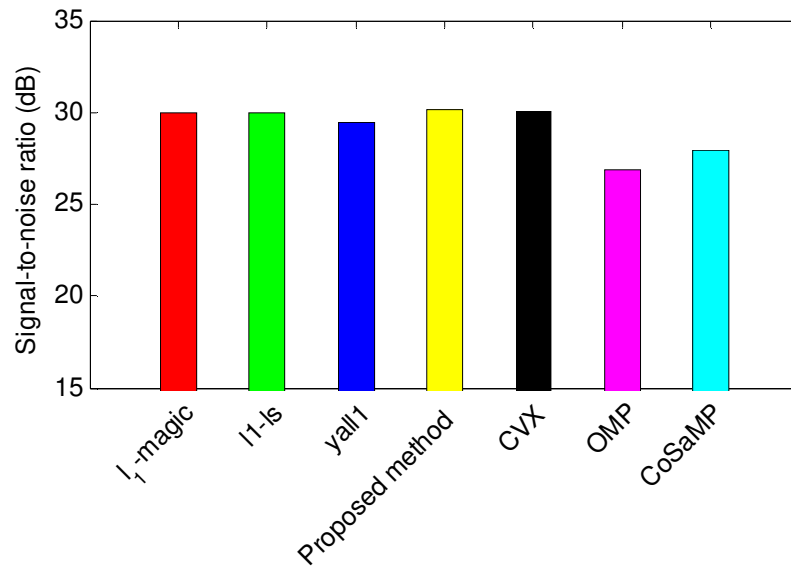


Fig. 6.1 Comparison of Signal-to-noise ratio Performance of the proposed matrix padding method with the other compressive sensing methods

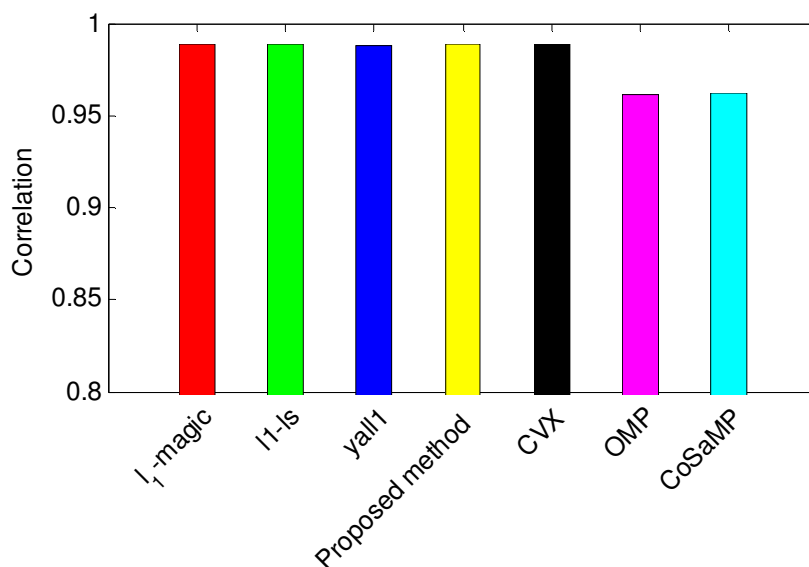


Fig. 6.2 Comparison of the Correlation Performance of the proposed matrix padding method with the other compressive sensing methods

From figure 6.2, it is clear that the proposed matrix padding method as well as the other convex optimization techniques give a correlation factor above 0.988, whereas the greedy methods offer a correlation factor close to 0.96. Similarly, from figure 6.3, it is clear that the proposed matrix padding method as well as other convex optimization techniques offer an MSE value close to 5×10^{-4} , whereas the MSE value of greedy methods are as high as 1.8×10^{-3} .

These plots reveal that the ℓ_1 -ls, ℓ_1 -magic, YALL1, CVX and the proposed method give comparable and good performance under noiseless scenarios, whereas the signal-to-noise ratio, correlation and mean squared error values of OMP and CoSaMP show that these greedy methods do not guarantee adequate performance. This improvement in performance of the proposed matrix padding method is due to the robustness offered by LMS adaptation.

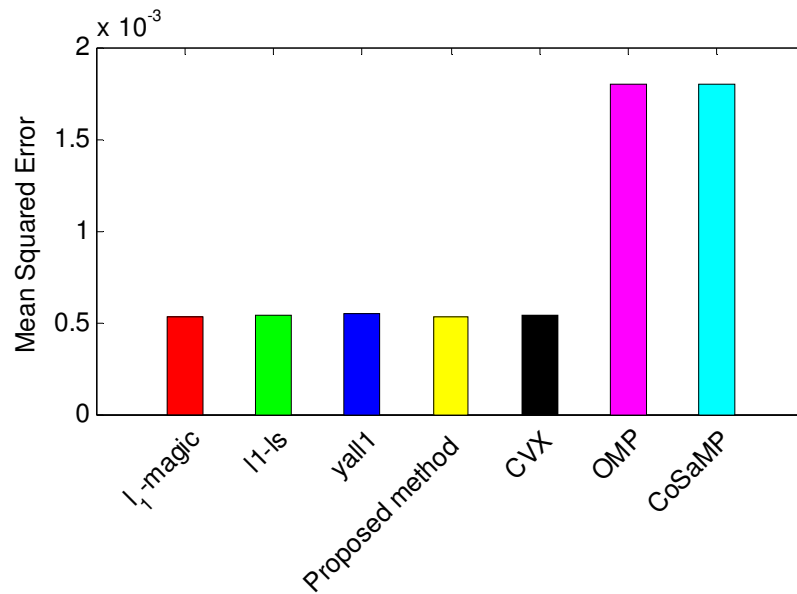


Fig. 6.3 Comparison of the Mean Squared Error Performance of the proposed matrix padding method with the other compressive sensing methods

6.2.2 Performance Comparison under Gaussian Noise

Figures 6.4, 6.5 and 6.6 show the comparison of the performances of the proposed matrix padding method with the widely used compressive sensing recovery methods, ℓ_1 -magic, ℓ_1 -ls, YALL1, CVX, OMP and CoSaMP, under noisy environment. The plots show the variations of output signal-to-noise ratio, correlation and mean squared error with respect to the SNR variation at the input.

It can be seen from figure 6.4 that YALL1 and ℓ_1 -magic offer similar SNR performances. OMP and CoSaMP offer better performances compared to ℓ_1 -ls, which is better than YALL1 and ℓ_1 -magic. The proposed matrix padding method as well as CVX offers good performances even at low SNR input values.

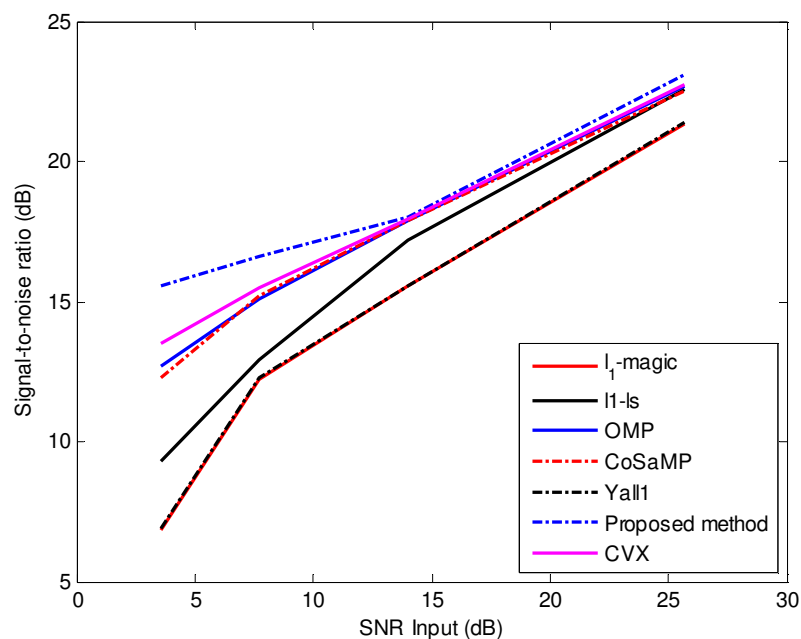


Fig. 6.4 Comparison of Signal-to-noise ratio Performance of the proposed matrix padding method with the other compressive sensing methods

As shown in figure 6.5, the proposed matrix padding method as well as CVX offer reasonable correlation performances even at low SNR inputs, while others do not guarantee good performance at low SNR inputs.

The simulation studies thus demonstrate the feasibility of improving sparse recovery using the proposed matrix padding technique in both ideal and noisy environments. The mean square error performance of this method is found to be negligibly small when compared to the other compressive sensing algorithms as shown in figure 6.6. Thus, the proposed matrix padding sparse recovery algorithm can be effectively used in practical communication scenarios.

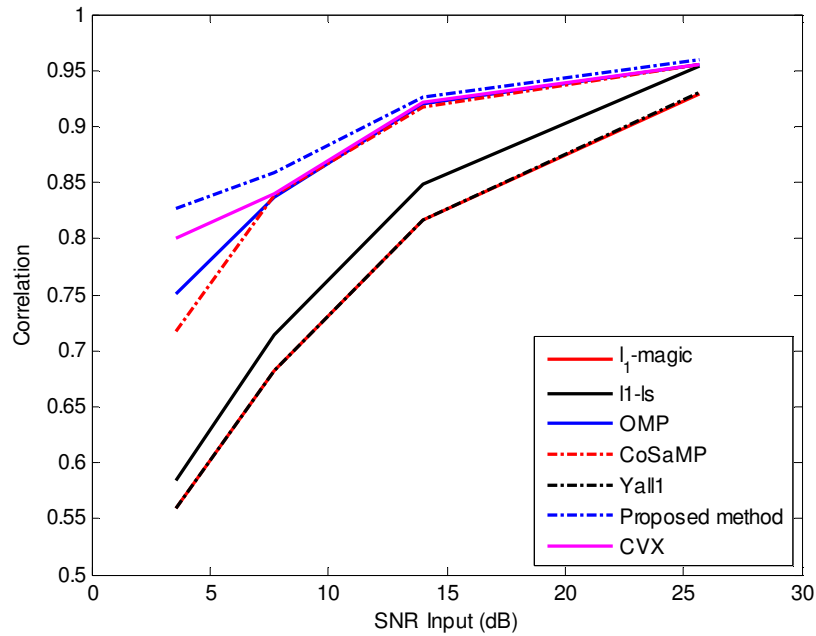


Fig. 6.5 Comparison of the Correlation Performance of the proposed matrix padding method with the other compressive sensing methods

At high input signal-to-noise ratios, all the methods show comparable performances. But, as the input signal-to-noise ratio decreases the performance of the proposed method is much better than that of the rest of the methods. CVX also performs good even at low input signal-to-noise ratios. OMP and CoSaMP also perform better compared to l_1 -magic, l_1 -ls and YALL1 as the SNR at the input decreases. Thus, the noise immunization of the proposed matrix padding method is better compared to the other recovery algorithms considered.

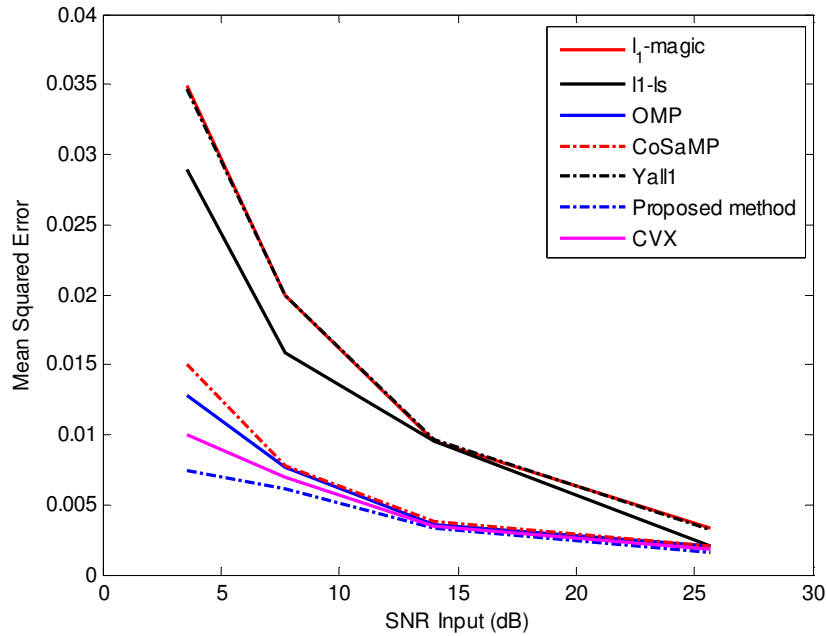


Fig. 6.6 Comparison of the Mean Squared Error Performance the proposed matrix padding method with the other compressive sensing methods

6.3 BER Performance of OFDM for Undersea Acoustic Links

The system model of OFDM has been given in section 4.4. OFDM has been simulated using a data stream comprising of 2048 bits per OFDM symbol using 16-QAM and a comparison of the bit-error-rates under various Signal to Noise Ratio conditions have also been simulated for AWGN and Underwater Channels and is plotted as in Figure 6.7. As expected, the bit-error-rate of AWGN channel is smaller than that of underwater acoustic channel for all SNR values.

The 16-PSK based OFDM for an undersea channel has also been simulated. Figures 6.8 and 6.9 show the constellation diagram for the

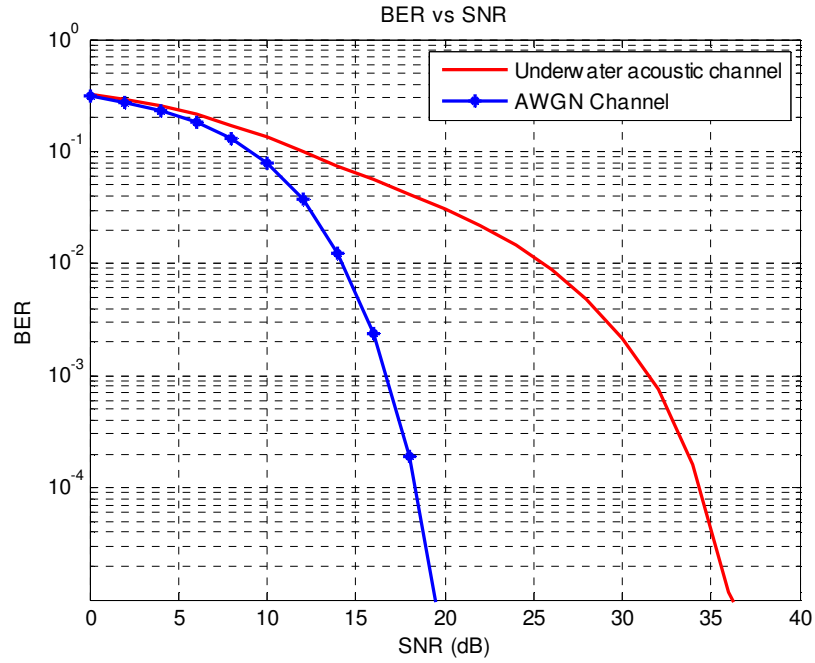


Fig. 6.7 Comparison of bit-error-rate performances of the AWGN channel with an Underwater Acoustic channel

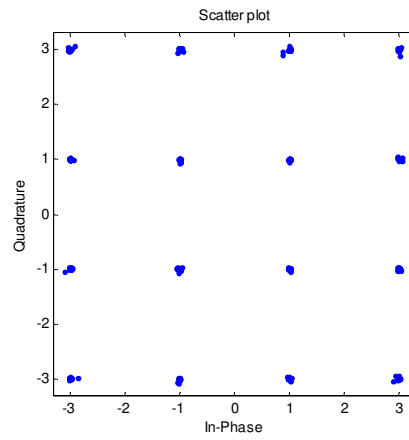


Fig. 6.8 Constellation Diagram of Received 16-QAM Symbols

received 16-QAM and 16-PSK symbols respectively. From the simulation studies, it has been observed that 16-QAM based OFDM offers lower bit-error-rates than that for the 16-PSK based OFDM, due to larger distance between the closest points in the constellation diagram. Figure 6.10 shows the variation of BER for 16-QAM and 16-PSK based OFDM with respect to the SNR variations whereas figure 6.11 shows the plot of a few of original and recovered data for 16-QAM based OFDM through the underwater channel.

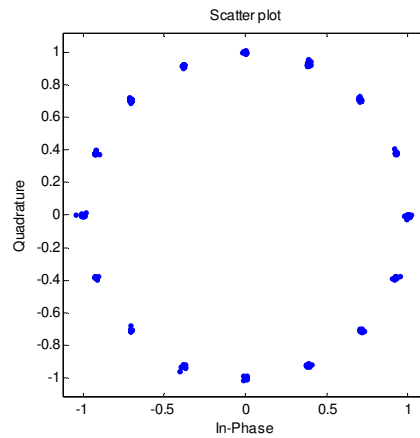


Fig. 6.9 Constellation Diagram of Received 16-PSK Symbols

The order of QAM has also been varied for QAM based OFDM systems, to study the trend of bit-error-rate performances. As the number of points in the constellation plot of QAM increases, the bit-error-rate increases, due to decrease in the distance between the points in the constellation plot. Figure 6.12 show the variation of BER for 4-QAM, 16-QAM and 256-QAM based OFDM systems. Among the three schemes compared, it was found that 4-QAM offers lower bit-error-rates.

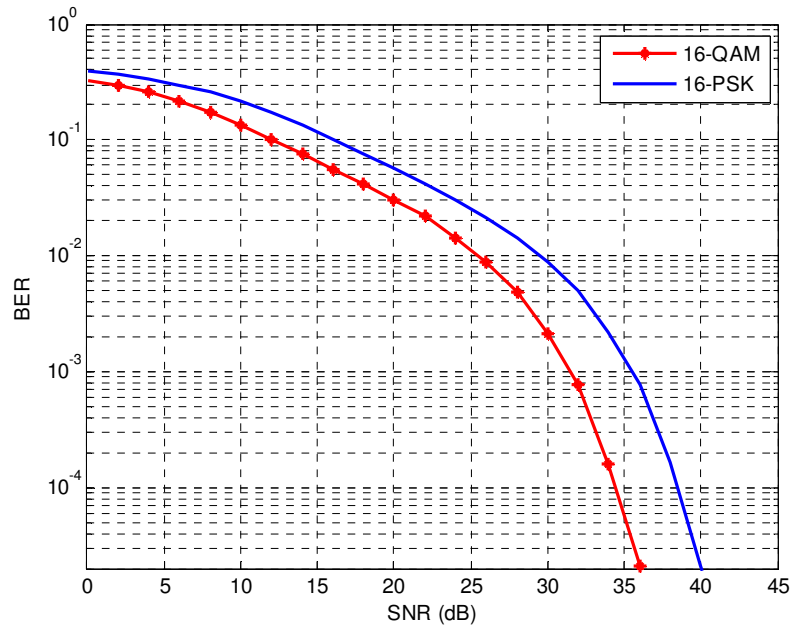


Fig. 6.10 Comparison of bit-error-rate performances of 16-QAM and 16-PSK based OFDMs for an Undersea Acoustic channel

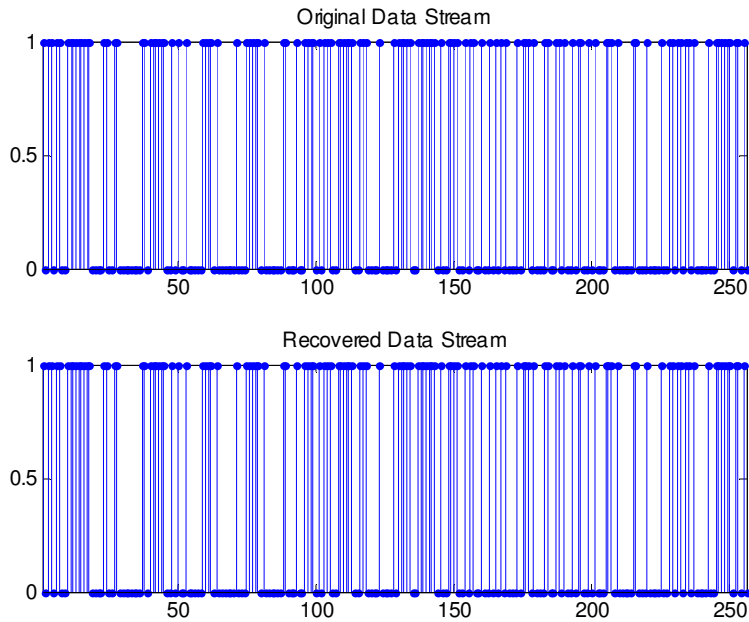


Fig. 6.11 Original and recovered data stream for 16-QAM based OFDM through underwater channel

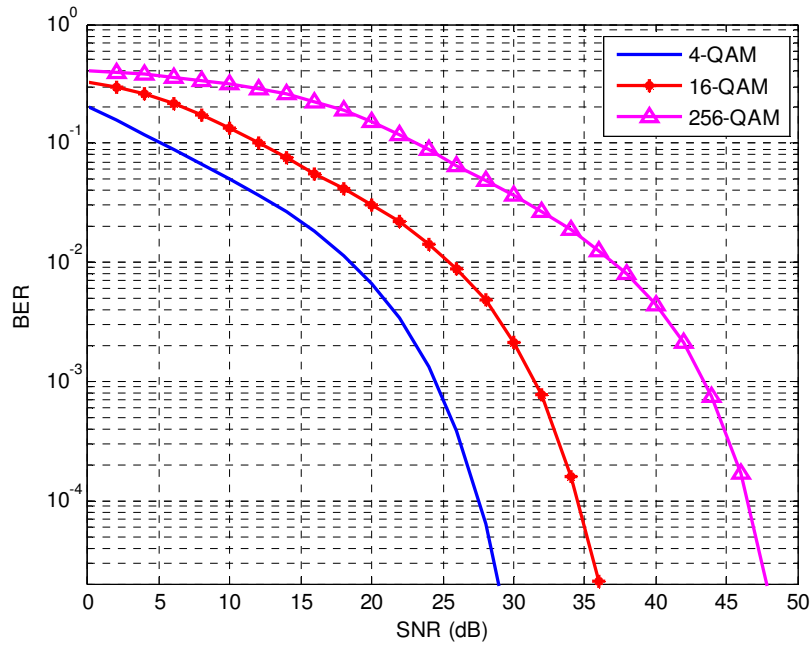


Fig. 6.12 Comparison of bit-error-rate performances of 4-QAM, 16-QAM and 256-QAM based OFDMs for an Undersea Acoustic channel

Figure 6.13 shows a comparison of bit-error-rate performances of BPSK, QPSK and 16-PSK based OFDM systems for an Undersea Acoustic channel. It has been observed for PSK also, that as the order decreases, the BER performance improves. As the number of points in the constellation plot decreases, the bit-error-rate decreases, due to increase in the distance between the points in the constellation plot. The simulation parameters for PSK based OFDM are furnished in Table 6.1. The center frequency of the OFDM band is taken to be 10kHz and the bandwidth is also taken to be 10kHz.

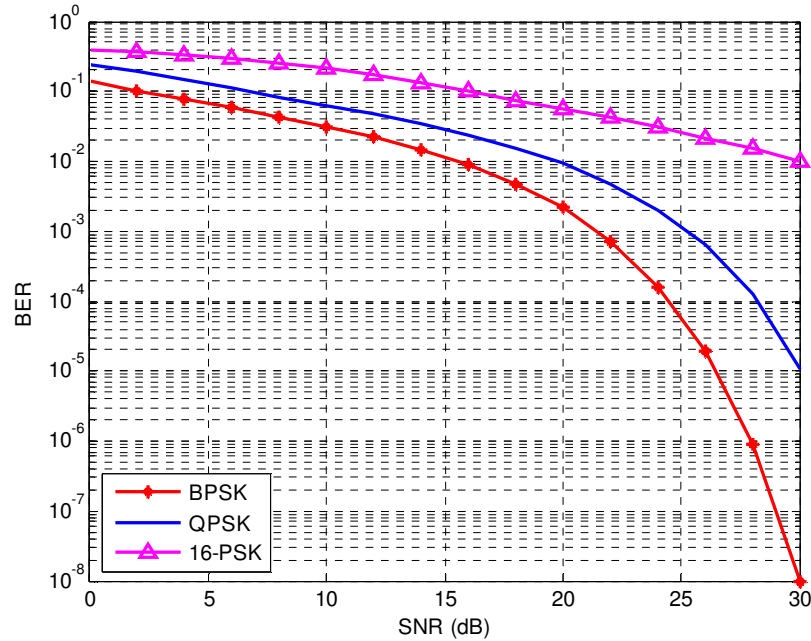


Fig. 6.13 Comparison of bit-error-rate performances for BPSK, DPSK, QPSK and 16-PSK based OFDMs for an Undersea Acoustic channel

Table 6.1 Simulation Parameters for PSK based OFDM

Mapping Scheme	BPSK	QPSK	16-PSK
Parameter			
Number of subcarriers: N	64	32	16
Subcarrier bandwidth: $\Delta f = BW/N$	156.25Hz	312.5Hz	625Hz
Valid symbol duration:	6.4ms	3.2ms	1.6ms

6.4 BER Performance of Coded OFDM for Undersea Acoustic Links

The system model of coded OFDM has been given in section 4.5. The bit-error-rate performances of the coded OFDM have been computed by pumping out 10^9 bits under various SNR conditions using the BPSK and

DPSK mapping with convolutional as well as BCH (7, 4) coded schemes with and without interleaving. The center frequency of the OFDM band is taken to be 10kHz.

6.4.1 Simulation Parameters

In this section, BPSK and DPSK based OFDM has been simulated for an ocean channel. The parameters used for comparing the performances by simulating the normal, convolutional coded as well as BCH coded OFDM systems are furnished in Table 6.2. Simulation has been performed using a data stream comprising of 64 bits per OFDM symbol, which gets converted to 128 bits after convolutional coding and 112 bits after BCH (7,4) encoding leading to a requirement of 128 and 112 subcarriers for convolutional coded and BCH coded OFDM systems respectively. It has been assumed that the receiver has complete channel state information. In addition, perfect frequency and phase synchronization are assumed.

Table 6.2 Simulation Parameters for Coded OFDM

Parameter	Normal OFDM	Convolutional Coded OFDM	BCH (7,4) Coded OFDM
No. of transmitted bits	10 ⁹		
Mapping Scheme	BPSK, DPSK		
Carrier frequency	10kHz		
Signal frequency band: BW	10kHz		
Number of subcarriers: N	64	128	112
Subcarrier bandwidth: $\Delta f = \text{BW}/N$	156.25Hz	78.125Hz	89.285Hz
Valid symbol duration:	6.4ms	12.8ms	11.2ms

6.4.2 Simulation Results

Figure 6.14 shows the BER performances of BPSK based normal OFDM, convolutional coded OFDM as well as BCH coded OFDM with and without interleaving. It can be observed that both the coded OFDM schemes with interleaving perform better than the normal OFDM. The error rate performance of convolutional coded OFDM is higher compared to BCH coded OFDM up to a crossover SNR value; beyond which the error rate of the convolutional coded OFDM with interleaving decreases. BCH coded OFDM with interleaving offers lower BER compared to normal OFDM at all SNR values. It has also been observed that coded schemes with interleaving perform much better than their counterparts without interleaving. As a result of interleaving and deinterleaving, the

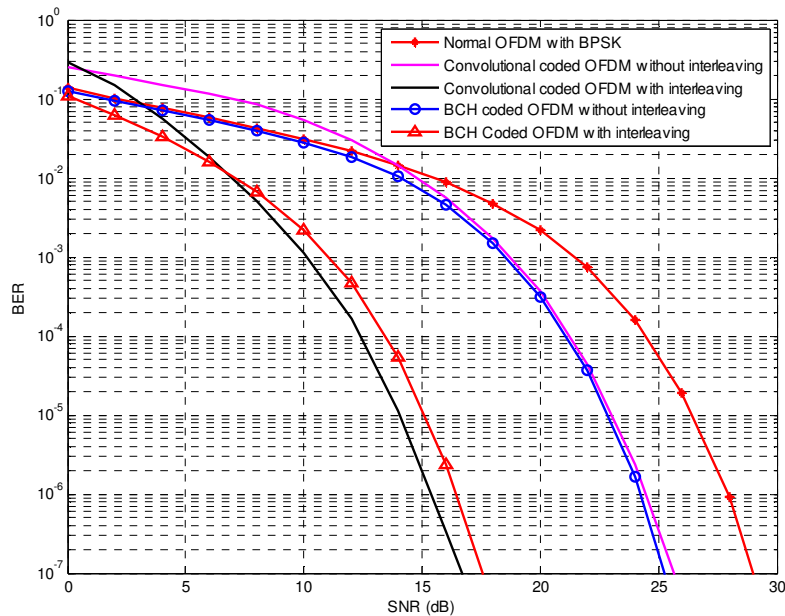


Fig. 6.14 Comparison of bit-error-rate performances of normal OFDM as well as Convolutional Coded and BCH coded OFDMs, with and without interleaving for an undersea acoustic channel using BPSK modulation

error bursts get spread out in time and hence, the process of interleaving improves the error rate performance of the coded OFDM systems. Thus, it can be concluded that both the convolutional and BCH coded OFDM systems with interleaving offers commendable improvement in performances. The bit-error-rates for various SNR values for BPSK based OFDM systems are tabulated in Table 6.3.

The differential PSK system is expected to give a performance which is nearly as good as coherent systems, but with less complex implementation. Differential phase shift keying (DPSK), which is a differentially encoded BPSK signal, is often used instead of BPSK, in practice, since DPSK receiver does not require a carrier synchronization circuit. In DPSK, the information is represented with relative phase, rather than the actual phase of the carrier.

Table 6.3 Bit-error-rates for various SNR for BPSK based OFDM system

SNR (dB)	Normal OFDM with BPSK	BCH coded OFDM	Convolutio nal coded OFDM	BCH coded OFDM	Convolutional coded OFDM
		(without interleaving)		(interleaved)	
0	0.1374	0.1243	0.2530	0.1081	0.2911
2	0.1032	0.0936	0.1945	0.0627	0.1507
4	0.0773	0.0710	0.1520	0.0333	0.0571
6	0.0579	0.0534	0.1168	0.0161	0.0181
8	0.0430	0.0394	0.0843	0.0067	0.0051
10	0.0312	0.0280	0.0543	0.0022	0.0011
12	0.0219	0.0184	0.0302	0.47592×10^{-3}	0.16563×10^{-3}
14	0.0145	0.0104	0.0143	0.5509×10^{-4}	0.1143×10^{-4}
16	0.0089	0.0046	0.0056	0.2340×10^{-5}	0.33×10^{-6}
18	0.0048	0.0015	0.0017	4×10^{-8}	1×10^{-8}

The performances of coded OFDM techniques with and without interleaving have also been simulated for DPSK based OFDM systems and the results of this simulation are depicted in Figure 6.15. DPSK based OFDM systems are also found to perform satisfactorily when the data is subjected to coding and interleaving. Thus, in addition to improving transmission security, coding combined with interleaving offer significant improvement in bit-error-rate performances. The bit-error-rates for various SNR values for DPSK based OFDM systems are tabulated in Table 6.4.

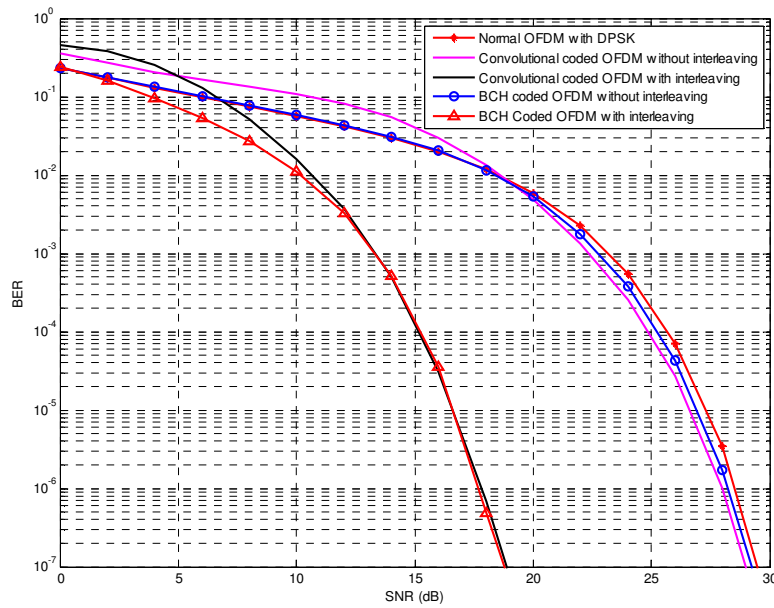


Fig. 6.15 Comparison of bit-error-rate performances of normal OFDM as well as Convolutional Coded and BCH Coded OFDMs, with and without interleaving for an undersea acoustic channel using DPSK modulation

A comparison of Tables 6.3 and 6.4 show that in the case of BPSK based systems, for SNR above 8dB, coded OFDM with interleaving shows tremendous improvement in performance compared to their counterparts without interleaving, whereas in DPSK based OFDM systems, for SNR above 12dB, coded OFDM systems with interleaving performs much better

when compared to their counterparts without interleaving. Thus, coding when suitably combined with interleaving, improves the performance of the system significantly. Moreover, as can be seen from the Tables, the bit-error-rate performance of BPSK based interleaved convolutional coded OFDM is superior when compared to the DPSK based system, since errors tend to propagate in the case of a DPSK based system.

Table 6.4 Bit-error-rates for various SNR for DPSK based OFDM system

SNR (dB)	Normal OFDM with DPSK	BCH coded OFDM	Convolutional coded OFDM	BCH coded OFDM	Convolutional coded OFDM
		(without interleaving)		(interleaved)	
0	0.2304	0.2345	0.3569	0.2393	0.4509
2	0.1751	0.1762	0.2727	0.1606	0.3801
4	0.1314	0.1323	0.2070	0.0967	0.2558
6	0.0996	0.1006	0.1638	0.0539	0.1309
8	0.0758	0.0768	0.1331	0.0270	0.0522
10	0.0571	0.0579	0.1077	0.0111	0.0162
12	0.0421	0.0430	0.0820	0.0032	0.0037
14	0.0298	0.0307	0.0545	5.237×10^{-3}	4.9867×10^{-3}
16	0.0198	0.0203	0.0302	3.575×10^{-4}	3.106×10^{-4}
18	0.0118	0.0115	0.0136	4.9×10^{-7}	6.8×10^{-7}

6.4.3 Performance Comparison of BCH (15, 11) and (15, 7) Coded OFDM for Undersea Acoustic Links

Simulation studies have also been carried out for the BPSK based BCH coded OFDM for an undersea acoustic link using BCH (15, 11) and (15, 7) codes, by pumping out 10^9 bits under various SNR conditions. BCH (15, 11) codes are single error correcting, whereas BCH (15, 7) codes are

double error correcting ones. Table 6.5 furnishes the simulation parameters used for the BPSK based normal as well as BCH Coded OFDMs.

Table 6.5 Simulation Parameters for BCH Coded OFDM

Parameters	Normal OFDM	BCH Coded OFDM	
		(15, 11)	(15, 7)
No. of transmitted bits	10 ⁹		
Mapping Scheme	BPSK		
Carrier frequency	10kHz		
Signal frequency band: BW	10kHz		
Number of subcarriers: N	308	420	660
Subcarrier bandwidth: $\Delta f = BW/N$	32.467Hz	23.8Hz	15.15Hz
Valid symbol duration:	30.8ms	42ms	66ms

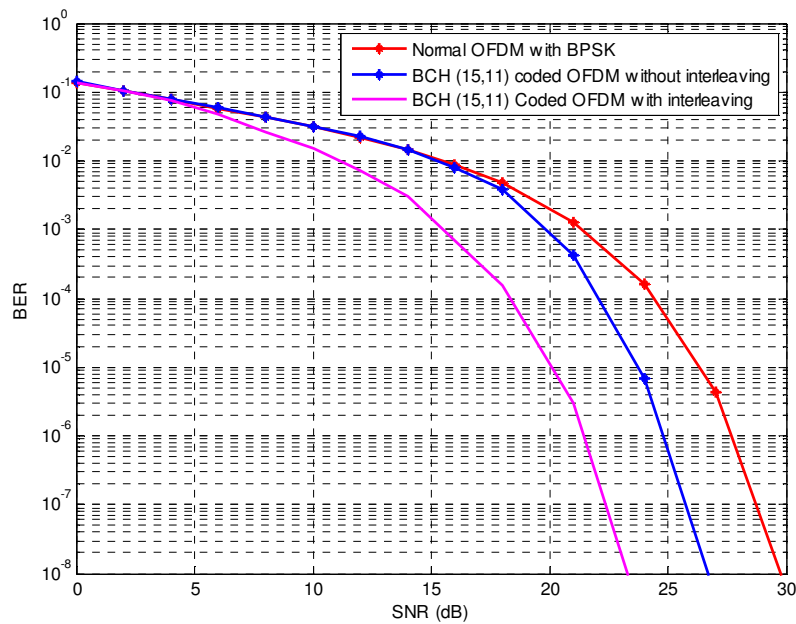


Fig. 6.16 Comparison of bit-error-rate performance of normal OFDM as well as BCH (15, 11) coded OFDM with and without interleaving

Figure 6.16 shows the BER performances of a BPSK based normal OFDM as well as BCH (15, 11) coded OFDMs, with and without

interleaving. It can be observed that compared to normal OFDM, BCH coded OFDM with interleaving performs significantly better in terms of the bit-error-rates. The plots of BCH coded OFDM with and without interleaving reveal that shuffling the orders of the bits at the transmitting end and later reordering it at the receiving end, will help in reducing the effects of burst errors, thus enhancing the bit-error-rate performances of the overall system.

Figure 6.17 shows the BER performances of a BPSK based normal OFDM as well as BCH (15, 7) coded OFDM with and without interleaving. This figure also reveals that the BCH coded OFDM with interleaving performs significantly better in terms of the bit-error-rates, compared to normal OFDM as well as its counterpart without interleaving. Thus, coding combined with interleaving provides improved error rate performances as well as higher transmission security.

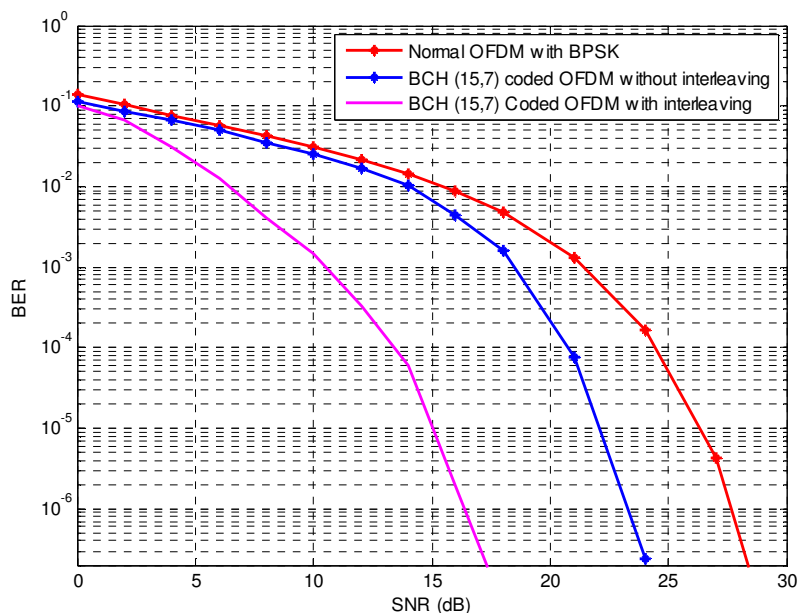


Fig. 6.17 Comparison of bit-error-rate performances of normal OFDM as well as BCH (15, 7) coded OFDM with and without interleaving

The BER values at various SNR levels for BPSK based OFDM systems have been tabulated in Table 6.6. In the case of BCH (15, 11) codes, for SNR above 15dB, the coded OFDM with interleaving shows significant improvement in performance compared to normal OFDM and its counterpart without interleaving, whereas in the case of (15, 7) codes, for SNR above 9dB, the coded OFDM with interleaving shows considerable improvement in performance. For an SNR of 18dB, BCH (15, 11) coded OFDM with interleaving has been found to have a BER value of 0.1527×10^{-3} , whereas BCH (15, 7) coded OFDM with interleaving exhibits a BER value of 0.6429×10^{-7} . This behavior is expected, as the BCH (15, 11) codes are single error correcting codes, whereas (15, 7) codes can correct up to 2 errors.

Table 6.6 BER values for normal OFDM as well as BCH (15, 11) and (15, 7) Coded OFDM systems, with and without interleaving, under various SNR conditions

SNR (dB)	Normal OFDM with BPSK	BCH (15,11) coded OFDM		BCH (15,7) coded OFDM	
		Without Interleaving	With Interleaving	Without Interleaving	With Interleaving
0	0.1378	0.1397	0.1380	0.1146	0.0999
2	0.1032	0.1040	0.1041	0.0850	0.0680
4	0.0774	0.0776	0.0760	0.0672	0.0315
6	0.0581	0.0597	0.0477	0.0501	0.0125
8	0.0429	0.0431	0.0265	0.0350	0.0041
10	0.0312	0.0315	0.015	0.0251	0.0015
12	0.0220	0.0229	0.0072	0.0170	0.3267×10^{-3}
14	0.0146	0.0142	0.0031	0.0102	0.6005×10^{-4}
16	0.0088	0.0078	0.0072	0.0045	0.2004×10^{-5}
18	0.0048	0.0039	0.1527×10^{-3}	0.0016	0.6429×10^{-7}

6.5 Performance of Space-Time Block Coding for Undersea Acoustic Links

This section gives the results of simulating normal as well as coded STBC for undersea acoustic links.

6.5.1 Simulation Steps

The script for simulation performs the following

- a. Generate random binary sequence of 1's and 0's.
- b. Perform modulation on the sequence
- c. Code the sequence as per the Alamouti Space Time code, include the channel effects as in section 5.6.2 and then add noise.
- d. Perform STBC decoding on the received symbols
- e. Perform demodulation
- f. Compute the bit errors
- g. Repeat for multiple values of SNR and plot the simulation results.

For the proposed coded interleaved STBC, in addition to the above steps, encoding as well as interleaving have to be performed before step b and deinterleaving and decoding have to be performed after step e.

6.5.2 Simulation Results

The block schematic of normal STBC has been given in section 4.7.1. The performance of STBC, using 16-QAM and 16-PSK based 2x1 systems have been analyzed for a Rayleigh fading underwater channel. Figure 6.18 shows the BER comparison of a 16-QAM and a 16-PSK based 2x1 Alamouti STBC system for a shallow water medium range underwater acoustic channel. As seen from the plot, 16-QAM offers lower bit-error-rate performance compared to 16-PSK system. The performance of STBC for an underwater acoustic channel has also been analyzed for 16-QAM

based 2x1 and 2x2 systems. As seen from the plot, the use of an additional receiver offers lower bit-error-rate performances, since a better estimate of the transmitted data can be made at the receiving system by combining the signals from the two receivers.

The system model for the proposed coded STBC has already been described in section 4.7.2. The performances of a 2x2 STBC system for 16-QAM with and without BCH (7,4) coding have been simulated. The channel coding offers improved security and interleaving helps to reduce the effects of the burst errors. Figure 6.19 shows the BER comparison of a 2x2 STBC system with and without coding using 16-QAM for an underwater acoustic channel. As seen from the plot, coding and interleaving offers significant improvement in the error rate performance of the system.

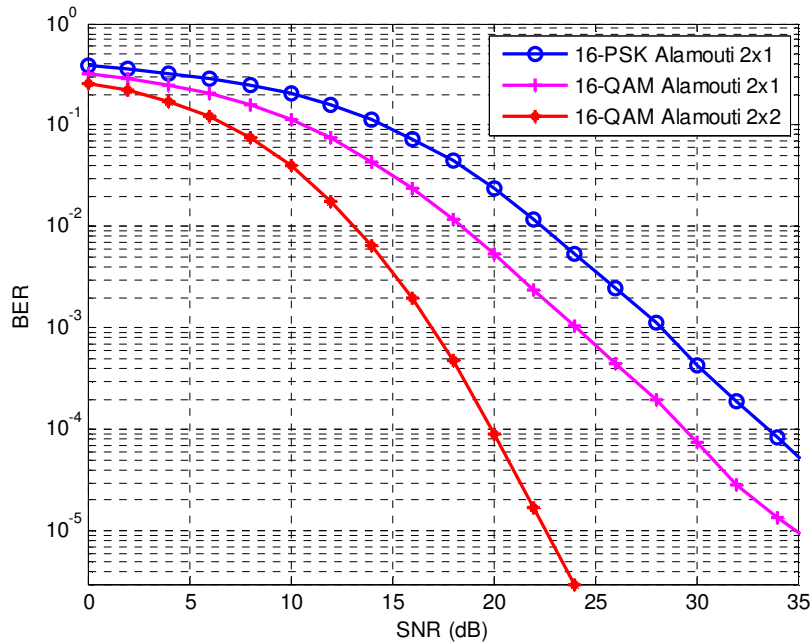


Fig. 6.18 Comparison of bit-error-rate performances of 16-QAM and 16-PSK for a 2x1 case, as well as 2x1 and 2x2 cases, for 16-QAM based system

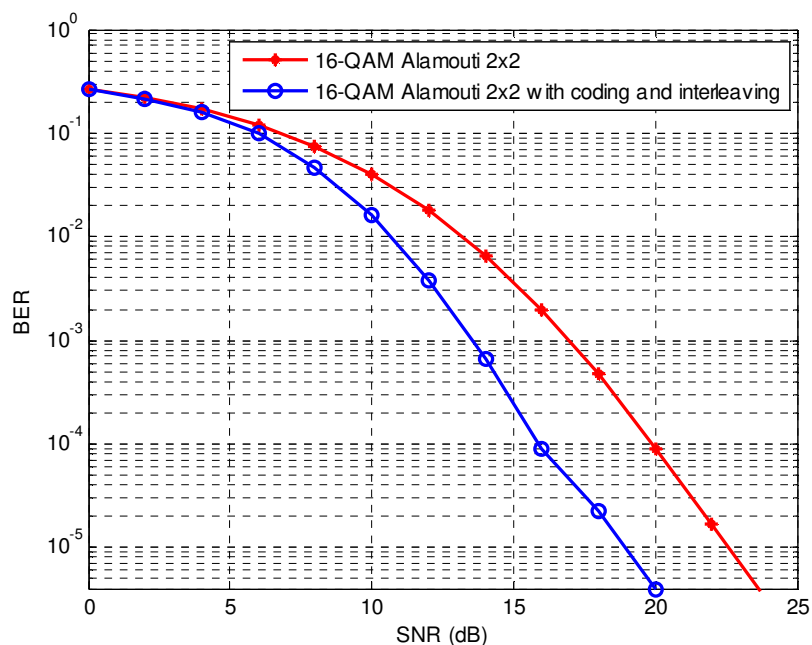


Fig. 6.19 Comparison of bit-error-rate performances of a 2x2 STBC system for 16-QAM modulation with and without coding

Table 6.7 BER values 16-QAM and 16-PSK based STBC systems

SNR (dB)	16-PSK (2x1)	16-QAM (2x1)	16-QAM (2x2)	Proposed coded interleaved STBC system
0	0.3882	0.3186	0.2618	0.2656
2	0.3611	0.2862	0.2197	0.2166
4	0.3274	0.2490	0.1707	0.1591
6	0.2896	0.2054	0.1208	0.0985
8	0.2480	0.1595	0.0749	0.0469
10	0.2030	0.1133	0.0404	0.0160
12	0.1567	0.0745	0.0179	0.0037
14	0.1122	0.0436	0.0064	6.6797x10 ⁻⁴
16	0.0733	0.0238	0.0020	8.7891x10 ⁻⁵
18	0.0440	0.0116	4.834x10 ⁻⁴	2.2461x10 ⁻⁵
20	0.0239	0.0054	8.9844x10 ⁻⁵	3.9063x10 ⁻⁶

The BER values at various SNR levels for 16-PSK and 16-QAM based 2x1 STBC systems, 16-QAM based 2x2 STBC system and 16-QAM based 2x2 STBC system with coding and interleaving are tabulated in Table 6.7. It can be seen that for SNR above 16dB, 2x2 16-QAM based STBC system performs much better compared to 2x1 STBC systems. It can also be seen that for SNR above 12dB, 2x2 STBC system with coding and interleaving performs much better compared to all others schemes compared. Thus, the proposed coded STBC system offers improved performance in terms of bit-error-rate for the undersea acoustic channel.

6.6 Effect of channel on BER Performance

6.6.1 Synchronization

Symbol time offset occurs when the transmitter and receiver do not have a common time reference and hence, the receiver needs to find symbol boundaries to avoid inter symbol interference. Carrier frequency offset occurs due to frequency differences between the transmitter and receiver oscillators, Doppler shift of mobile channels or oscillator instabilities, leading to inter carrier interference.

The STO estimation methods under consideration are well suited for fast-changing channels, because the delay time can be updated on per-symbol basis. Table 6.8 lists a comparison of STO estimation by correlation and difference methods and it can be seen from this table that the difference method outperforms the correlation method for STO estimation.

Figure 6.20 shows a comparison of BER for an undersea acoustic channel using BPSK based OFDM modulation for various CFO values. It has been observed that as CFO value increases, the BER performance

deteriorates. Figure 6.21 shows a comparison of CFO estimation using cyclic prefix and pilot based methods for a CFO of 0.15 and it has been observed that pilot based method gives a better CFO estimation, even though it causes additional processing overhead.

Table 6.8 STO Estimation by correlation and difference methods

Actual STO		-5	-4	-3	-2	-1	0	1	2	3	4	5
STO Estimated by	Correlation Method	-4	-4	-3	-2	-1	0	1	2	3	3	5
	Difference Method	-5	-4	-3	-2	-1	0	1	2	3	4	5

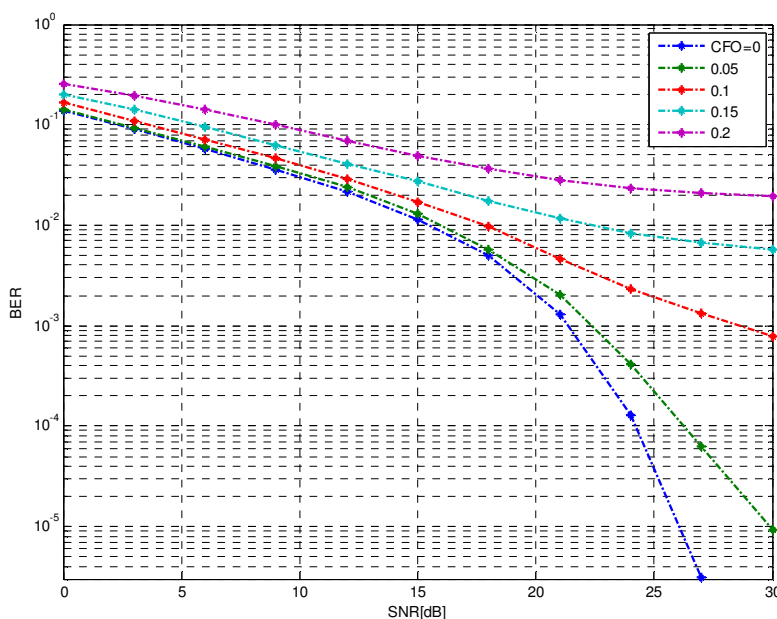


Fig. 6.20 Effect of CFO on bit-error-rate under various SNR conditions for BPSK based OFDM in an undersea acoustic channel

6.6.2 Channel Estimation

Pilots are inserted at specific locations within each OFDM symbol for enabling channel estimation.

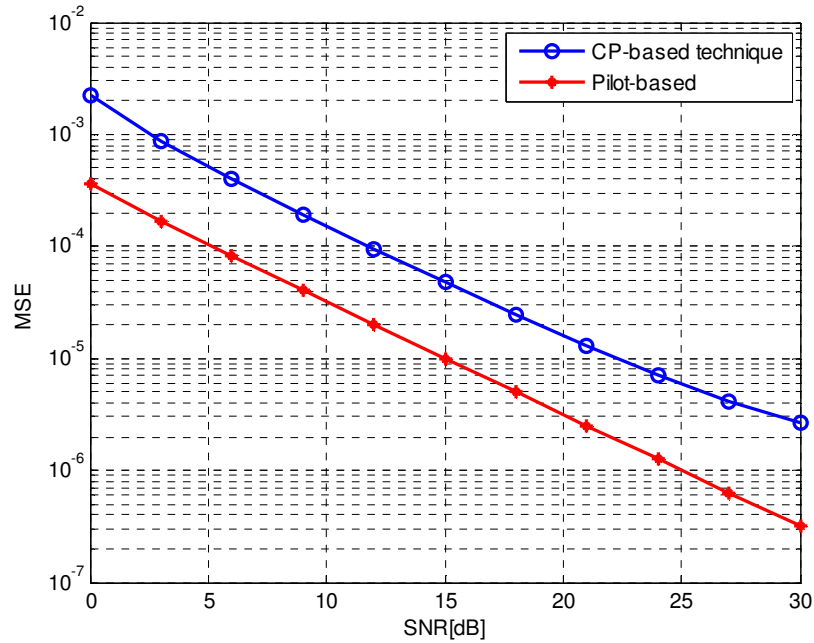


Fig. 6.21 Comparison of CFO Estimation by using Cyclic Prefix and Pilot based approaches for an Undersea Acoustic channel

Table 6.9 Simulation Parameters for channel estimation

Parameters	Values
Number of transmitted bits	10 ⁹
Symbol mapping scheme	BPSK
Carrier frequency (f_c)	10kHz
Signal frequency bandwidth (BW)	10kHz
Number of subcarriers (N)	64
Number of pilot subcarriers (P)	4, 8 and 16
Subcarrier spacing ($\Delta f = BW/N$)	156.25Hz
Valid Symbol duration (T)	6.4ms

6.6.2.1 Simulation Parameters

In this section, BPSK modulation has been used for implementing OFDM for an ocean channel. The simulation parameters for channel estimation are furnished in Table 6.9. The number of subcarriers has been

chosen to be 64 and it is assumed that the receiver has complete state information and Doppler effect has been neglected. In addition, perfect frequency and phase synchronization have been assumed.

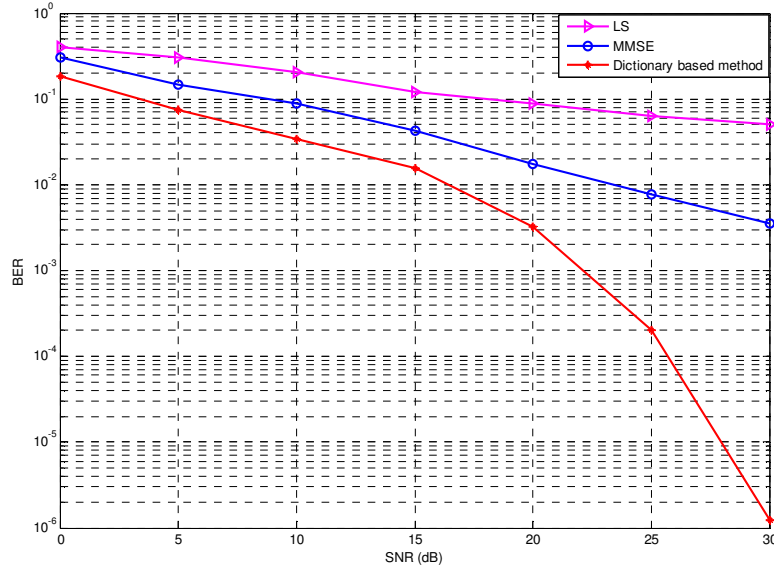


Fig. 6.22 Comparison of bit-error-rate performances of LS, MMSE and the dictionary based sparse channel estimation method using 16 pilots for an Undersea Acoustic channel

6.6.2.2 Simulation Results

Figure 6.22 shows the comparison of LS and MMSE estimation methods with that of the dictionary based sparse channel estimation for a range of 1km using 16 pilots. It can be seen that the performance of the dictionary based sparse channel estimation method is far superior compared to that of the LS and MMSE estimation methods. Hence, the dictionary based sparse channel estimation method with 4, 8 and 16 pilots have been used for computing the bit-error-rates for different ranges and the results have been compared with an ideal receiver having a known channel state information (CSI).

Figures 6.23 to 6.26 show the BER performance vs. SNR for a BPSK based OFDM for the ranges 200m, 500m, 1km and 10km, respectively. It has been noticed that BER increases as the distance between source and receiver increases. Also, the error rate decreases with increase the number of pilots. The minimum number of pilots required for an L -sparse channel can be computed using equation (5.22).

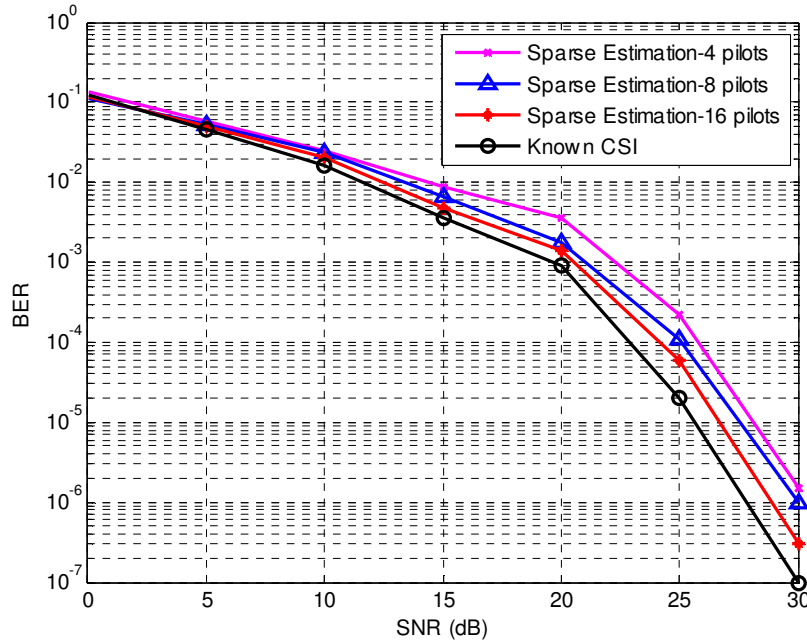


Fig. 6.23 Comparison of bit-error-rate performances using different number of pilots for a BPSK based OFDM for a range of 200m

Figure 6.23 shows the bit-error-rate performance of a BPSK based OFDM system for a range of 200m. At SNR of 30dB, it can be seen that using 16, 8 and 4 pilots, the error rates achieved are 3×10^{-7} , 10^{-6} and 1.5×10^{-6} , as compared to the ideal case in which, the achieved bit-error-rate is 10^{-7} . Similarly, figure 6.24 and 6.25 show the bit-error-rate performance of a BPSK based OFDM system for a range of 500m and 1km respectively. As seen from the plots, the error rate decreases with increase the number of

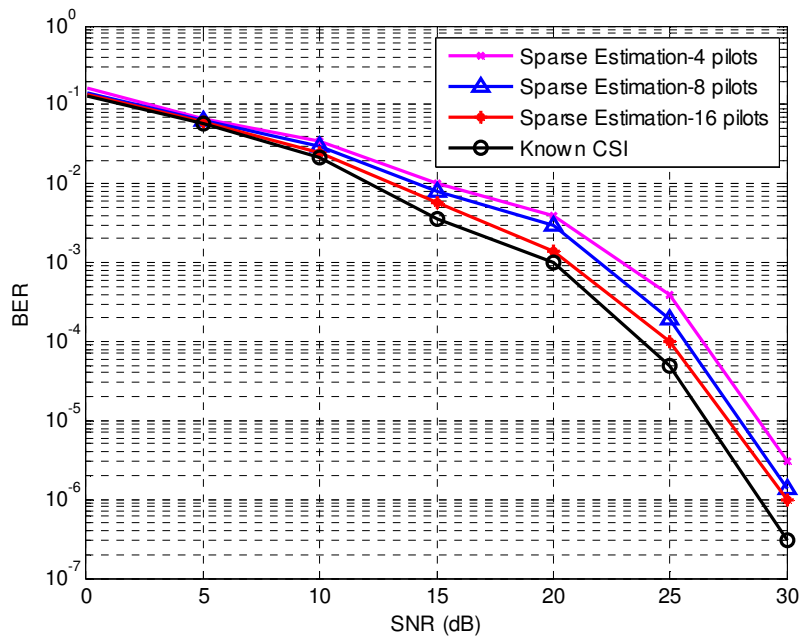


Fig. 6.24 Comparison of bit-error-rate performances using different number of pilots for a BPSK based OFDM for a range of 500m

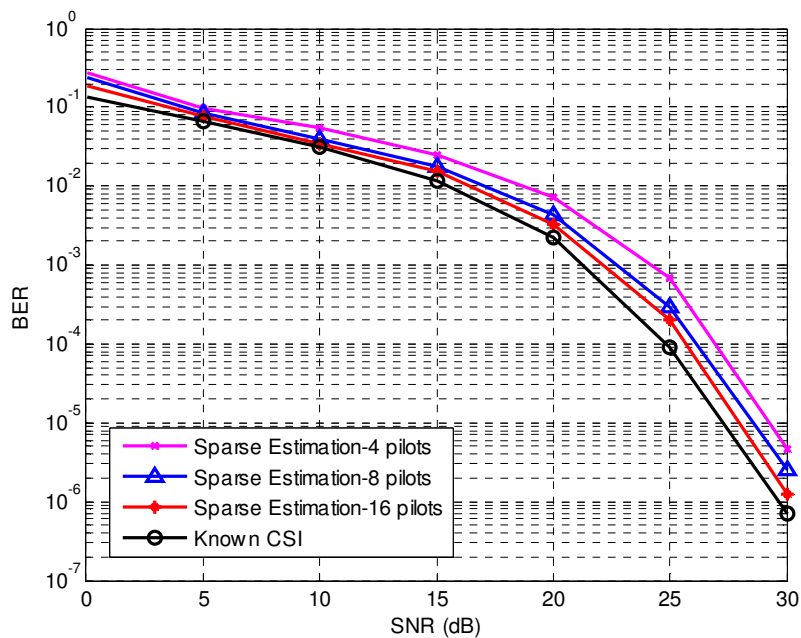


Fig. 6.25 Comparison of bit-error-rate performances using different number of pilots for a BPSK based OFDM for a range of 1km

pilots. At SNR of 30dB, it can be seen that using 16, 8 and 4 pilots, the error rates achieved are 10^{-6} , 1.4×10^{-6} and 3×10^{-6} , for the case of 500m. At SNR of 30dB, it can be seen that using 16, 8 and 4 pilots, the error rates achieved are 1.25×10^{-6} , 2.5×10^{-6} and 4.6×10^{-6} , for the case of 1km.

Table 6.10 BER values for various ranges for channel estimated using 16 pilots for channel estimation

Range SNR	200m	500m	1km	10km
0	0.117	0.1357	0.1857	0.2001
5	0.0494	0.0594	0.0754	0.1901
10	0.0202	0.0244	0.0344	0.129
15	0.0048	0.0058	0.0158	0.069
20	1.4×10^{-3}	1.4×10^{-3}	3.24×10^{-3}	0.0311
25	6×10^{-5}	1×10^{-4}	2×10^{-4}	0.0121
30	3×10^{-7}	1×10^{-6}	1.25×10^{-6}	0.006

Table 6.10 shows the bit-error-rate values at various SNR values for various ranges using 16 pilots for channel estimation. It can be seen that the error rate increases with increase in distance between source and receiver.

The level of sparsity has been quantified by the number of channel taps in the Bellhop model. The number of significant channel taps and the minimum number of pilots required for an L -sparse channel computed using equation (5.22), have been tabulated for various ranges and the results are furnished in Table 6.11. The minimum number of pilots needed for 200m, 500m and 1km ranges are seen to be 3 for the given environmental conditions. Hence, as shown, the channel state information has been estimated using 4 pilots per OFDM symbol with fairly acceptable

BER performance. For 10km range, under the given environmental conditions, the minimum number of pilots needed per OFDM symbol can be seen to be 10. Hence, as shown in figure 6.26, channel estimation using 4 and 8 pilots do not give acceptable BER performance, whereas use of 16 pilots per OFDM symbol can fully characterize the channel state information as evident from the BER performances.

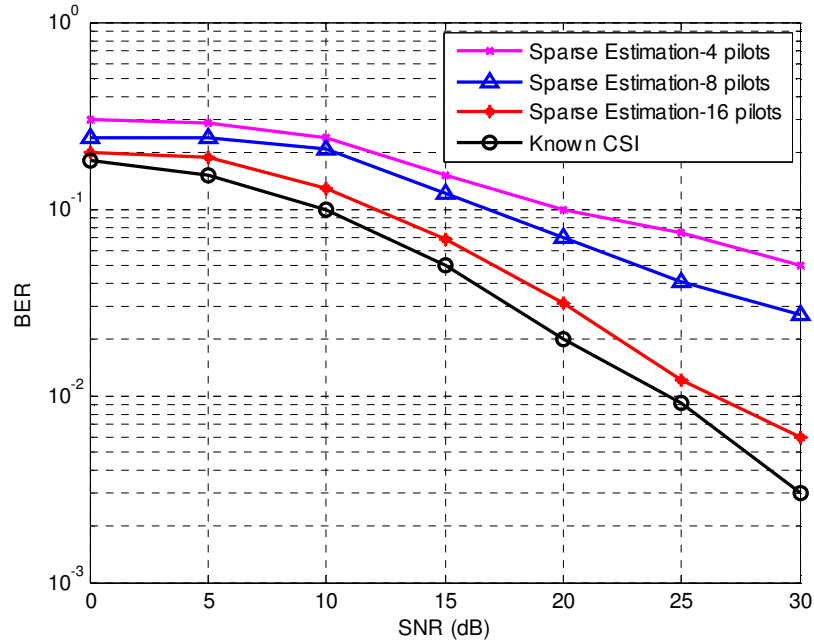


Fig. 6.26 Comparison of bit-error-rate performances using different number of pilots for a BPSK based OFDM for a range of 10km

Table 6.11 Minimum number of pilots needed for an L -sparse channel

Range/Distance (km)	No. of significant channel taps L (Sparsity)	Minimum number of pilots needed, M
0.2	2	3
0.5	2	3
1	2	3
10	15	10

Pilot overhead, which is the ratio of number of pilots to the total number of subcarriers, has been computed and the BER values for an SNR of 25dB has been plotted against the pilot overhead and its effect is depicted in figure 6.27. It can be seen that as the pilot overhead increases, BER performance improves significantly until a pilot overhead value of 0.25, beyond which, increase in pilot overhead do not have much significant effect on the BER performance. Thus, channel state estimation using 16 pilots give reasonably good BER performance.

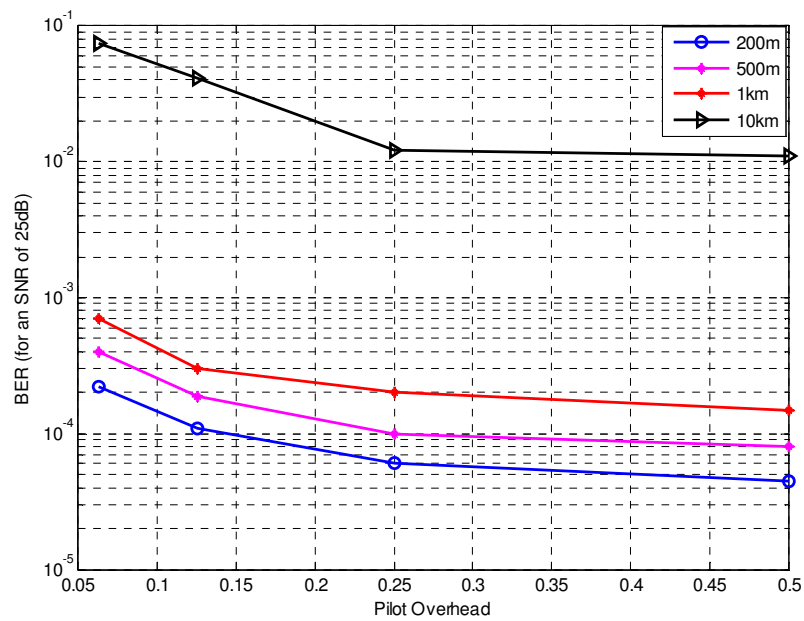


Fig. 6.27 Bit-error-rate plotted against Pilot Overhead for an SNR of 25dB

6.7 Data Rate Computation for OFDM in undersea acoustic links

Data Rate is a function of the modulation (BPSK, QPSK, 16-QAM and 64-QAM) and the code rate. The data rate is calculated using, [91]

$$Data\ Rate = \frac{bits_{symbol}N_{carrier}CR}{T_{sym}}, \quad (6.4)$$

where $bits_{symbol}$ is the number of bits per symbol, $N_{carrier}$ is the number of data subcarriers, CR is the code rate and T_{sym} is the OFDM symbol duration. The length of the guard band should be greater than the expected multipath spread and so, the duration of cyclic prefix is taken to be $T_G = 5ms$.

6.7.1 Comparison of Data Rates for BPSK, QPSK and 16-PSK based OFDM schemes

Computation of data rates for BPSK, QPSK and 16-PSK using equation (6.4) and Table 6.1, has been tabulated as in Table 6.12. It can be seen from Table 6.12 that 16-PSK offers the highest data rate among all the three schemes compared since it accommodates more bits per symbol.

Table 6.12 Data Rate Computation for PSK based OFDM schemes

Modulation scheme	BPSK	QPSK	16-PSK
Number of subcarriers	64	32	16
Bits per symbol	1	2	4
Total symbol duration	11.4ms	8.2ms	6.6ms
Data Rate	5.61kbps	7.804kbps	9.697kbps

6.7.2 Comparison of Data Rates for normal OFDM, Convolutional Coded OFDM and BCH Coded OFDM schemes

Computation of data rates for BPSK based normal, convolutional coded and BCH coded OFDM schemes using equation (6.4) and Table 6.2, has been tabulated as in Table 6.13. It can be seen from Table 6.13 that as

the code rate decreases, the data rate also decreases and convolutional coded OFDM offers the lowest data rate among the three schemes compared.

Table 6.13 Data Rate Computation for BPSK based OFDM schemes with and without coding

Coding scheme	No coding	Convolutional coded OFDM	BCH coded OFDM
Number of subcarriers	64	128	112
Total symbol duration	11.4ms	17.8ms	16.2ms
Code Rate	1	1/2	4/7
Data Rate	5.61kbps	3.596kbps	3.951kbps

6.7.3 Comparison of Data Rates for normal OFDM with pilot based scheme for channel estimation

Computation of data rates for BPSK based normal OFDM schemes with and without pilots using equation (6.4) and Table 6.9, have been

Table 6.14 Data Rate Computation for BPSK based OFDM schemes with and without pilots

Number of pilots per OFDM symbol	No pilots	4 pilots	8 pilots	16 pilots
Number of subcarriers	64			
Total symbol duration	11.4ms			
Number of data subcarriers	64	60	56	48
Data Rate	5.61kbps	5.263kbps	4.9122kbps	4.210kbps

tabulated as in Table 6.14. It can be seen from Table 6.14 that as the number of pilots increases, the data rate decreases and hence the choice of the number of pilots should be a compromise between the acceptable bit-error-rate and the required data rate.

6.8 Summary

The results of comparison of matrix padding method with that of the other compressive sensing recovery algorithms have been presented in this chapter. The bit-error-rates under various Signal to Noise Ratio conditions have been simulated for AWGN and Underwater Channels for 16-QAM based OFDM. The performances of OFDM for 16-QAM and 16-PSK based modulation techniques as well as various orders of QAM based OFDM have been compared. The bit-error-rate performances of normal as well as coded OFDM with and without interleaving schemes have also been simulated for various signal-to-noise ratio levels for both convolutional and BCH codes. The performances of Alamouti STBC for a 2x1 and a 2x2 system were compared with the proposed coded STBC system. The performances of various STO as well as CFO estimation methods have been compared and the channel has been estimated for various ranges using different number of pilots.

CHAPTER 7

CONCLUSIONS

Ocean exploration activities have been steadily increasing and there is need to transmit the data collected by the sensors placed underwater to the surface of ocean or even to terrestrial networks. This thesis addresses one of the emerging topics in Underwater Acoustics, *viz.* the various modulation and coding techniques for realising reliable OFDM for Undersea Acoustic Links. This thesis proposed a matrix padding method for sparse recovery, which is robust even in the presence of noise. Orthogonal Frequency Division Multiplexing and coded interleaved OFDM as well as coded interleaved STBC have been investigated. The synchronization and channel estimation problems in OFDM systems have also been investigated. This chapter brings out the salient highlights of the research work undertaken for realizing an underwater acoustic communication system and the general inferences gathered. This chapter also enlists the scope and directions for future research in this area.

7.1 Background

Wireless acoustic transmission through the ocean is the enabling technology for the development of undersea sensor networks. Applications of undersea sensor networks include instrument monitoring, pollution control, climate recording, prediction of natural disturbances, search and rescue missions and study of marine life. This thesis addresses some of the emerging techniques in signal processing for underwater acoustic

communications. This chapter also consolidates the highlights of the thesis as well as the future scope for research in the area of undersea acoustic networks.

7.2 Highlights of the Thesis

The study of underwater acoustic communication has gained significant attention due to its strategic and commercial applications. The work reported in the thesis entitled *Sparse Signal Processing for Undersea Acoustic Links* addresses one of the emerging topics in Ocean Engineering. The practical applications of the work include numerous military applications as well as civilian application like the real-time remote monitoring of oceanic parameters like dissolved oxygen, salinity variation, pressure variation, etc. The following are the salient highlights of this thesis.

7.2.1 Importance of Undersea Sensor Networks

Optical as well as electromagnetic waves do not propagate over long distances in water. Cables provide robust communication performance; however, the deployment and maintenance cost is very high. Even though complex, a reliable communication is provided by acoustic waves in water. An undersea sensor network is a set of autonomous nodes that are deployed over a particular region which can communicate with each other to form a network, detect and measure certain parameters of the region in which they are deployed and forward the requisite data to a control station without any human intervention. The importance of acoustic communication underwater as well as various topologies for underwater acoustic sensor networks have been elaborated. Various challenges involved in the propagation of sound in water as well as

modeling of undersea scenario using Bellhop and Rayleigh models have also been discussed.

7.2.2 Matrix Padding method for Sparse Signal Reconstruction

Compressive sensing recently gained immense attention due to the commendable advantages the technique offers in signal manipulation at comparatively low bit rate requirements. With the help of compressive sensing, the salient information in a signal can be preserved in a relatively small number of linear projections which helps in saving memory. Compressive sensing has applications in communication, speech signal processing, image processing, etc. This thesis proposed a *matrix padding method* for sparse recovery, which is robust even in the presence of noise. In practical scenarios, the noise cannot be eliminated and hence, the proposed robust signal recovery method is of great importance. The simulation studies demonstrate that the proposed algorithm can effectively improve sparse recovery with the help of matrix padding and LMS based adaptation in both ideal and noisy environments.

7.2.3 OFDM for Undersea Acoustic Links

Modulation and Demodulation of OFDM is achieved easily using IFFT and FFT techniques. With the help of Bellhop, the underwater environment has been simulated and the bit-error-rates have been computed for 16-QAM and 16-PSK based OFDM schemes. It was found that 16-QAM offers lower bit-error-rates compared to 16-PSK based OFDM. The performances of 4-QAM, 16-QAM and 256-QAM based OFDM systems have been compared. Among the three schemes compared, 4-QAM has been found to offer lower bit-error-rates. Similarly, a comparison of bit-error-rate performances of BPSK, QPSK and 16-PSK based OFDM systems for an undersea acoustic channel has been performed. It has been

observed for PSK also, that as the order decreases, the BER performance improves.

7.2.4 Effect of Coding and Interleaving on BER performance of OFDM systems

The bit-error-rate performances of normal as well as coded OFDM with and without interleaving schemes have been simulated for various signal-to-noise ratio levels. For BPSK based OFDM, the BCH coder with interleaving gives better performance compared to convolutional coder with interleaving for very low SNR values, whereas for SNR levels higher than a cross over SNR value, convolutional coder with interleaving gives improved error rate performance. However, for DPSK based OFDM, the error rate performance of BCH coded system with interleaving is found to be better for SNR levels typically below a cross over SNR value, beyond which both the BCH and convolutional coded systems with interleaving exhibit the same bit-error-rate performances. It has also been observed that the performances of coded OFDM with interleaving is superior compared to coded OFDM schemes without interleaving. Thus, the cumulative effect of coding and interleaving improves the overall bit-error-rate performance of OFDM substantially.

7.2.5 BER performance of BCH Coded OFDM systems

A comparison of the BCH (15, 11) and (15, 7) coded BPSK based OFDM systems have also been made and the results clearly indicate that BCH (15, 7) coded system perform significantly better in terms of bit-error-rate performances since BCH (15, 7) is double error correcting whereas BCH (15, 11) is a single error correcting code. It has been found that the process of interleaving improves the performance of coded OFDM systems significantly. Thus, interleaved coded OFDM has been found to be a good

choice for undersea acoustic links as well as for channels where burst errors occur.

7.2.6 Normal STBC and Coded STBC for Undersea Acoustic Links

Space-time block coding offers higher link reliability by purposefully introducing redundancy. Alamouti STBC offers good performance and improved robustness without any sacrifice on the data rate, by using special signal processing at the receiver to sort out the multiple symbols received to regenerate the transmitted data stream. It has been observed that a 2x2 system offers better performance compared to a 2x1 STBC system. It has also been observed that the proposed STBC system with coding and interleaving offers better performance compared to the normal 2x1 and 2x2 STBC systems.

7.2.7 Synchronization and Channel Estimation for an Undersea Acoustic Link

The OFDM transmission is very sensitive to receiver synchronization imperfections. The performances of various STO as well as CFO estimation methods have been compared. It has been observed that STO estimation using difference method and CFO estimation using pilot based method guarantee good performances. It has been further noted that the dictionary based sparse channel estimation method outperforms the channel estimation by LS and MMSE estimations. The channel has been estimated for various ranges using different number of pilots and the effect of varying the number of pilots for channel estimation has been studied, in terms of BER performance. This study further reveals that using 16 pilots, acceptable performance can be achieved for a pilot overhead of 0.25.

7.3 Future Scope for Research

The work presented in this thesis has a significant role to play in view of its practical applications for undersea acoustic links. This work also has substantial scope for further research for improving the overall system performance. Some of the possible proposals for future work in this area are enlisted below.

7.3.1 Trials in the Open Ocean

For the studies of the work presented in the thesis, underwater acoustic communication environment has been simulated. Experimental evaluation of the work presented in the thesis in the open ocean is very expensive as well as time consuming and hence, will have to be taken up as a separate major project from appropriate interest groups and funding agencies.

7.3.2 Use of other Modeling techniques/simulators for Undersea Acoustic Communication

The question of statistical channel modeling is still a controversial one for undersea acoustic links. Hence, other models like Rician models, Nakagami or K-distribution can also be used for modeling the underwater acoustic communication scenario. Simulators like NS2 [159], NS3 [160], Aqua-Sim [161], etc. are also available. The one which gives more closer results to the field trials has to be used for further studies.

7.3.3 Other coding schemes

Other coding schemes, like turbo codes or Low Density Parity Check codes (LDPC), which are more powerful than convolutional and BCH codes, can as well be used for implementing Coded OFDM for Undersea Acoustic Links.

7.3.4 Coded STBC-OFDM for Undersea Acoustic Links

Multiple transmitters and receivers can be combined with OFDM to improve the capacity and reliability of communications. The combination of the reliability of an STBC system with the robustness of orthogonal frequency division multiplexing against frequency-selective fading caused by severe multipath is a very promising basis for future high speed data communications. The performance can be further improved by incorporating error correcting codes as well as interleaving into the STBC-OFDM system. Thus, a coded STBC-OFDM system will offer a spectrally efficient and reliable undersea acoustic link, while keeping a simple equalizer structure.

7.3.5 Possibility of utilization of proposed technique for real-time data transmission in the SOFAR channel

The *SOFAR* channel is a deep sound channel that can act as a waveguide for sound, and low frequency sound waves within the channel may travel thousands of miles. The coded interleaved OFDM as well as coded STBC techniques proposed in the thesis can be effectively utilized in the deep sound channel, so as to make long range underwater acoustic communication more effective.

7.4 Summary

An attempt has been made in this chapter to bring out the salient highlights of the work and the general inferences gathered. A judicious selection of modulation scheme, coding, transmission and reception techniques is needed for the successful design and implementation of an undersea acoustic communication link. The scope and directions for future research in this area have also been proposed.

References

- [1] Tri Budi Santoso, Wirawan and Gamantyo Hendrantoro, “Development of Underwater Acoustic Communication Model: Opportunities and Challenges”, in *Int. Conf. Inform. and Commun. Technol. (ICoICT)*, 2013.
- [2] Ian F. Akyildiz, Dario Pompili and Tommaso Melodia, “Underwater acoustic sensor networks: research challenges”, *Elsevier, Ad Hoc Networks*, vol. 3, no. 3, pp. 257–279, May 2005.
- [3] *Underwater Wireless Communication Networks*, Broadband Wireless Networking Lab, School of Electrical and Computer Engineering, Georgia Institute of Technology. [Online] Available: <http://bwn.ece.gatech.edu/Underwater/Projectdescription.html>
- [4] Robert J. Urick, *Principles of Underwater Sound*, 2nd Edition, McGraw-Hill, 1975.
- [5] Paul C. Etter, *Underwater Acoustic Modeling - Principles, techniques and applications*, 2nd Edition, E & FN Spon, 1996.
- [6] Walter H. Munk, “Sound channel in an exponentially stratified ocean, with application to SOFAR”, *J. Acoust. Soc. Am.*, vol. 55, no. 2, Feb. 1974.
- [7] Milica Stojanovic and James Preisig, “Underwater Acoustic Communication Channels: Propagation models and Statistical Characterization”, *IEEE Commun. Mag.*, pp 84-89, Jan. 2009.
- [8] Fangkun Jia, En Cheng, Fei Yuan, “The Study On Time-variant Characteristics Of Under Water Acoustic Channels”, in *Int. Conf. Syst. and Informatics (ICSAI)*, May 2012.
- [9] Gordon M. Wenz, “Acoustic Ambient Noise in the Ocean: Spectra and Sources”, *J. Acoust. Soc. Am.*, vol. 34, no. 12, Dec. 1962.
- [10] A. B. Baggeroer, *Sonar Signal Processing - Applications of Digital Signal Processing*, Alan V. Oppenheim (editor), Prentice-Hall, Inc., 1978.
- [11] William C. Knight, Roger G. Pridham and Steven M. Kay, “Digital Signal Processing for Sonar”, *Proc. IEEE*, vol. 69, no. 11, Nov. 1981.

References

- [12] L. M. Brekhovskikh and Yu. P. Lysanov, *Fundamentals of Ocean Acoustics*, 2nd Edition, Springer-Verlag, Oct. 1990.
- [13] R. J. Urick, “Sonar Design In The Real Ocean: Multipath Limitations On Sonar Performance”, in *IEEE Int. Conf. Acoust., Speech, and Signal Process., ICASSP '76*, vol. 1, Apr. 1976.
- [14] John G. Proakis, *Digital Communications*, 4th Edition, McGraw-Hill, Int. Edition, 2001.
- [15] A. D. Waite, *Sonar for Practising Engineers*, 3rd Edition, John Wiley & Sons Ltd., 2002.
- [16] Joseph Rice, “Seaweb Acoustic Communication and Navigation Networks”, in *Proc. Underwater Acoust. Measurements: Technologies & Results*, Heraklion, Crete, Greece, 28th June – 1st July 2005.
- [17] Milica Stojanovic, “On the relationship between capacity and distance in an underwater acoustic communication channel,” in *WUWNet '06, Proc. 1st ACM Int. Workshop Underwater Networks, (New York, USA)*, pp. 41–47, 2006.
- [18] Mandar Chitre, Shiraz Shahabudeen, Lee Freitag, Milica Stojanovic, “Recent Advances in Underwater Acoustic Communications & Networking”, in *IEEE-OCEANS*, 2008.
- [19] Andrew C. Singer, Jill K. Nelson and Suleyman S. Kozat, “Signal Processing for Underwater Acoustic Communications”, *IEEE Commun. Mag.*, Jan. 2009.
- [20] Nejah Nasri, Abdennaceur Kachouri, Laurent Andrieux and Mounir Samet, “Design Considerations For Wireless Underwater Communication Transceiver”, in *Int. Conf. Signals, Circuits and Syst.*, Nov. 2008.
- [21] Joël Trubuil and Thierry Chonavel, “Accurate Doppler estimation for underwater acoustic communications”, in *OCEANS - Yeosu*, May 2012.

- [22] J. Poncela, M. C. Aguayo, P. Otero, “Wireless Underwater Communications”, *Wireless Pers. Commun.* (2012), 64, pp. 547–560, 2012.
- [23] F. De Rango, F. Veltri, P. Fazio, “A Multipath Fading Channel Model for Underwater Shallow Acoustic Communications”, in *IEEE Int. Conf. Commun.* (ICC), June 2012.
- [24] José S. G. Panaro, Fábio R. B. Lopes, Leonardo M. Barreira, Fidel E. Souza, “Underwater Acoustic Noise Model for Shallow Water Communications”, in *Brazilian Telecommun. Symp.*, Sept., 2012.
- [25] Michael B. Porter and Martin Siderius, “Acoustic Propagation in Very Shallow Water”, in *Int. Waterside Security Conf. (WSS)*, Nov. 2010.
- [26] Nan Jing, Weihong Bi, Qing Yue, “Attack Simulation Model and Channel Statistics in Underwater Acoustic Sensor Networks”, *Elsevier - Tsinghua Sci. and Technol.*, vol. 16, no. 6, pp. 611–621, Dec. 2011.
- [27] Emmanuel J. Candès, “Compressive sampling”, in *Proc. Int. Cong. Mathematicians*, Madrid, Spain, vol. 3, pp. 1433–1452, 2006.
- [28] Justin Romberg, “Imaging via Compressive Sampling”, *IEEE Signal Process. Mag.*, Mar. 2008.
- [29] Xiao Wang, Zhifeng Zhao, Ning Zhao and Honggang Zhang, “On the Application of Compressed Sensing in Communication Networks”, in *5th Int. ICST Conf. Commun. and Networking, China (CHINACOM)*, Aug. 2010.
- [30] Saad Qaisar, Rana Muhammad Bilal, Wafa Iqbal, Muqaddas Naureen, and Sungyoung Lee, “Compressive Sensing: From Theory to Applications, a Survey”, *J. Commun. and Networks*, vol. 15, no. 5, Oct. 2013.
- [31] Richard G. Baraniuk, “Compressive Sensing”, *IEEE Signal Process. Mag.*, vol. 24, no. 4, pp. 118-120,124, July 2007.
- [32] Thong T. Do, Lu Gan, Nam H. Nguyen and Trac D. Tran, “Fast and Efficient Compressive Sensing Using Structurally Random Matrices”, *IEEE Trans. Signal Process.*, vol. 60, no. 1, Jan. 2012.

References

- [33] Mark D. Plumbey, Thomas Blumensath, Laurent Daudet, Remi Gribonval and Mike Davis, "Sparse Representations in Audio and Music: From Coding to Source Separation", *Proc. IEEE*, vol. 98, no. 6, pp. 995-1005, June 2010.
- [34] Supatana Auethavekiat, "Introduction to the Implementation of Compressive Sensing", *AU J. Technol. (AU J.T.)*, vol. 14, no. 1, pp. 39-46, July 2010.
- [35] Joel A. Tropp and Stephen J. Wright, "Computational Methods for Sparse Solution of Linear Inverse Problems", *Proc. IEEE*, vol. 98, no. 6, pp. 948-958, June 2010.
- [36] Joel A. Tropp and Anna C. Gilbert, "Signal Recovery From Random Measurements Via Orthogonal Matching Pursuit", *IEEE Trans. Inf. Theory*, vol. 53, no. 12, pp. 4655-4666, Dec. 2007.
- [37] Joel A. Tropp, "Greed is Good: Algorithmic Results for Sparse Approximation", *IEEE Trans. Inf. Theory*, vol. 50, no. 10, Oct. 2004.
- [38] Jagdeep Kaur, Kamaljeet Kaur, Monika Bharti, Pankaj Sharma and Jatinder Kaur, "Reconstruction Using Compressive Sensing: A Review", *Int. J. Advanced Research Comput. and Commun. Eng.*, vol. 2, no. 9, Sept. 2013.
- [39] Shuai Yu, Rui Wang, Wanggen Wan, Linfeng Du, Xiaoqing Yu, "Compressed Sensing in Audio Signals and It's Reconstruction Algorithm", in *Int. Conf. Audio, Language and Image Process. (ICALIP)*, July 2012.
- [40] Deanna Needell and Joel A. Tropp, "CoSaMP: Iterative Signal Recovery from Incomplete and Inaccurate Samples", *Appl. and Computational Harmonic Anal.*, vol. 26, no. 3, pp. 301-321, May 2009.
- [41] R. Baraniuk, Mark A. Davenport, Marco F. Duarte, and Chinmay Hedge, eds., "An Introduction to Compressive Sensing", *Connexions*, Rice Univ., Houston, Texas, 2011, Available: <http://cnx.org/content/col11133/1.5/>

- [42] Emmanuel J. Candes and Michael B. Wakin, “An Introduction to Compressive Sampling”, *IEEE Signal Process. Mag.*, pp. 21-30, Mar. 2008.
- [43] Christian R. Berger, Zhaohui Wang, Jianzhong Huang, Shengli Zhou, “Application of Compressive Sensing to Sparse Channel Estimation”, *IEEE Commun. Mag.*, pp. 164-174, Nov. 2010.
- [44] Richard Baraniuk, M. Davenport, R. DeVore, and M. Wakin, “A simple proof of the restricted isometry property for random matrices,” *Constructive Approx.*, vol. 28, no. 3, pp. 253–263, Dec. 2008.
- [45] Emmanuel Candes, Justin Romberg and Terence Tao, “Stable Signal Recovery from Incomplete and Inaccurate Measurements”, *Commun. Pure Appl. Math.*, vol. 59, no. 8, pp. 1207-1223, Aug. 2006.
- [46] Farokh Marvasti, Arash Amini, Farzan Haddadi, Mahdi Soltanolkotabi, Babak Hossein Khalaj, Akram Aldroubi, Saeid Sanei and Jonathon Chambers, “A unified approach to sparse signal processing”, *EURASIP J. Advances Signal Process.*, 2012.
- [47] Emmanuel J. Candes and Terence Tao, “Decoding by Linear Programming”, *IEEE Trans. Inf. Theory*, vol. 51, no. 12, Dec. 2005.
- [48] Mihailo Stojnic, Weiyu Xu and Babak Hassibi, “Compressed sensing of approximately sparse signals”, in *IEEE Int. Symp. Inform. Theory*, ISIT 2008, July 2008.
- [49] Vidya L, Vivekanand V, ShyamKumar U., Deepak Mishra and Lakshminarayanan R., “Feasibility Study of Applying Compressed Sensing Recovery Algorithms for Launch Vehicle Telemetry”, in *IEEE Int. Conf. Microelectronics, Commun. and Renewable Energy (ICMiCR-2013)*, 2013.
- [50] Vivekanand V., Vidya L., Shyam Kumar U. and Deepak Mishra, “Noise Immunity Analysis of Compressed Sensing Recovery Algorithms”, in *IEEE Int. Conf. Signal Process. and Integrated Networks*, 2014.
- [51] Radomir Mihajlović, Marijana Šćekić, Andjela Draganić and Srdjan Stanković, “An Analysis of CS Algorithms Efficiency for Sparse

References

- Communication Signals Reconstruction”, in *3rd Mediterranean Conf. Embedded Computing MECO*, 2014.
- [52] Moreno-Alvarado and Mauricio Martinez-Garcia, “DCT-Compressive Sampling of Frequency-sparse Audio Signals”, in *Proc. World Congr. Eng. 2011*, vol. ii, London, UK, July 6-8, 2011.
- [53] R. G. Moreno-Alvarado, Mauricio Martinez-Garcia, “DCT-Compressive Sampling applied to speech signals”, in *21st Int. Conf. Elect. Commun. and Comput. (CONIELECOMP)*, Mar. 2011.
- [54] Deanna Needell, “Noisy Signal Recovery via Iterative Reweighted ℓ_1 -Minimization”, in *Conf. Record 43rd Asilomar Conf. Signals, Syst. and Comput.*, Nov. 2009.
- [55] Emmanuel Candes and Justin Romberg, “ ℓ_1 -magic : Recovery of Sparse Signals via Convex Programming”, Oct. 2005. Available: <http://users.ece.gatech.edu/~justin/l1magic/>
- [56] Seung-Jean Kim, K. Koh, M. Lustig, S. Boyd, and D. Gorinevsky, “An Interior-Point Method for Large-Scale ℓ_1 -Regularized Least Squares”, *IEEE J. Sel. Topics Signal Process.*, pp. 606–617, Dec. 2007.
- [57] Behtash Babadi, Nicholas Kalouptsidis and Vahid Tarokh, “SPARLS: The Sparse RLS Algorithm”, *IEEE Trans. Signal Process.*, vol. 58, no. 8, pp. 4013-4025, Aug. 2010.
- [58] Yin Zhang, Junfeng Yang, Wotao Yin, “User’s Guide for YALL1: Your Algorithm for L1 Optimization”, Dept. of CAAM., Rice Univ., Texas, USA. Available: <http://yall1.blogs.rice.edu/>
- [59] Junfeng Yang and Yin Zhang, “Alternating Direction Algorithms For ℓ_1 -Problems In Compressive Sensing”, *SIAM J. Sci. Comput.*, vol. 33, no. 1, pp. 250–278, 2011.
- [60] Stephen Boyd and Lieven Vandenberghe, *Convex Optimization*, Cambridge Univ. Press, 2004.

- [61] Richard G. Baraniuk, Emmanuel Candes, Michael Elad and Yi Ma, “Applications of Sparse Representation and Compressive Sensing”, *Proc. IEEE*, vol. 98, no. 6, pp. 906-912, June 2010.
- [62] Richard G. Baraniuk, Volkan Cevher, and Michael B. Wakin, “Low-Dimensional Models for Dimensionality Reduction and Signal Recovery: A Geometric Perspective”, *Proc. IEEE*, vol. 98, no. 6, pp. 959-971, June 2010.
- [63] CVX Research, Inc. CVX: Matlab software for disciplined convex programming, version 2.0. [Online] Available: <http://cvxr.com/cvx>, Apr. 2011.
- [64] Hamada Esmail, Danchi Jiang, “Review Article: Multicarrier Communication for Underwater Acoustic Channel”, *Int. J. Commun., Network and Syst. Sci.*, 6, pp. 361-376, 2013.
- [65] Jeong-woo Han, Se-young Kim, Ki-man Kim, Won-seok Choi, Min-jae Kim, Seung-yong Chun, Kwon Son, “A Study on the Underwater Acoustic Communication with Direct Sequence Spread Spectrum”, in *2010 IEEE/IFIP Int. Conf. Embedded and Ubiquitous Computing (EUC)*, Dec. 2010.
- [66] Jeong-woo Han, Se-young Kim, Ki-man Kim, Seung-yong Chun and Kwon Son, “Design of OFDM System for High Speed Underwater Communication”, in *2009 Int. Conf. Computational Sci. and Eng. (CSE)*, Aug. 2009.
- [67] Prashant Kumar and Preetam Kumar, “DCT Based OFDM for Underwater Acoustic Communication”, in *1st Int. Conf. Recent Advances Inform. Technol. (RAIT-2012)*, Mar. 2012.
- [68] M. C. Domingo, “Overview of channel models for underwater wireless communication networks,” *Elsevier, Physical Commun.*, vol. 1, no. 3, pp. 163–182, 2008.
- [69] T.C. Yang and Wen-Bin Yang, “Low signal-to-noise-ratio underwater acoustic communications using direct-sequence spread spectrum signals”, in *IEEE OCEANS – Europe*, June 2007.

References

- [70] Wang Yonggang, "Underwater Acoustic Channel Estimation for Pilot Based OFDM", in *IEEE Int. Conf. Signal Process., Commun. and Computing (ICSPCC)*, Sept. 2011.
- [71] S.S.Ghorpade, S.V.Sankpal, "Behavior of OFDM System Using MATLAB Simulation", *Int. J. Innovative Technol. and Research*, vol. 1, no. 3, pp. 249 – 252, Apr. - May 2013.
- [72] Rehan Khan, Qiao Gang, Asim Ismail and Khurram Mehboob, "Investigation of Channel Modeling and Simulation of OFDM Based Communication Near Northern Regions of Arabian Sea", *Research J. Appl. Sci., Eng. and Technol.*, vol. 5, no. 04, pp. 1169-1182, 2013.
- [73] Ashok Kamboj and Geeta Kaushik, "Study and Simulation of OFDM System", *Int. J. Modern Eng. Research (IJMER)*, vol. 2, no.1, pp. 235-241, Jan-Feb 2012.
- [74] Neha Pathak, "OFDM (Orthogonal Frequency Division Multiplexing) Simulation Using Matlab", *Int. J. Eng. Research & Technol. (IJERT)*, vol. 1, no. 6, Aug. 2012.
- [75] Guoqing Zhou and Taebo Shim, "Simulation Analysis of High Speed Underwater Acoustic Communication Based on a Statistical Channel Model", in *IEEE Congr. Image and Signal Process.*, 2008.
- [76] Andreja Radosevic, Rameez Ahmed, Tolga M. Duman, John G. Proakis and Milica Stojanovic, "Adaptive OFDM Modulation for Underwater Acoustic Communications: Design Considerations and Experimental Results", *IEEE J. Ocean. Eng.*, vol. 39, no. 2, Apr. 2014.
- [77] Bertrand Muquet, Zhengdao Wang, Georgios B. Giannakis, Marc de Courville and Pierre Duhamel, "Cyclic Prefixing or Zero Padding for Wireless Multicarrier Transmissions?", *IEEE Trans. Commun.*, vol. 50, no. 12, Dec. 2002.
- [78] Lu Yin, Bing Chen, Ping Cai, "Implementation and Design of Underwater Acoustic Speech Communication System Based on OFDM Technology", in *2012 AASRI Conf. Computation Intell. and Bioinformatics (CIB2012)*, pp. 46-51, 2012.

- [79] Prafulla. D. Gawande and Sirdharth. A. Ladhake, “BER Performance of OFDM System with Cyclic Prefix & Zero Padding”, *Int. J. Advances Eng. and Technol.*, vol. 6, no. 1, pp. 316-324, Mar. 2013.
- [80] Baosheng Li, Shengli Zhou, Milica Stojanovic, Lee Freitag, and Peter Willett, “Multicarrier Communication Over Underwater Acoustic Channels With Non uniform Doppler Shifts”, *IEEE J. Ocean. Eng.*, vol. 33, no. 2, Apr. 2008.
- [81] Xuefei Ma, Gang Qiao and Chunhui Zhao, “The OFDM Underwater Communication Frequency Equalization based on LMS Algorithm and Pilot Sequence”, in *5th Int. Conf. Wireless Commun., Networking and Mobile Computing*, 24-26 Sept. 2009.
- [82] Prashant Kumar and Preetam Kumar, “A Comparative Study of Spread OFDM with Transmit Diversity for Underwater Acoustic Communications”, *Wireless Pers. Commun.*, Feb. 2015.
- [83] Prashant Kumar, Vinay Kumar Trivedi and Preetam Kumar, “Performance Evaluation of DQPSK OFDM for Underwater Acoustic Communications”, in *Underwater Technol. 15*, Feb. 2015.
- [84] Prashant Kumar and Preetam Kumar, “Performance Evaluation of $\pi/4$ -DQPSK OFDM over Underwater Acoustic Channels”, *Wireless Pers. Commun.*, vol. 91, no. 3, pp. 1137–1152, Dec. 2016.
- [85] Yiyang Wu and William Y. Zou, “Orthogonal Frequency Division Multiplexing: A Multi-Carrier Modulation Scheme”, *IEEE Trans. Consum. Electron.*, vol. 41, no. 3, Aug. 1995.
- [86] Suzi Seroja Sarnin, Nani Fadzlina Naim, Wan Nor Syafizan W. Muhamad, “Performance Evaluation of Phase Shift Keying Modulation Technique Using BCH Code, Cyclic Code and Hamming Code Through AWGN Channel Model in Communication System”, in *3rd Int. Conf. Inform. Sci. and Interaction Sci. (ICIS)*, pp. 60 – 65, June 2010.
- [87] Mahmoud A. Smadi, “Performance Analysis Of BPSK System With Hard Decision (63, 36) BCH Code”, *J. Theoretical and Appl. Inform. Technol.*, vol.13, no. 2, 2010.

References

- [88] Jitendra Prakash Shreemukh and Prof. (Dr.) B.S. Rai, "Simulation and Analysis of Puncturing in Turbo Code using MATLAB", *Int. J. Advanced Research Comput. and Commun. Eng.*, vol. 3, no. 4, Apr. 2014.
- [89] Jyoti Kataria, Pawan Kumar, Tilak Raj, "A Study and Survey of OFDM versus COFDM" *Int. J. Sci. and Modern Eng. (IJISME)*, vol. 1, no. 5, Apr. 2013.
- [90] Ch Sekhararao K., S.S.Mohan Reddy, K. Ravi Kumar, "Performance of Coded OFDM in Impulsive Noise Environment", *Int. J. Syst. and Technologies*, vol. 5, no. 1, 2012.
- [91] Fernando H. Gregorio, "802.11a - OFDM PHY Coding and Interleaving", *Helsinki Univ. Technol.*, vol. 4, no. 8, pp. 1-6, 2006.
- [92] Mandar Chitre, S.H.Ong and John Potter, "Performance of coded OFDM in very shallow water channels and snapping shrimp noise", in *IEEE OCEANS 2005*, 17-23 Sept. 2005.
- [93] W.Aziz, G.Abbas, E.Ahmed, S.Saleem, Q.Islam, "Time Offset Estimation for OFDM Using MATLAB", *J. Expert Syst. (JES)*, vol. 1, no. 2, 2012.
- [94] Praween Kumar Nishad and P. Singh, "Carrier Frequency Offset Estimation in OFDM Systems", in *IEEE Conf. Inform. and Commun. Technologies (ICT)*, 11-12 Apr. 2013.
- [95] Abdul Gani Abshir, M. M. Abdullahi, Md. Abdus Samad, "A Comparative Study of Carrier Frequency Offset (CFO) Estimation Techniques for OFDM Systems", *IOSR J. Electron. and Commun. Eng. (IOSR-JECE)*, vol. 9, no. 4, ver. IV, pp. 01-06, Jul - Aug. 2014.
- [96] W.Aziz, E.Ahmed, G.Abbas, S.Saleem and Q.Islam, "Performance Analysis of Carrier Frequency Offset (CFO) in OFDM using MATLAB", *J. Eng. (JOE)*, vol. 1, no. 1, 2012.
- [97] Mahmood A.K. Abdulsattar and Raed Sattar Jebur, "DSP-based Synchronization Algorithm Implementation for OFDM", *Int. J. Comput. Applicat. (0975 – 8887)*, vol. 107, no. 9, Dec. 2014.

- [98] Fan Wu and Mosa Ali Abu-Rgheff, “Time and Frequency Synchronization Techniques for OFDM Systems operating in Gaussian and Fading Channels: A Tutorial”, in *8th Annu. Postgraduate Symp. The Convergence of Telecommun., Networking and Broadcast. (PGNET)*, Liverpool John Moores Univ., 28th - 29th June 2007.
- [99] Michael Speth, Stefan A. Fechtel, Gunnar Fock, and Heinrich Meyr, “Optimum Receiver Design for Wireless Broad-Band Systems Using OFDM—Part I”, *IEEE Trans. Commun.*, vol. 47, no. 11, Nov. 1999.
- [100] Michael Speth, Stefan Fechtel, Gunnar Fock, and Heinrich Meyr, “Optimum Receiver Design for OFDM-Based Broadband Transmission—Part II: A Case Study”, *IEEE Trans. Commun.*, vol. 49, no. 4, Apr. 2001.
- [101] Ferdinand Classen, Heinrich Meyr, “Frequency Synchronization Algorithms for OFDM Systems suitable for Communication over Frequency Selective Fading Channels”, in *Proc. IEEE Int. Conf. Veh. Technol., Stockholm, Sweden*, pp. 1655–1659, June 1994.
- [102] Seung Hee Han, Jae Hong Lee, “An Overview of Peak-To-Average Power Ratio Reduction Techniques for Multicarrier Transmission”, *IEEE Wireless Commun.*, vol. 12, no. 2, Apr. 2005.
- [103] Mohammed Melood A. Abdased, Mahamod Ismail, Rosdiadee Nordin, “PAPR Performance Comparison between Localized and Distributed-Based SC-FDMA Techniques”, in *Proc. of World Cong. Multimedia and Comput. Sci.*, 2013.
- [104] C. C. Leroy, “Development of Simple Equations for Accurate and More Realistic Calculation of the Speed of Sound in Seawater”, *J. Acoust. Soc. Am.*, vol. 46, no. 1 (Part 2), pp. 216-226, 1969.
- [105] Michael B. Porter and Homer P. Bucker, “Gaussian beam tracing for computing ocean acoustic fields”, *J. Acoust. Soc. Am.*, Oct. 1987.
- [106] Orlando Camargo Rodriguez, “General description of the BELLHOP ray tracing program(June 2008 release)”, [Online] Available: <http://oalib.hlsresearch.com/Rays/GeneralDescription.pdf>
- [107] Michael B. Porter, “The BELLHOP Manual and User’s Guide: PRELIMINARY DRAFT”, [Online] Available: <http://oalib.hlsresearch.com/Rays/HLS-2010-1.pdf>

References

- [108] Peter King, Ramachandran Venkatesan, and Cheng Li, “An Improved Communications Model for Underwater Sensor Networks”, in *Global Telecommun. Conf., IEEE GLOBECOM*, Dec. 2008.
- [109] Lars Michael Wolff, Erik Szczepanski, and Sabah Badri-Hoehner, “Acoustic Underwater Channel and Network Simulator”, in *IEEE OCEANS*, May 2012.
- [110] Sudip Misra, Ghosh A., “The Effects of Variable Sound Speed on Localization in Underwater Sensor Networks”, in *Proc. Australian Telecommun. Networks and Applicat. Conf. (ATNAC)*, Melbourne, Australia, Nov 9-11, 2011.
- [111] Peter King, Ramachandran Venkatesan, and Cheng Li, “A study of channel capacity for a seabed underwater acoustic sensor network”, in *IEEE OCEANS 2008*, 15-18 Sept, 2008.
- [112] Sumi A. Samad, S. K. Shenoy, G. Santhosh Kumar and P.R.S. Pillai, “A Survey of Modeling and Simulation Tools for Underwater Acoustic Sensor Networks”, *Int. J. Research and Reviews Comput. Sci. (IJRRCS)*, SI: Simulation, Benchmarking and Modeling of Systems and Communication Networks, Apr. 2011.
- [113] Hou Pin Yoong, Kiam Beng Yeo, Kenneth Tze Kin Teo, Wei Loong Wong, “Underwater Wireless Communication System: Acoustic Channel Modeling and Carry Frequency Identification”, *Int. J. Simulation Syst., Sci. and Technol. (IJSSST)*, vol. 13, no. 3c, June 2012.
- [114] Mario A. Muñoz Gutiérrez, Pedro L. Próspero Sanchez and Jose V. do Vale Netob, “An eigen path underwater acoustic communication channel simulation”, in *IEEE OCEANS*, 2005.
- [115] Jesse Cross, “Underwater Acoustic Channel Estimation and Analysis”, in *Proc. 5th Annu. ISC Research Symp. ISCRS 2011*, Apr., 2011.
- [116] Ethem M. Sozer, Milica Stojanovic, and John G. Proakis, “Underwater Acoustic Networks”, *IEEE J. Ocean. Eng.*, vol. 25, no. 1, Jan. 2000.

- [117] Xueyi Geng and Adam Zielinski, “An eigenpath underwater acoustic communication channel model”, in *OCEANS '95, MTS/IEEE, Challenges of Our Changing Global Environment Conf. Proc. (vol. 2)*, Oct.- Nov. 1995.
- [118] S. Bonnifay, K. Yao and C. Jutten, “Underwater Acoustic Signal Separation Based on Prior Estimation of the Channel Impulse Response”, in *Int. Conf. Acoust., Speech, and Signal Process., ICASSP '00*, 2000.
- [119] Milica Stojanovic, “Underwater Acoustic Communications: Design Considerations on the Physical Layer”, in *5th Annu. Conf. Wireless Demand Network Syst. and Services WONS*, Jan. 2008.
- [120] Muhammad Ali Raza Anjum, “Underwater Acoustic Channel Modeling, Simulation, and Estimation”, in *Proc. Int. Bhurban Conf. Appl. Sci. and Technol.*, Islamabad, Pakistan, Jan. 10 - 13, 2011.
- [121] Anuj Sehgal, Daniel Cernea, Andreas Birk, “Modeling Underwater Acoustic Communications for Multi-Robot Missions in a Robotics Simulator”, in *IEEE OCEANS - Sydney*, May 2010.
- [122] Parastoo Qarabaqi, and Milica Stojanovic, “Statistical Characterization and Computationally Efficient Modeling of a Class of Underwater Acoustic Communication Channels”, *IEEE J. Ocean. Eng.*, vol. 38, no. 4, Oct. 2013.
- [123] John Heidemann, Milica Stojanovic and Michele Zorzi, “Underwater sensor networks: applications, advances and challenges”, *Phil. Trans. R. Soc. A* (2012) 370, pp. 158–175, 2012.
- [124] Wenli Lin, Deshi Li, Ying Tan, Jian Chen, Tao Sun, “Architecture of Underwater Acoustic Sensor Networks : A Survey”, in *1st Int. Conf. Intelligent Networks and Intelligent Syst.*, ICINIS, pp. 155 – 159, Nov. 2008.
- [125] M. S. Chavan, R. H. Chile and S. R. Sawant, “Multipath Fading Channel Modeling and Performance Comparison of Wireless Channel Models”, *Int. J. Electron. and Commun. Eng.*, vol. 4, no. 2, pp. 189-203, 2011.

References

- [126] Joaquín Aparicio, Fernando J. Álvarez¹, Ana Jiménez, Carlos De Marziani², Jesús Ureña, Cristina Diego, “Underwater Channel Modeling for a Relative Positioning System”, in *IEEE OCEANS - Spain*, June 2011.
- [127] Bernard Widrow and Samuel D. Stearns, *Adaptive Signal Processing*, Prentice-Hall signal process. series, 1985.
- [128] Simon Haykin, *Adaptive Filter Theory*, 3rd Edition, Prentice Hall, 1996.
- [129] Yilun Chen, Yuantao Gu and Alfred O. Hero III, “Sparse LMS for system identification”, in *ICASSP*, pp. 3125 – 3128, Apr. 2009.
- [130] Yuantao Gu, Jian Jin and Shunliang Mei, “ ℓ_0 Norm Constraint LMS Algorithm For Sparse System Identification”, *IEEE Signal Process. Lett.*, vol. 16, no. 9, pp. 774-777, Sept. 2009.
- [131] Ons Benrhouma, Sebastien Houcke, Ammar Bouallegue, “A Statistical Modeling of the Underwater Acoustic Channel”, in *12th IEEE Int. Conf. Electron., Circuits and Syst. (ICECS)*, Dec. 2005.
- [132] Oe-Hyung Lee, Yoon-Jun Son and Ki-Man Kim, “Underwater digital communication using acoustic channel estimation”, in *OCEANS '02 MTS/IEEE*, Oct. 2002.
- [133] B. Jagdishwar Rao and T. Prabhakar, “Underwater Acoustic Wireless Communication Channel Model and Bandwidth”, *Int. J. Appl. Eng. Research*, vol. 6, no.18, pp. 2625-2629, 2011.
- [134] Nina Wang, Guan Gui, Zhi Zhang and Ping Zhang, “Suboptimal sparse channel estimation for multicarrier underwater acoustic communications”, *Int. J. Physical Sci.*, vol. 6(25), pp. 5906-5911, Oct., 2011.
- [135] Shane F. Cotter and Bhaskar D. Rao, “Sparse Channel Estimation via Matching Pursuit With Application to Equalization”, *IEEE Trans. Commun.*, vol. 50, no. 3, Mar. 2002.

- [136] C. Qi, X. Wang and L. Wu, “Underwater acoustic channel estimation based on sparse recovery algorithms”, *IET Signal Process.*, vol. 5, iss. 8, pp. 739–747, Dec. 2011.
- [137] Jun Tao, Yahong Rosa Zheng, Chengshan Xiao, T. C. Yang and Wen-Bin Yang “Channel Estimation, Equalization and Phase Correction for Single Carrier Underwater Acoustic Communications”, in *Proc. OCEANS’08*, Kobe, Apr. 2008.
- [138] Jianzhong Huang, Christian R. Berger, S. Zhou, J. Huang, “Comparison of basis pursuit algorithms for sparse channel estimation in underwater acoustic OFDM”, in *Proc. OCEANS Sydney*, May 24-27, 2010.
- [139] Sichuan Guo, Zhiqiang He, Weipeng Jiang, Yue Rong and Michael Caley, “Channel Estimation Based on Compressed Sensing in High-speed Underwater Acoustic Communication”, in *9th Int. Conf. Inform., Commun. and Signal Process. (ICICS)*, Dec. 2013.
- [140] Guan Gui, Qun Wan, Wei Peng and Fumiyuki Adachi, “Sparse Multipath Channel Estimation Using Compressive Sampling Matching Pursuit Algorithm”, in *IEEE Asia Pacific Wireless Commun. Symp. (APWCS)*, 2010.
- [141] Mauro Biagi, Stefano Rinauro and Roberto Cusani, “Channel Estimation or Prediction for UWA?”, in *IEEE OCEANS - Bergen*, 10-14 June 2013.
- [142] Srishtansh Pathak and Himanshu Sharma, “Channel Estimation in OFDM Systems”, *Int. J. Advanced Research Comput. Sci. and Software Eng.*, vol. 3, no. 3, Mar. 2013.
- [143] Sinem Coleri, Mustafa Ergen, Anuj Puri and Ahmad Bahai, “A study of Channel Estimation in OFDM Systems”, in *IEEE 56th Veh. Technol. Conf. (VTC 2002)*, 2002.
- [144] Thomas Pedersen, Alex Bloomberg, “OFDM Pilot-Aided Underwater Acoustic Channel Estimation”, (*IJEECS*) *Int. J. Elect., Electron. and Comput. Syst.*, vol. 9, no. 3, 2012.

References

- [145] Shengli Zhou and Zhaohui Wang, *OFDM for Underwater Acoustic Communications*, John Wiley & Sons Ltd., Apr. 2014.
- [146] Sajjad Ahmed Ghauri, SherazAlam, M. Farhan Sohail, AsadAli and FaizanSaleem, "Implementation of OFDM and Channel Estimation using LS and MMSE Estimators", *Int. J. Comput. and Electron. Research*, vol. 2, no. 1, Feb. 2013.
- [147] Sanjay Kumar Khadagade, N.K.Mittal, "Comparison of BER of OFDM system using QPSK and 16-QAM over Multipath Rayleigh fading channel using pilot-based Channel Estimation", *Int. J. Eng. and Advanced Technol. (IJEAT)*, vol. 2, no. 3, Feb 2013.
- [148] Kavitha K.V.N., Abhishek Jaiswal and Sibaram Khara, "Performance analysis of MISO-OFDM & MIMO-OFDM Systems", *Int. J. Eng. and Technol.*, vol. 5, no. 3, Jun-Jul 2013.
- [149] Sinem Coleri, Mustafa Ergen, Anuj Puri, and Ahmad Bahai, "Channel Estimation Techniques Based on Pilot Arrangement in OFDM Systems", *IEEE Trans. Broadcast.*, vol. 48, no. 3, Sept. 2002.
- [150] Chunguo Li, Kang Song, Luxi Yang, "Low computational complexity design over sparse channel estimator in underwater acoustic OFDM communication system", *IET Commun.*, vol. 11, no. 7, pp. 1143-1151, 2017.
- [151] Siavash M. Alamouti, "A Simple Transmit Diversity Technique for Wireless Communications", *IEEE J. Sel. Areas Commun.*, vol. 16, no. 8, Oct. 1998.
- [152] R.F. Ormondroyd, J.S. Dhanoa, "Comparison of Space-Time Block Code and Layered Space-Time MIMO Systems for an Underwater Acoustic Channel", *IEEE OCEANS - Europe 2005*, June 2005.
- [153] Baosheng Li and M. Stojanovic, "Alamouti Space Time Coded OFDM for Underwater Acoustic Channels", in *IEEE OCEANS Sydney*, May 2010.

- [154] Eduard Valera Zorita and Milica Stojanovic, "Space-Frequency Block Coding for Underwater Acoustic Communications", *IEEE J. Ocean. Eng.*, Vol. 40, No. 2, Apr. 2015.
- [155] Yamini Devlal, Meenakshi Awasthi, "MIMO performance analysis with Alamouti STBC code and V-Blast Detection Scheme", *Int. J. Sci., Eng. and Technol. Research (IJSETR)*, vol. 4, no. 1, Jan. 2015.
- [156] B.-C. Gwun, J.-W. Han, K.-M. Kim, and J.-Won Jung, "MIMO Underwater Communication with Sparse Channel Estimation," in *2013 5th Int. Conf. Ubiquitous and Future Networks (ICUFN)*, pp. 32–36, July 2013.
- [157] Fengzhong Qu, Zhenduo Wang, and Liuqing Yang, "Differential Orthogonal Space-Time Block Coding Modulation for Time-Variant Underwater Acoustic Channels", *IEEE J. Oceanic Eng.*, vol. 42, no. 1, January 2017.
- [158] Moore–Penrose inverse [Wikipedia]
https://en.wikipedia.org/wiki/Moore%E2%80%93Penrose_pseudoinverse
- [159] The Network Simulator - ns-2 [Online] Available:
<https://www.isi.edu/nsnam/ns/>
- [160] ns-3 Tutorial [Online] Available:
<https://www.nsnam.org/docs/tutorial/html/>
- [161] Peng Xie, Zhong Zhou, Zheng Peng, Hai Yan, Tiansi Hu, Jun-Hong Cui, Zhijie Shi, Yunsi Fei, Shengli Zhou, "Aqua-Sim: An NS-2 based simulator for underwater sensor networks", *MTS/IEEE Biloxi - Marine Technology for Our Future: Global and Local Challenges, OCEANS*, Oct. 2009.

References

Publications brought out in the field of research

1. Sabna N., Supriya M.H., and P.R. Saseendran Pillai, "Computationally Efficient Sparse Reconstruction of Underwater Signals," in *Int. Symp. Ocean Electron. (SYMPOL 2013)*, IEEE Xplore 10.1109/SYMPOL.2013.6701916, Oct. 2013.
2. Sabna N., and P.R. Saseendran Pillai, "Matrix Padding Method for Sparse Signal Reconstruction," *Signal Process.: Int. J. (SPIJ)*, vol. 9, no. 1, pp. 1-13, 2015.
3. Sabna N., and P.R. Saseendran Pillai, "Effect of Ambient Noise on OFDM Signals," in *Underwater Technol. 2015 (UT 15)*, IEEE Xplore 10.1109/UT.2015.7108291, 23-25 Feb. 2015.
4. Sabna N., Revathy R. and P.R. Saseendran Pillai, "Space-Time Block Coding for Undersea Acoustic Links," *Proc. Meeting Acoust. (POMA)*, Vol. 25, 070001, pp. 1-7, 2015.
5. Sabna N. and P.R. Saseendran Pillai, "BPSK based BCH Coded OFDM for Undersea Acoustic Links," in *Int. Symp. Ocean Electron. (SYMPOL 2015)*, IEEE Xplore 10.1109/SYMPOL.2015.7581172, 18-20 Nov. 2015.
6. Sabna N., and P.R. Saseendran Pillai, "Error Rate Performance of Interleaved Coded OFDM for Undersea Acoustic Links," *Signal Process.: Int. J. (SPIJ)*, vol. 10, no. 3, pp. 41-49, 2016.
7. Sabna N., and P.R. Saseendran Pillai, "Channel Estimation in an OFDM System for Undersea Acoustic Links", *Int. J. Commun. (IJC)*, vol. 5, pp. 1-11, 2016.
8. Sabna N., and P.R. Saseendran Pillai, "Bit Error Rate Performance of Underwater Channels for OFDM Data," *J. Mar. Biol. Ass. India*, vol. 58, no. 2, July-December 2016.

Other Publications

1. Sabna N., Suraj Kamal, Supriya M.H. and P.R. Saseendran Pillai, "Implementation of an Underwater Image Classifier using Neural Networks," *Int. Symp. Ocean Electron. (SYMPOL 2011)*, IEEE Xplore 10.1109/SYMPOL.2011.6170512, Nov. 2011.

Subject Index

Subject Index

- A**
- adaptive filter..... 43, 71, 72
 - Alamouti 18, 19, 48, 49, 83, 84, 106, 107, 108, 110, 121, 123, 145, 159, 165, 184, 185
 - ambient noise .. 1, 2, 6, 10, 17, 23, 24, 27, 65, 74, 80, 86, 115
 - Ambient Noise 115
 - attenuation 1, 2, 6, 7, 8, 22, 23, 26, 27, 42, 44, 52, 61
- B**
- BCH code..... 37, 99
 - BELLHOP 40, 179
 - BPSK xxv, 36, 37, 47, 48, 81, 82, 83, 86, 93, 94, 124, 135, 136, 137, 138, 139, 140, 141, 142, 143, 144, 148, 149, 150, 152, 153, 155, 156, 157, 158, 163, 164, 177, 187
- C**
- Carrier Frequency Offset.. xxv, 18, 38, 65, 85, 87, 115, 118, 178
 - channel estimation 16, 18, 20, 21, 35, 44, 45, 46, 47, 48, 50, 57, 61, 62, 63, 85, 86, 112, 115, 123, 125, 149, 150, 151, 154, 155, 158, 161, 165, 182, 183
 - Coded OFDM.. 59, 81, 82, 136, 137, 141, 142, 144, 157, 164, 166, 178, 184, 187
 - compressive sensing ... xiii, 14, 16, 17, 19, 20, 21, 28, 29, 30, 31, 32, 33, 43, 44, 45, 48, 49, 52, 53, 54, 56, 62, 66, 89, 111, 124, 125, 126, 127, 128, 129, 130, 131, 163
 - correlation 19, 24, 72, 117, 123, 125, 126, 127, 128, 129, 148, 149
 - CoSaMP..... xxv, 16, 19, 21, 29, 30, 44, 46, 55, 123, 125, 127, 128, 130, 172
 - CVX. 16, 33, 55, 114, 116, 127, 128, 129, 130, 175
- D**
- DCT..... xxv, 17, 32, 34, 65, 68, 69, 70, 71, 174, 175
 - dictionary. 17, 20, 51, 53, 55, 62, 63, 86, 113, 114, 115, 123, 125, 151, 165
 - diversity techniques..... 16, 21, 66, 103, 121
- E**
- environmental file..... 15
- G**
- greedy algorithm..... 46
- H**
- Hybrid Topology..... 5
- I**
- incoherence 29, 30, 66
 - interleaving 18, 19, 37, 39, 59, 65, 81, 82, 83, 84, 89, 90, 102, 121, 123, 124, 137, 138, 139, 140, 141, 142, 143, 144, 145, 146, 148, 159, 164, 165

Subject Index

L

l_1xxv, 16, 19, 21, 32, 45, 55, 123, 125,
127, 128, 130
 l_1 -magic.....16, 19, 21, 32, 55, 123, 125, 127,
128, 130, 174
least squares 41, 45, 48, 55
LMS .xxv, 17, 35, 43, 65, 71, 72, 86, 124, 125,
127, 163, 177, 182

M

matrix padding.....16, 17, 19, 65, 70, 86, 123,
124, 126, 127, 128, 129, 159, 161, 163
MIMO.....xxv, 48, 49, 83, 110, 111, 184, 185
modulation 16, 17, 18, 19, 21, 26, 33, 34, 35,
36, 37, 48, 49, 50, 57, 58, 59, 80, 83, 84,
89, 90, 93, 94, 95, 115, 123, 124, 138,
140, 145, 147, 148, 150, 156, 159, 161,
167
multipath . 1, 2, 11, 12, 15, 22, 23, 24, 26, 34,
40, 42, 44, 47, 58, 59, 62, 77, 80, 90, 91,
96, 103, 112, 157, 167

O

Orthogonal Frequency Division Multiplexing
.xiii, xxv, 16, 17, 18, 34, 37, 51, 58, 89, 90,
92, 161, 176, 177
Orthogonal Matching Pursuit xxv, 16, 55, 172

P

PAPR34, 39, 60, 96, 97, 179

pilot overhead..... 62, 156, 165

R

Rayleigh.. 1, 14, 15, 16, 20, 21, 34, 41, 43, 47,
48, 145, 163, 184
Relaxation methods 54

S

sensor networks.....5, 20, 21, 22, 41, 42, 161,
162, 169, 181, 185
sensor nodes..... xiii, 2, 3, 4, 5, 25
Sonar 2
sound speed.....2, 8, 9, 12, 14, 18, 23, 25, 42,
43, 65, 77, 78
Space-time block coding 18, 65, 83, 107, 165
STO estimation..... 19, 117, 123, 148, 165
synchronization.....16, 21, 38, 50, 60, 85, 86,
116, 124, 137, 139, 151, 161, 165

T

thermocline..... 10, 23, 25
Three-dimensional underwater networks ... 4
two-dimensional underwater networks 3

Y

YALL1....xxvi, 16, 19, 21, 32, 45, 55, 123, 125,
127, 128, 130, 174